Nuclear Reactor Physics

lecture notes AP3341

prof.dr.ir. H. van Dam
prof.dr.ir. T.H.J.J. van der Hagen
dr.ir. J.E. Hoogenboom

Delft University of Technology

Physics of Nuclear Reactors

Mekelweg 15, 2629 JB Delft

The Netherlands

April 2005

Contents

Chapter 1

Nuclear reactors and nuclear reactions

1.1. Principle of a nuclear reactor

In a nuclear reactor certain very heavy nuclei (e.g. $^{235}_{92}U$) can be split into two fragments by neutrons, whereby a relatively large amount of energy is released and, moreover, a few new neutrons, which in their turn can cause new fissions. If on average one of the neutrons released in a fission causes a new fission, a steady state chain reaction is initiated, whereby energy is continuously being released. A fission releases *circa* 200 MeV (1 eV = $1.6 \cdot 10^{-19}$ J). Compared with a chemical reaction, in which a few eV are released (for example, compare the combustion of 1 m^3 of natural gas with an energy content of 30 MJ), this is an enormous amount of energy. Although it is possible to sustain a chain reaction with a ball of $^{235}_{92}U$ a little bit larger than a tennis-ball, such a structure is unsuitable for generating a large amount of energy. To that end, one applies a coolant that can effectively remove the heat and a much larger amount of uranium is placed in the reactor core. Moreover, pure $^{235}_{92}U$ does not occur in nature. The composition of natural uranium, which is found in various ore layers in the earth's crust, consists of the isotopes ^{234}U, ^{235}U and ^{238}U with weight percentages as stated in Table 1.1.

Table 1.1. Composition of natural uranium

Isotope	weight percentage	mass number	radioactive half-life
$^{234}_{92}U$	0.006	234.0409	2.4 10^5 a
$^{235}_{92}U$	0.712	235.0439	7.0 10^8 a
$^{238}_{92}U$	99.282	238.0508	4.5 10^9 a

Hereafter, it will become evident why e.g. ^{238}U is much less suited for fission by neutrons, because of which the percentage ^{235}U, the degree of enrichment, is very important. For economic reasons, one chooses a degree of enrichment for the nuclear fuel in a reactor of about 3 %. A reactor core is formed by placing together a large number of fuel elements in a large reactor vessel. A fuel element consists of a number of slender, long rods with uranium (usually in the form of UO$_2$) in a rectangular fuel lattice, between which the coolant (mostly water)

flows. In order to prevent chemical reactions between the coolant and the nuclear fuel, the nuclear fuel is housed in a metal cladding.
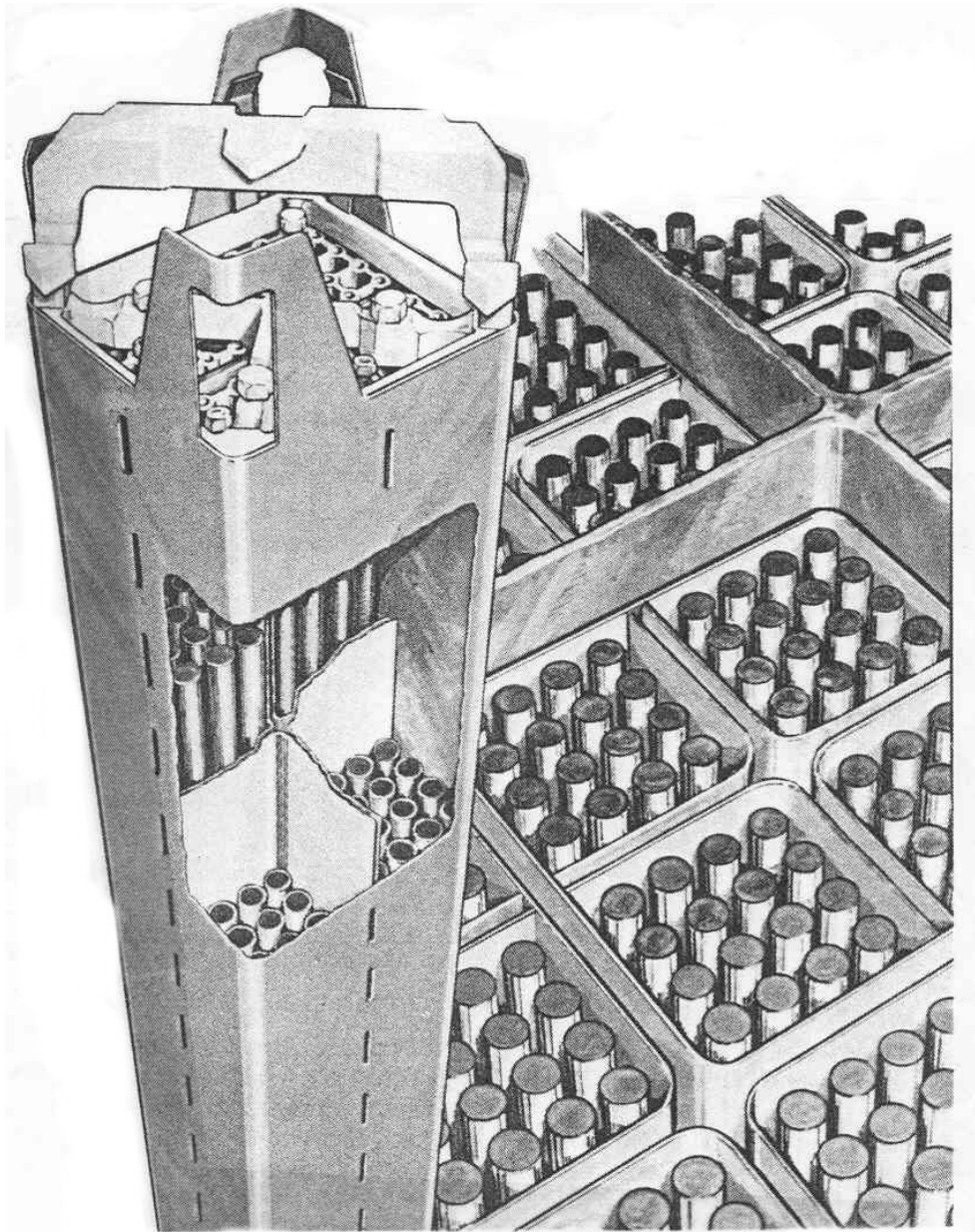
Figure 1.1. Fuel elements in a reactor

Figure 1.1 shows a possible shape of a fuel assembly. The heat generated in the nuclear fuel is transferred to the cooling water, which is pumped upward along the rods. The water can start to boil by this. The steam is subsequently led to a steam turbine, in which the blades are driven and a rotation is induced. The turbine shaft subsequently drives an electrogenerator, which generates the electric energy and supplies it to the electrical power network. The expanded steam from the turbine is condensed, after which the water is pumped through the core again. Cooling water, which is drawn from river or seawater, is used for condensation of the steam, or one applies a cooling tower. Figure 1.2 shows a schematic drawing of such a so-called boiling-water reactor.

6
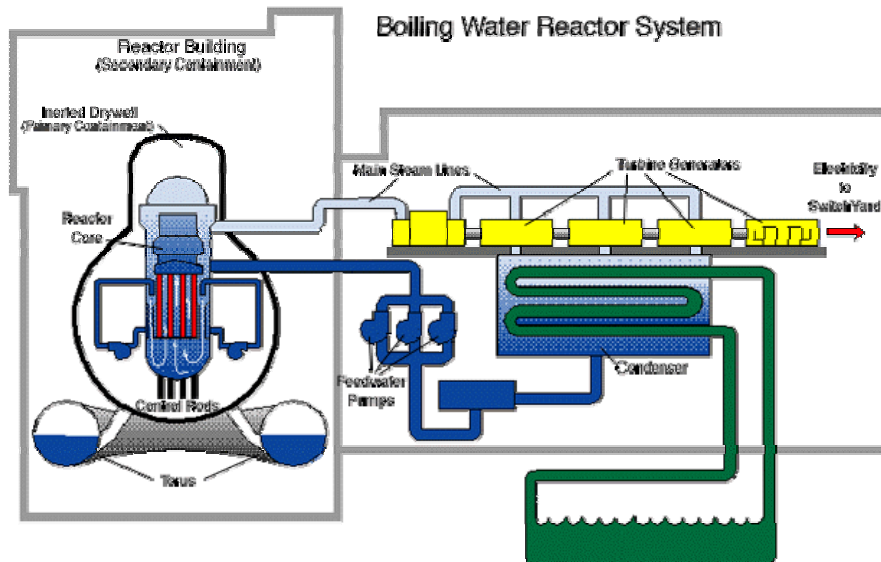
Figure 1.2. Principle sketch of a boiling-water reactor

In a so-called pressurized-water reactor (see Figure 1.3) the pressure of the water in the reactor is kept much higher, so that boiling in the core does not occur. The heated water is led to a steam generator, in which heat is transferred to water from the secondary side, which is under a lower pressure, so that it starts boiling. The steam is then led to the turbine again.
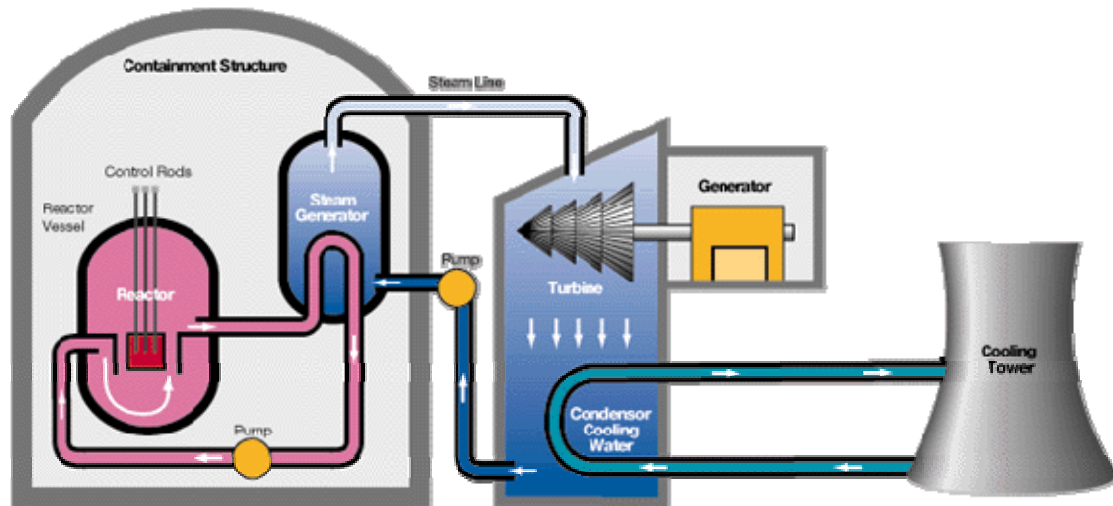
Figure 1.3. Principle sketch of a pressurized-water reactor

The water in a boiling-water or pressurized-water reactor not only serves as coolant, but also for slowing down the neutrons in their energy. The neutrons released during fission have a high energy, as we will see in the next section, whereas the chance of causing a new fission is larger if the neutrons have a low energy. By collisions with light nuclei such as hydrogen in water, the neutrons lose energy, so that the water also works as moderator.

Finally, the neutrons get an energy distribution that corresponds with the heat movement of the atomic nuclei. Therefore, reactors in which a moderator is applied are also referred to as thermal reactors. In reactors in which no moderator is applied, the neutrons predominantly keep a high energy. These reactors are called fast reactors. In the next sections, first we will go into the fission process in order to understand why energy is released in nuclear fission and why only certain nuclei can be used. Further, other possible interactions of neutrons with a nucleus will be discussed and the chance of interactions will be quantified. In the next chapter, an equation can then be derived, which describes the transport of neutrons in a reactor core. From the solution of this equation (or a simplified form thereof), the conditions that a reactor core must satisfy in order to enable a self-sustaining chain reaction of fissions can be derived.

1.2. The fission process

The protons and neutrons in an atomic nucleus are held together by the nuclear forces (strong force). Therefore, energy is required for breaking apart the nucleus into the separate nuclear particles or nucleons. This binding energy of a nucleus is obtained by imaginary composition of the nucleus from the separate nucleons, because the mass of the whole nucleus is less than the sum of the masses of the separate nucleons. According to the relation of Einstein $E=mc^2$, this so-called mass defect has been converted into potential energy: the binding energy E_b. For a nucleus with A nucleons (A is the so-called mass number), the binding energy per nucleon E_b/A can be calculated. This is shown in Figure 1.4 as a function of the mass number.

For low mass numbers it increases rapidly, with some irregularities in the case of light nuclei, reaches a maximum of 8.8 MeV at A=60 and after that decreases slowly. From this figure it becomes evident that energy can be produced by fusion of light nuclei or by fission of heavy nuclei.
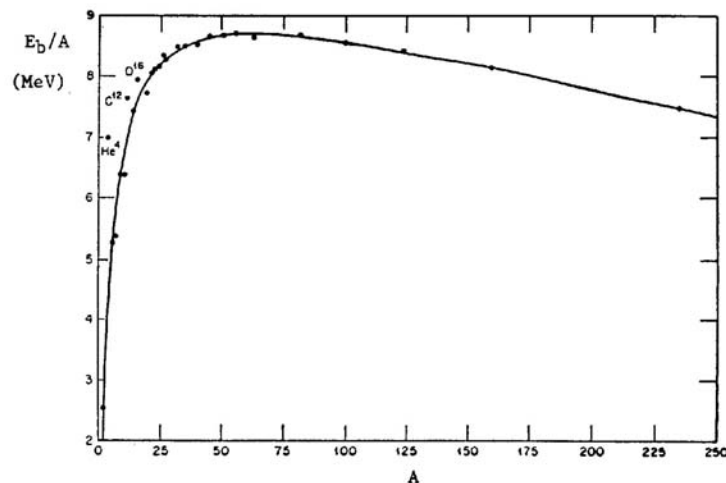

Figure 1.4. Binding energy per nucleon as a function of the mass number A

The binding energy of atomic nuclei as a function of the mass number A and the number of protons Z can be described with the following semi-empirical equation:

$$E_b(MeV) = 15.76\,A - 17.81\,A^{2/3} - 0.711\frac{Z^2}{A^{1/3}} - 23.702\frac{(N-Z)^2}{A} \pm 34\,A^{-3/4} \qquad (1.1)$$

The physical meaning of this equation will now be discussed term by term. Seeing that the attracting forces between the nucleons mainly operate via direct neighbours, the positive first term in (1.1) will be proportional to the number of nucleons A in the nucleus. One can call this the *volume term*. Hereby it is neglected, however, that particles at the surface of the nucleus are not completely surrounded by other particles. Consequently, the binding energy has been overestimated with an amount that must be proportional to the surface area of the nucleus. By analogy with a liquid drop this effect is indicated as the *surface tension effect*. This term (*surface term*) must be proportional to the surface area, so with $A^{2/3}$. The third term is connected with the coulomb interaction between the protons, which lowers the binding energy because of the repulsion between charges of equal sign. The potential energy of an electrically charged sphere is proportional to Z^2/R, whereby R is proportional to $A^{1/3}$, which yields the third term (*coulomb term*).

The last two terms in (1.1) cannot be described as 'classically' as the first three. In atomic nuclei there is a tendency to form groups of neutron/proton pairs. Especially in the case of light nuclei, one sees that those with an equal number of protons and neutrons are very stable. The heavier stable nuclei, however, contain more neutrons than protons. This excess of neutrons is necessary in order that the attractive forces between the neutrons and between the neutrons and protons can provide some compensation for the repulsion between the protons (third term). At the same time, however, some instability is introduced because the surplus of neutrons occupies a number of energy levels in the nucleus, which do not contain protons. A correction factor must be introduced for this, the so-called *symmetry term*, which is also important in the case of a proton surplus; therefore this term is quadratic in N-Z.

The last term is the *pairing term*, which accounts for the fact that nucleons have a spin moment of momentum or 'spin'. This spin effect finds expression in the fact that nuclei with an even number of protons and an even number of neutrons are very stable thanks to the occurrence of 'paired spin'. When a nucleus contains an odd number of both particle types, it is nearly always unstable; the only exceptions are ^2_1H, ^6_3Li, $^{10}_5B$ and $^{14}_7N$.

For this fifth term the following 'recipe' holds:

even/even nuclei	: pairing term *positive*
odd/odd nuclei	: pairing term *negative*
even/odd or odd/even nuclei	: pairing term = 0

With the aid of (1.1) the binding energy can be calculated fairly accurately and it can be determined, for example, at which value of A for a given Z the binding energy is maximum, *i.e.* which nuclides have the largest stability (for example $^{27}_{13}\text{Al}$ and $^{64}_{28}\text{Ni}$).

Table 1.2 shows the influence of the various effects on the binding energy for a light, medium-weighted and heavy nuclide.

Table 1.2. Binding energy (in MeV) for some nuclides

Effect	$^{40}_{20}\text{Ca}$	$^{107}_{47}\text{Ag}$	$^{238}_{92}\text{U}$
volume term	630	1686	3751
surface term	-208	-401	-684
coulomb term	-83	-331	-971
symmetry term	0	-37	-290
pairing term	+2	0	+0.6
calculated E_b	341	917	1806
measured E_b	342	915	1802
measured E_b/A	8.6	8.6	7.6

From Figure 1.4 we see that, if we can split a $^{235}_{92}\text{U}$ nucleus into two parts, the binding energy of the fragments (A ≈ 120) together is larger than that of the original nucleus, whereby *circa* 235 x (8.5 − 7.6) ≈ 200 MeV is released.

The fission process consists of splitting a nucleus into roughly equal parts. In principle, any nucleus, if brought into sufficiently high excited state, can be split. The amount of excitation energy that is required to enable nuclear fission can be estimated from the magnitude of the electrostatic barrier and the dissociation energy of the fission in question.

In Figure 1.5 the potential energy of two fission fragments has been sketched as a function of the distance between their centres. The height of the potential barrier is approximately given by $E_C = Z_1 Z_2 e^2 / \{4\pi\varepsilon_0 (R_1 + R_2)\}$ in which R_1 and R_2 are the respective nuclear radii and ε_0 is the permittivity of the vacuum. To the left of the maximum, a bound state occurs as a result of the nuclear forces.

The dissociation energy E_d is equal to the difference between the binding energy of the compound nucleus and the sum of the binding energies of the fission fragments and can thus be estimated with (1.1). The minimum activation energy E_a that has to be added to a nucleus to cause fission is thus $E_C − E_d$.

10
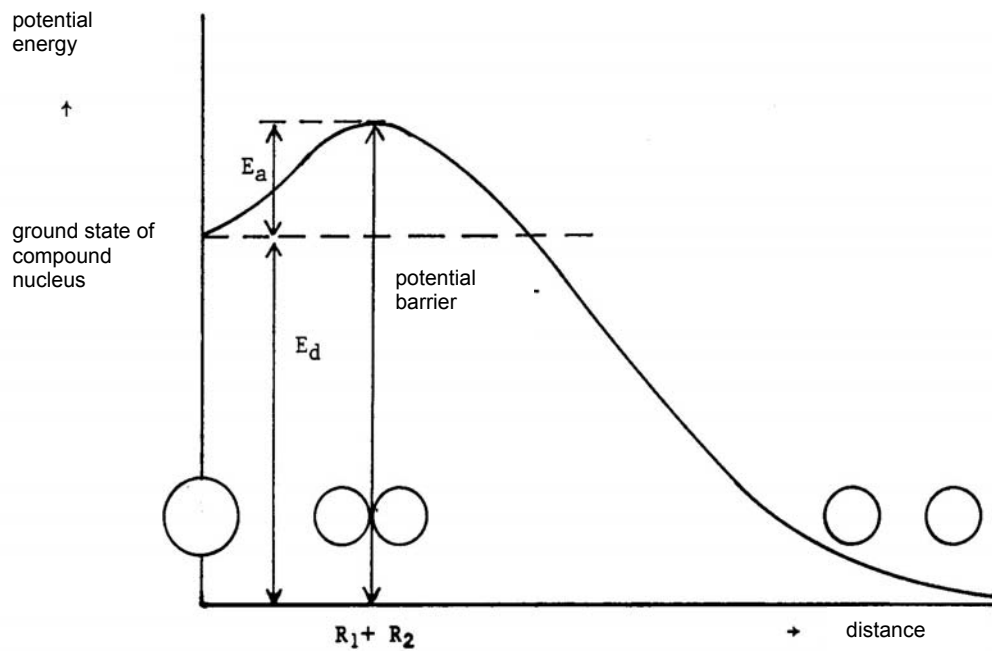
Figure 1.5. Potential energy as a function of the distance between two fission fragments

When the mass of a nucleus is larger than the sum of the masses of the fragments into which the nucleus can be separated, the first will show a tendency towards instability, because fission is accompanied by the release of energy. This tendency is thus present in nuclei sufficiently far from the 'binding energy maximum' in Figure 1.4, so for A > 100. However, seeing that the activation energy E_a of nuclides with mass numbers below about 230 is very large, spontaneous fission of these nuclides does not occur; for A > 260, E_a is negative, so that these nuclei have a very short radioactive life. Table 1.3 gives the minimum activation energy for fission of a number of nuclei.

Table 1.3. Energy values (in MeV) important for fission

	mass number A					
	16	60	100	140	200	236
potential barrier E_C	4	32	62	110	175	210
dissociation energy E_d	-12.7	-16	15	48	135	205
activation energy E_a	18.5	48	47	62	50	~5

The excitation energy can be added to a nucleus by bombardment with photons or particles. With the aid of gamma bombardment one can determine the value of E_a. For example, the following values have been found:

11

^{236}U : E_a = 5.3 MeV

^{239}U : E_a = 5.5 MeV

The most attractive method of causing fission, however, is by forming a compound nucleus with the aid of a neutron. Indeed, by absorption of a neutron, both the kinetic energy and the binding energy of the neutron become available for bringing the compound nucleus into an excited state, while no coulomb forces need to be overcome such as in the case of charged particles. If the excited state in the energy diagram of Figure 1.5 is above the potential barrier, then the possibility of fission occurs. By applying (1.1) one finds that by absorption of a neutron in ^{235}U an amount of binding energy becomes available of:

$$E_b(^{236}U) - E_b(^{235}U) = 6.6 \text{ MeV}$$

In the case of ^{238}U one finds:

$$E_b(^{239}U) - E_b(^{238}U) = 5.1 \text{ MeV}$$

From this it follows that for fission of ^{238}U the neutron must have a minimum kinetic energy of 5.5 − 5.1 = 0.4 MeV, while absorption of a neutron without kinetic energy can already cause fission of ^{235}U. In general, heavy nuclei with an odd number of neutrons (^{233}U, ^{235}U, ^{239}Pu) can easily be split, because the neutron that is absorbed to form a compound nucleus with these nuclei is an 'even' neutron, so that the binding energy due to the pairing effect is large. On the other hand, the heavy 'even' nuclei (^{232}Th, ^{238}U, ^{240}Pu, ^{242}Pu) have an energy threshold for fission by neutrons, because the absorbed neutron is an 'odd' neutron, which makes relatively little binding energy available. For these nuclides fission is thus a threshold reaction.

When a nucleus is excited above the potential barrier, fission need not always occur. It is also possible that the excitation energy rapidly dissipates by emission of gammas; in this case the reaction is referred to as a capture reaction or (n,γ) reaction. This is detrimental to sustaining the chain reaction in a reactor.

During the spontaneous fission reaction, immediately a few neutrons are emitted as a result of the large neutron surplus in the fission products. The average number (v) increases with increasing excitation energy, so with the kinetic energy of the absorbed neutron. For example, in the case of ^{235}U:

$$v(E) = 2.44 + 0.095 \text{ E (MeV)}$$

12

with E the kinetic energy of the neutron in MeV.
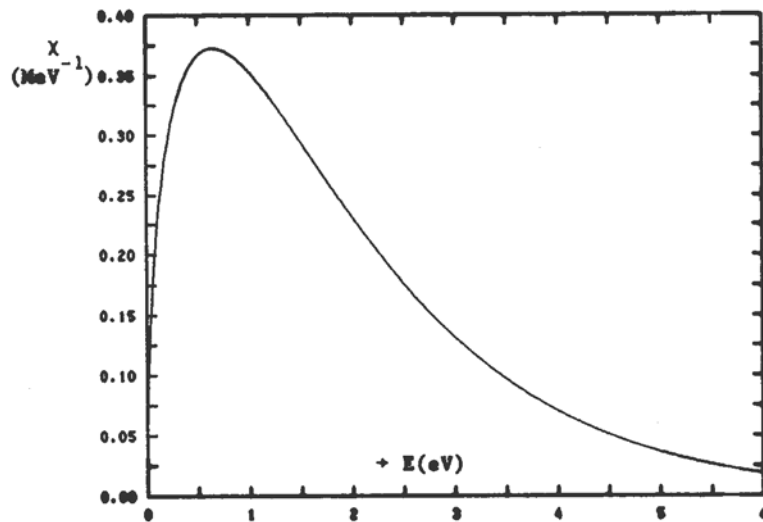
Figure 1.6. The fission spectrum of ^{235}U

The neutrons emitted during fission have an energy distribution as sketched in Figure 1.6, which in analytical form can be written as:

$$\chi(E) - \frac{2}{\sqrt{\pi T^3}}\sqrt{E}e^{-E/T} \qquad (1.2)$$

in which T is a fictitious temperature in units of energy (T = 1.3 MeV) and χ (E)dE the fraction of neutrons with an energy between E and E + dE; the average neutron energy is 3/2 T $\approx$ 2 MeV.
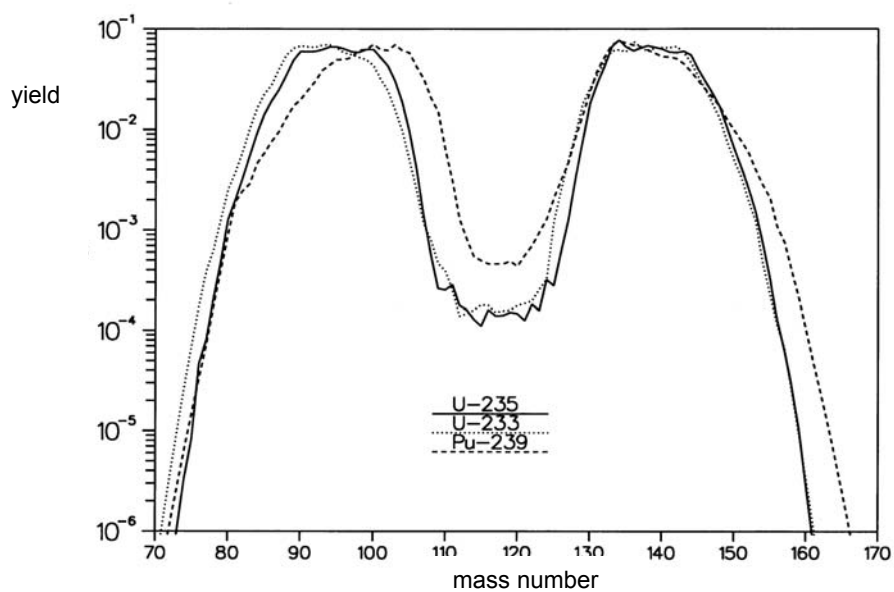
Figure 1.7. Yield of fission products

There are about 60 primary fission products, the yield of which per fission is distributed according to the 'camel curve' sketched in Figure 1.7. From this figure a preference appears for asymmetric fission. The primary fission products, which are in a highly excited state, lose their redundant energy by decay. This can happen by emission of photons and neutrons. When the excitation energy has become smaller than the binding energy of the neutrons in the fission fragments, the prompt neutron emission stops and the remaining energy will be released in the form of photons, the so-called prompt gamma radiation.

Fallen back into the ground state the fragments will still be unstable. As the fragments then still have a neutron surplus, it is obvious that most fission fragments will decay into a more stable state through β emission. Often a multi-stage β decay is necessary for obtaining a stable nucleus, for example:

$$^{135}_{52}Te \xrightarrow[18s]{\beta^-} {}^{135}_{53}I \xrightarrow[6.6h]{\beta^-} {}^{135}_{54}Xe \xrightarrow[9.2h]{\beta^-} {}^{135}_{55}Cs \xrightarrow[2.10^6 a]{\beta^-} {}^{135}_{56}Ba \ (stable)$$

or

$$^{149}_{60}Nd \xrightarrow[1.7h]{\beta^-} {}^{149}_{61}Pm \xrightarrow[53h]{\beta^-} {}^{149}_{62}Sm \ (stable)$$
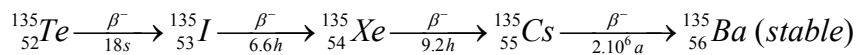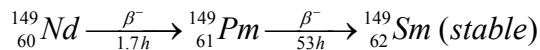
The largest part of the energy produced during fission (about 80 %) becomes available in the form of kinetic energy of the fission fragments. The other part is distributed over the kinetic energy of the neutrons and the radiation energy. The total energy amounts to about 203 MeV per fission, distributed as shown in Table 1.4. In a reactor, per fission *circa* 195 MeV becomes available, being the total energy minus the energy of the neutrinos. However, neutron capture processes in a reactor produce additional energy, by which the total energy becoming available amounts to about 200 MeV per fission. This means that *circa* $3.1 \cdot 10^{10}$ fissions per second are required to produce a power of 1 W and that burn-up of 1 g of uranium yields about 1 MWd (megawatt day) of energy (verify this!).

Table 1.4. Energy distribution during fission

	energy (MeV)
kinetic energy fission fragments	169.58
prompt γ radiation	6.96
kinetic energy fission neutrons	4.79
γ-energy fission products	6.26
β-energy fission products	6.43
neutrinos	8.68
total	202.70

1.3. Nuclear reactions and neutron cross sections

Atomic nuclei can undergo interactions with other nuclei, elemental particles (protons, neutrons, electrons) and electromagnetic radiation (photons). For reactor physics we can confine ourselves to interactions with neutrons, which due to their electrical neutrality do not experience coulomb repulsion and can thus become involved in interactions with nuclei already at very low energy. In the description of neutron-nucleus interactions the 'compound-nucleus model' proposed by Bohr in 1936 can be used. According to this model two consecutive phases can be discerned in a nuclear reaction:

1) The incident particle is absorbed by the nucleus and forms a compound nucleus with it.
2) After a short time the compound nucleus disintegrates by emission of a particle, which need not be equal to the incident particle.

Because a particle is absorbed in the target nucleus, an amount of energy will be added to the compound nucleus that is equal to the binding energy of the particle plus the kinetic energy of this particle. Because conservation of momentum must be satisfied, part of the total energy is converted into kinetic energy of the compound nucleus, while the remaining energy causes the compound nucleus to attain a high-energy state. The first part of the reaction can be written as follows:

$$_0^1 n + {}_Z^A X \rightarrow {}_Z^{A+1} X *$$
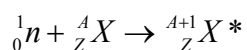
in which the asterisk indicates that the compound nucleus is in an excited state. Immediately after formation of the compound nucleus, all of the energy is concentrated around the captured particle. In consequence of the interactions between the nuclear particles, this energy will rapidly spread over all particles in the nucleus. This distribution has a statistical character, whereby it is possible that a particle gets an energy that is larger than its binding energy. The compound nucleus then can lose its excess energy by emission of this particle. In the previous section we already saw that in the case of very heavy nuclei it is possible that the energy is distributed in such a way that two fragments arise: the nuclear fission. Excess energy can also be emitted in the form of electromagnetic radiation (photons); in that case one speaks of a (n,γ) reaction.

The second phase of the neutron-nucleus interaction can now be written as follows:

$$
{}^{A+1}_{Z}X* \rightarrow
\begin{cases}
{}^{A}_{Z}X + {}^{1}_{0}n & (n, n') - reaction \\
{}^{A-1}_{Z}X + 2\,{}^{1}_{0}n & (n, 2n) - reaction \\
{}^{A}_{Z-1}Y + {}^{1}_{1}p & (n, p) - reaction \\
{}^{A-3}_{Z-2}Y + {}^{4}_{2}He & (n, \alpha) - reaction \\
{}^{A+1}_{Z}X + \gamma & (n, \gamma) - reaction \\
{}^{A_1}_{Z_1}Y_1 + {}^{A_2}_{Z_2}Y_2 + v\,{}^{1}_{0}n & (n, f) - reaction
\end{cases}
$$
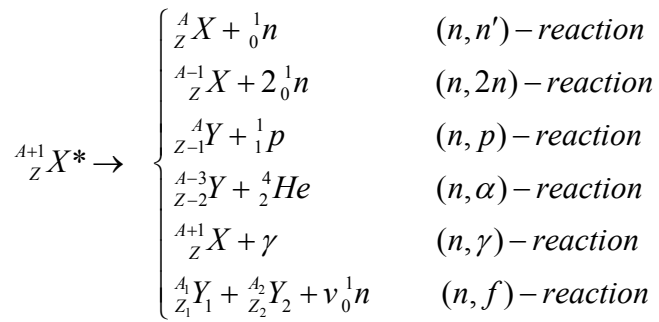
In the (n,n$'$) reaction or inelastic scattering, part of the excitation energy is emitted in the form of gamma radiation. The last reaction is the fission reaction. Hereby it must hold that $Z_1 + Z_2 = Z$ and $A_1 + A_2 + v = A + 1$.

The remaining nucleus after one of these reactions in many cases will not be stable and will transform into a more stable nucleus under emission of β and/or α particles, whereby often also photons are released.

For neutron-nucleus reactions the following division is used:
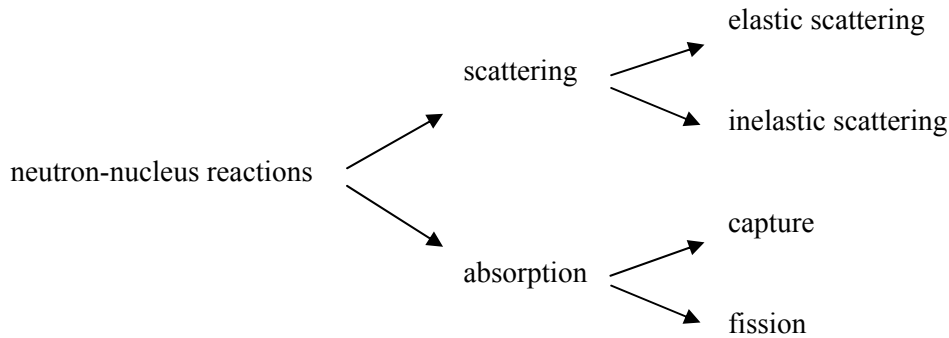
The concept of the microscopic cross section is introduced to represent the probability of a neutron-nucleus reaction. Suppose that a uniform beam of neutrons with intensity I cm^{-2} s^{-1} strikes a thin 'film' of atoms (one atomic layer thick) with N_a atoms/cm^2. Then the number of interactions C per cm^2 per second will be proportional to the intensity I and the atom density N_a. We define the proportionality factor as the microscopic cross section (or just cross section) σ.

$$C = \sigma N_a I \tag{1.3}$$

The microscopic cross section is often expressed in 'barns' (1 b = 10^{-24} cm^2); from this definition it follows that one can consider σ as the effective 'target area' that a nucleus presents to the neutron. The microscopic cross section in general is dependent on the neutron energy and the type of reaction. In accordance with the foregoing scheme one distinguishes:
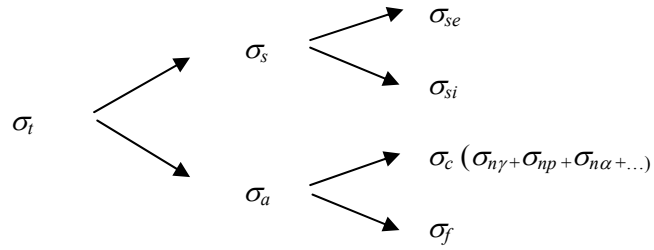
In order to be able to define the concept of the 'microscopic cross section', in the foregoing our starting point was a thin film of atoms. In order to be able to determine the microscopic cross section, transmission measurements are performed on plates of materials. Starting from the presumption that no fission or scattering occurs, the neutron attenuation by a plate with thickness x will be calculated (see Figure 1.8).
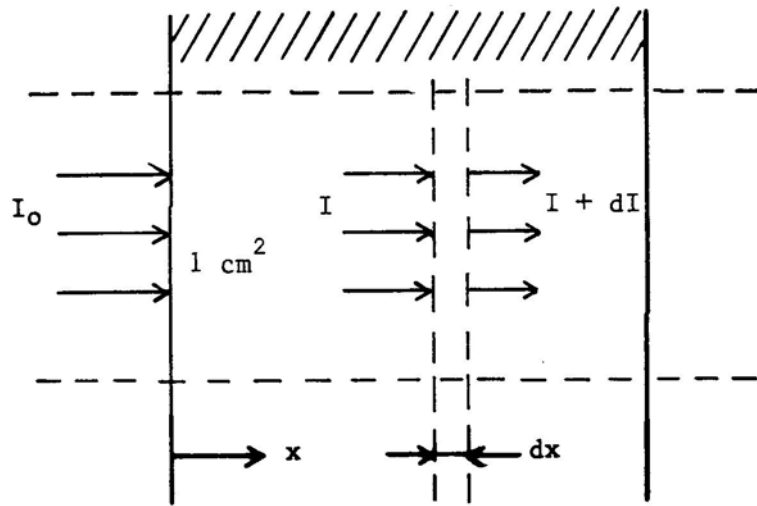
Figure 1.8. Neutron transmission through a plate

Assume that I_0 neutrons per cm^2 and per second perpendicularly strike a plate, the atomic number density of which is N (nuclei per cm^3). Of a layer dx in the plate, the nucleus density per unit area $N_a = Ndx$. Then, according to the definition of the microscopic cross section, the reaction rate per unit area is $N\sigma I(x)dx$. This is equal to the decrease of the beam intensity, so that:

$$-dI = N\sigma I dx \qquad (1.4)$$

Integration gives:

$$I(x) = I_0 e^{-N\sigma x} \qquad (1.5)$$

17

The microscopic cross section σ refers to one nucleus. The product

$$\Sigma = N\sigma \qquad (1.6)$$

refers to one cm^3 of material and is called the macroscopic cross section, which in fact is an incorrect name, because it is not a cross section (dimension L^{-1}). From (1.5) it follows that the probability P(x) that a neutron will travel a distance x in the material concerned without becoming involved in a reaction is:

$$P(x) = e^{-\Sigma x} \qquad (1.7)$$

The probability that a neutron will be involved in a reaction between x and x + dx is equal to Σdx, so that for the mean free path λ of the neutrons it follows that:

$$\lambda = \int_0^\infty x e^{-\Sigma x}\Sigma dx = \frac{1}{\Sigma} \qquad (1.8)$$

whereby one can distinguish λ_s, λ_a, etc. This quantity is also referred to as the *relaxation length*, because it is the distance in which the intensity of the neutrons that have not caused a reaction has decreased with a factor e.

If ρ represents the density of a material with mass number A, then the following holds:

$$N = \frac{\rho}{A} N_A \qquad (1.9)$$

in which N_A is Avogadro's number = $6.022 \cdot 10^{23}$ mol^{-1}. When one has a mixture of nuclei, it holds that:

$$\Sigma_{mixture} = \sum_i N_i \sigma_t \qquad (1.10)$$

in which N_i represents the number of nuclei of the i-th type per cm^3 in the mixture concerned.

1.4. Energy dependence of neutron cross sections

Besides a ground state, atomic nuclei also have higher energy levels, which can be excited. The lowest energy levels of the compound nucleus, which is formed in a neutron-nucleus interaction, are relatively far apart; for medium-weighted nuclei (A = 100 – 150) *circa* 0.1 MeV. The high energy levels become closer and closer to each other. For an excitation energy of about 8 MeV, as is the case after capture of a neutron with low kinetic energy, the separation between the levels is only 1 – 10 eV. Figure 1.9 schematically indicates the position of the energy levels during the formation of a compound nucleus.
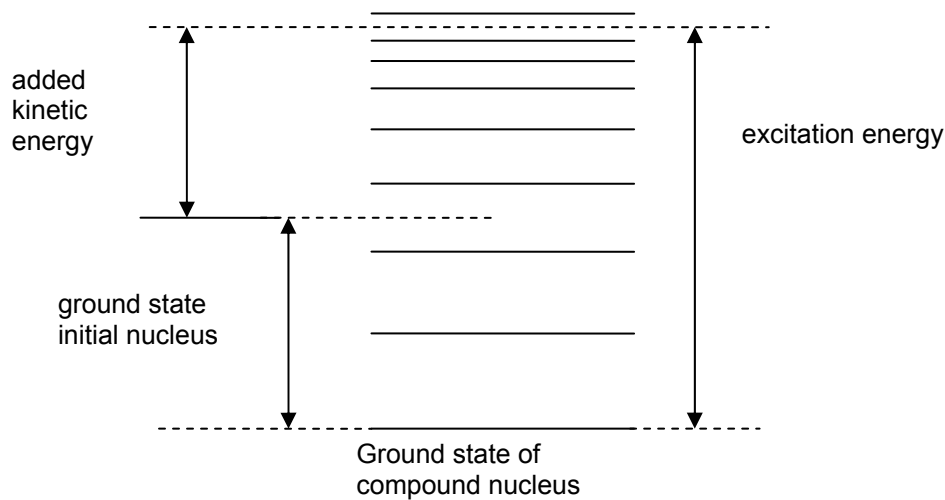
Figure 1.9. Energy diagram of a neutron-nucleus interaction

The energy levels of a nucleus are no sharp 'lines', but show a certain width Γ, which according to the uncertainty principle of Heisenberg is connected with the average time before a nucleus in an excited state decays by emission of a photon or other particle. If there are several decay possibilities for the compound nucleus (emission of a photon, neutron, etc. or fission), we distinguish partial level widths Γ_γ, Γ_n, Γ_f, etc., which summed yield the total level width Γ.

If the excitation energy of the compound nucleus corresponds with one of the level energies, the probability of an interaction is large: resonance occurs. As the excitation energy depends on the kinetic energy of the neutron, the probability of an interaction and thus the microscopic cross section varies strongly with the energy of the neutron. Breit and Wigner, on the ground of quantum-mechanic considerations, have derived the following expression for the microscopic cross section σ_{na} for an interaction whereby the neutron is included in the nucleus and a particle a (possibly the same neutron again) is emitted:

$$\sigma_{na}\left(E\right) = \frac{\lambda^2}{4\pi} \frac{\Gamma_n \Gamma_a}{\left(E - E_r\right)^2 + \left(\Gamma/2\right)^2} \tag{1.11}$$

in which $\lambda = h/mv$ is the de Broglie wavelength of the neutron and E_r the resonance energy. The microscopic cross section shows a maximum if the kinetic energy E of the neutron equals E_r. If $E = E_r \pm \Gamma/2$, the value of the microscopic cross section is halved, so that Γ indicates the width of the resonance peak at half height. As the level widths are often small, the resonance peaks can be very sharp. Figure 1.10 gives an example.
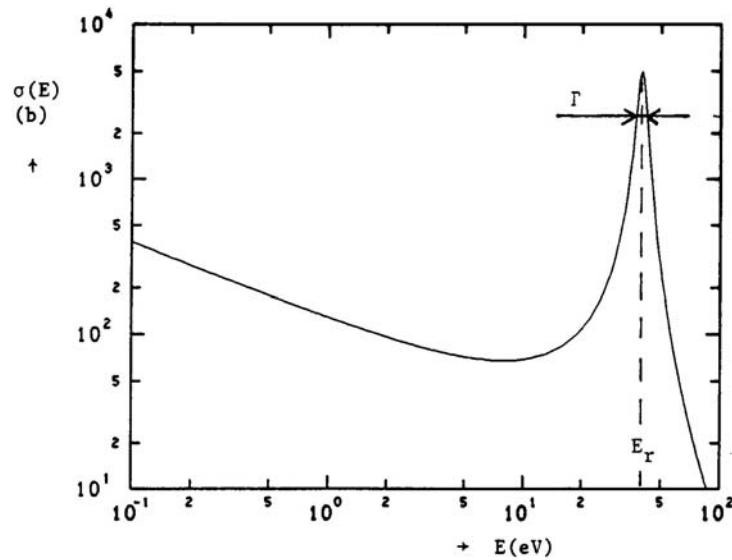
Figure 1.10. Microscopic cross section at a resonance

According as the neutron energy increases, the peak height of the resonance decreases and the resonances become relatively closer to each other, so that they finally cannot be distinguished anymore (see Figure 1.11).
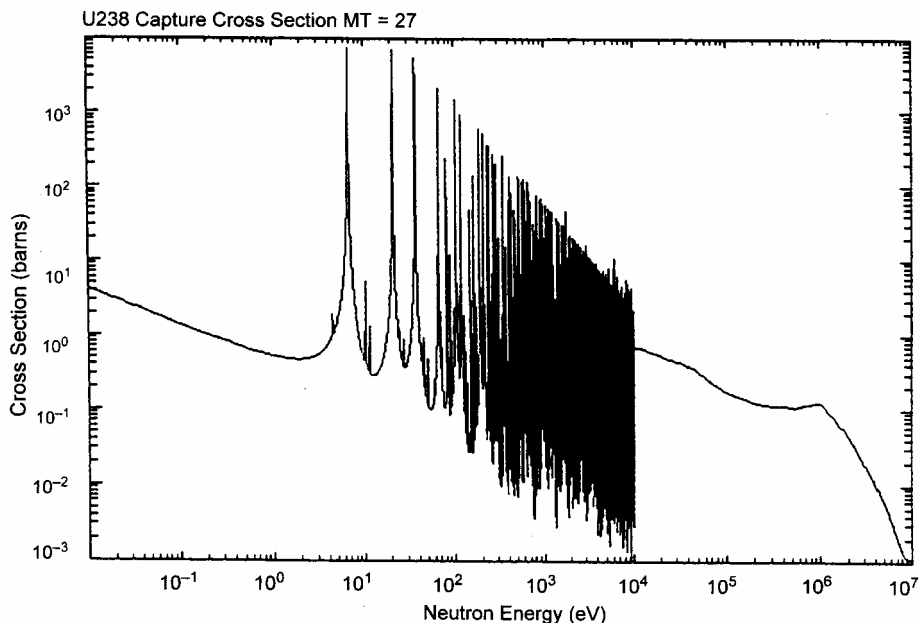
Figure 1.11. Microscopic cross section of a ^{238}U nucleus for neutron capture

For the derivation of the Breit-Wigner equation the starting point is an unmoving nucleus, which is struck by a neutron. In reality the nucleus will also have a kinetic energy as a result of heat movement. This expresses itself in the microscopic cross section, because averaging over the energy distribution of the nuclei must take place. Although the average energy of the nuclei is small, at room temperature 0.025 eV, this averaging still has noticeable consequences for the resonances, because the width of the resonances can be of the same order of magnitude. This leads to broadening of the resonances and lowering of the top value. This so-called Doppler effect is thus temperature dependent and plays an important role in reactors.

The microscopic cross section outside the resonance is also determined by the behaviour of the level widths Γ_n, Γ_γ, … as a function of the neutron energy. The level widths Γ_γ and Γ_f appear to be rather constant, whereas Γ_n increases approximately proportional to $\sqrt{E}$. From this it can be derived that for energies much lower than the lowest resonance energy, the capture and fission cross sections behave as follows

$$\sigma_\gamma, \sigma_f(E) \div \frac{1}{\sqrt{E}} \div \frac{1}{v} \tag{1.12}$$

One finds this '1/v-relation' for many nuclides and it means that the probability of such a reaction is proportional to the time that the incident neutron spends in the proximity of the nucleus.

For scattering, the microscopic cross section decreases sharply outside the resonance, and the so-called potential scattering will predominate, whereby the neutron is scattered by the potential field of the nucleus and does not form a compound nucleus. The potential-scattering cross section is constant over a large energy range, but decreases at high energies. For light nuclides, at low energies chemical-bonding effects can occur, by which the microscopic cross section is larger than that of the free atomic nucleus (e.g. H in H_2O).

In addition to elastic scattering, whereby the total kinetic energy of the particles is conserved, also inelastic scattering can occur. In that case the nucleus remains in an excited state after emission of the neutron and rapidly decays to the ground state under emission of a photon. The incident neutron then must have sufficient energy to be able to excite this level, so that inelastic scattering is a threshold reaction.

Numerical data for microscopic cross sections of many nuclides are available as computer data files (ENDF/B, Evaluated Nuclear Data File or JEF, Joint Evaluated File). The microscopic cross sections for many nuclides and various reactions can be represented graphically by various computer programs making use of these data files.

The energy dependence of the microscopic cross section can be summarised as:

capture and fission   :   1/v + resonances

elastic scattering   :   constant/decreasing + resonances

inelastic scattering   :   threshold reaction; for light nuclides a few MeV,

for heavy nuclides 10 – 100 keV

resonances   :   width Γ_γ, Γ_f constant; $\Gamma_n \div \sqrt{E}$

peak width decreasing with E

for light nuclides $E_r > 1$ MeV,

for heavy nuclides $E_r > 1$ eV

as a result of resonances at very low energy

e.g. 0.1 eV) deviations occur in the 1/v relation

Chapter 2

Neutron transport

2.1. The neutron transport equation

As the free neutrons play an essential part in sustaining the fission reactions in a nuclear reactor, studying the neutron distribution in a reactor is an important part of reactor physics. Generally put the question is: how do the free neutrons distribute themselves in place, energy, time and direction of movement? Hereby not the individual life histories of neutrons are concerned, but the statistical average behaviour of a very large number of neutrons. The mathematical description of the neutron distribution is based on a neutron balance equation, which is called the neutron transport equation. This equation is a linearized form of the Boltzmann equation, known from the kinetic gas theory. Linearization is possible because mutual interactions between neutrons are negligible in nuclear reactors; in other words, the neutron distribution is wholly determined by interactions between neutrons and nuclei of the medium.

The neutron distribution in a system is completely described by the differential neutron density $n(\underline{r},E,\underline{\Omega},t)$, defined as follows:

$n(\underline{r},E,\underline{\Omega},t)dVdEd\Omega$ = number of neutrons at time t in volume element dV, with energy between E and E + dE, which moves in a solid-angle element $d\Omega$ around the direction $\underline{\Omega}$. This quantity is thus a function of seven independent variables: three for the place, one for the energy, two for the direction and one for the time.

Instead of the neutron density, in reactor physics one usually uses the angle-dependent flux density ϕ:

$$\phi(\underline{r},E,\underline{\Omega},t) = n(\underline{r},E,\underline{\Omega},t)v \tag{2.1}$$

in which v is the neutron velocity. This quantity indicates the number of neutrons that, moving in direction $\underline{\Omega}$, passes through a unit area perpendicular to $\underline{\Omega}$ per unit time. Seeing that v is the distance covered per unit time, one can also interpret $\phi = nv$ as the total distance covered per unit volume and per unit time.

As Σ is the probability of interaction per unit path length, from this it follows that the number of interactions per unit volume and per unit time R equals

$$R = \Sigma \phi \qquad (2.2)$$

In reactor physics one often works with differential quantities, whereby for ease of notation's sake no differentiation signs are used, but by omission of variables over which has been integrated it is indicated how far the quantity is still 'differential', such as:

$$\phi(\underline{r},\underline{\Omega},t) = \int_0^\infty \phi(\underline{r},E,\underline{\Omega},t)dE \qquad (2.3)$$

$$\phi(\underline{r},E,t) = \int_{4\pi} \phi(\underline{r},E,\underline{\Omega},t)d\Omega \qquad (2.4)$$

$$\phi(\underline{r},t) = \int_0^\infty \int_{4\pi} \phi(\underline{r},E,\underline{\Omega},t)dEd\Omega = \int_0^\infty \phi(\underline{r},E,t)dE = \int_{4\pi} \phi(\underline{r},\underline{\Omega},t)d\Omega \qquad (2.5)$$

The last quantity $\phi(\underline{r},t)$ is the total neutron flux density, mostly called the flux. It can be interpreted as the number of neutrons per second moving through an imaginary small sphere with a cross section of 1 cm^2.

In order to develop an equation describing the transport of neutrons, we consider an arbitrary volume V, enclosed by a surface S, for which a balance is made. Our starting point is the number of neutrons in V with an energy between E and E + dE and with direction in the solid angle dΩ around $\underline{\Omega}$. This number is equal to

$$\int_V n(\underline{r},E,\underline{\Omega},t)dVdEd\Omega$$

The change of this number in time is the balance of all processes that make this number increase or decrease:

1. increase by the presence of neutron sources, among which fission,
2. increase by scattering of neutrons with other energies and directions to the energy range dE and solid angle dΩ,

3. decrease by net outflow of neutrons (this can also be negative, by which there is a net inflow of neutrons),
4. decrease by neutrons undergoing an interaction.

For the contribution under 1 we define the source strength $S(\underline{r},E,\underline{\Omega},t)$, so that the increase of the neutrons considered is

$$\int_V S(\underline{r},E,\underline{\Omega},t)dVdEd\Omega$$

For the contribution under 2 we introduce the macroscopic differential scattering cross section $\Sigma_s(\underline{r},E'\rightarrow E,\underline{\Omega}'\rightarrow\underline{\Omega})$ so that

$$\Sigma_s(\underline{r},E'\rightarrow E,\underline{\Omega}'\rightarrow\underline{\Omega})dEd\Omega$$

is the probability per path length for scattering of neutrons with energy E' and direction $\underline{\Omega}'$ to an energy between E and E + dE and direction in the solid angle $d\Omega$ around $\underline{\Omega}$. The increase of the number of neutrons then is

$$\int_V\int_0^\infty\int_{4\pi}\Sigma_s(\underline{r},E'\rightarrow E,\underline{\Omega}'\rightarrow\underline{\Omega})\phi(\underline{r},E',\underline{\Omega}',t)dE'd\underline{\Omega}'dVdEd\Omega$$

When calculating the decrease (or increase for a negative result) by net outflow of neutrons, the possibility that the direction $\underline{\Omega}$ of the neutrons need not be the same as that of the normal vector $\underline{n}$ at the surface (see Figure 2.1) must be taken into consideration.
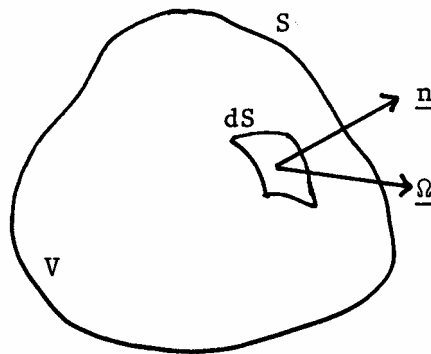
Figure 2.1. Leakage from volume V

The net outflow is now given by

$$\int_S \underline{n}\cdot\underline{\Omega}\,\phi(\underline{r},E,\underline{\Omega},t)dEd\Omega\,dS = \int_V \underline{\nabla}\cdot\underline{\Omega}\,\phi(\underline{r},E,\underline{\Omega},t)dVdEd\Omega$$

where use is made of the divergence theorem of Gauss for the conversion of the surface integral into the volume integral (see Appendix).

The decrease under 4 by all possible interactions is, conformably to (2.2), given by

$$\int_V \Sigma_t(\underline{r},E)\phi(\underline{r},E,\underline{\Omega},t)dVdEd\underline{\Omega}$$

The net result of all these contributions, whereby the first two must be counted positive and the last two negative, is

$$\frac{\partial}{\partial t}\int_V n(\underline{r},E,\underline{\Omega},t)dVdEd\Omega = \int_V S(\underline{r},E,\underline{\Omega},t)dVdEd\Omega$$

$$+ \int_V\int_0^\infty\int_{4\pi} \Sigma_s(\underline{r},E'\to E,\underline{\Omega}'\to\underline{\Omega})\phi(\underline{r},E',\underline{\Omega}',t)dE'd\Omega'dVdEd\Omega \qquad (2.6)$$

$$- \int_V \underline{\nabla}\cdot\underline{\Omega}\phi(\underline{r},E,\underline{\Omega},t)dVdEd\Omega - \int_V \Sigma_t(\underline{r},E)\phi(\underline{r},E,\underline{\Omega},t)dVdEd\Omega$$

This can be reduced to

$$\int_V\left(\frac{1}{v}\frac{\partial\phi(\underline{r},E,\underline{\Omega},t)}{\partial t} - S(\underline{r},E,\underline{\Omega},t) - \int_0^\infty\int_{4\pi}\Sigma_s(\underline{r},E'\to E,\underline{\Omega}'\to\underline{\Omega})\phi(\underline{r},E',\underline{\Omega}',t)dE'd\Omega' \right.$$

$$\left. + \underline{\Omega}\cdot\underline{\nabla}\phi(\underline{r},E,\underline{\Omega},t) + \Sigma_t(\underline{r},E)\phi(\underline{r},E,\underline{\Omega},t)\right)dV = 0 \qquad (2.7)$$

As this equation must hold for each volume V, the integrand of this volume integral must be zero, with which the neutron transport equation is obtained:

$$\frac{1}{v}\frac{\partial\phi(\underline{r},E,\underline{\Omega},t)}{\partial t} = S(\underline{r},E,\underline{\Omega},t) + \int_0^\infty\int_{4\pi}\Sigma_s(\underline{r},E'\to E,\underline{\Omega}'\to\underline{\Omega})\phi(\underline{r},E',\underline{\Omega}',t)dE'd\Omega'$$

$$- \underline{\Omega}\cdot\underline{\nabla}\phi(\underline{r},E,\underline{\Omega},t) - \Sigma_t(\underline{r},E)\phi(\underline{r},E,\underline{\Omega},t) \qquad (2.8)$$

This is the linear integro-differential equation for de angle-dependent neutron flux $\phi(\underline{r},E,\underline{\Omega},t)$, which even for very simple cases is difficult to solve analytically.

Boundary conditions and initial conditions go with this equation. If one considers a convex system placed in vacuum, so that no neutrons can enter the system from outside, then the boundary condition is

$$\phi(\underline{r}_s, E, \underline{\Omega}, t) = 0 \quad for \; \underline{n} \cdot \underline{\Omega} < 0 \tag{2.9}$$

for all points $\underline{r}_s$ at the surface of the system considered. As initial condition, the neutron flux $\phi(\underline{r}, E, \underline{\Omega}, t_0)$ at a certain time t_0 must be specified for all values of $\underline{r}$ in the system and all values of E and $\underline{\Omega}$.

If fission occurs in the system, taking into account the energy distribution $\chi(E)$ of fission neutrons and isotropy during their 'birth', the source as a result of fissions, is given by

$$S_f(\underline{r}, E, \underline{\Omega}, t) = \frac{1}{4\pi} \chi(E) \int_0^\infty \int_{4\pi} \nu(E') \Sigma_f(\underline{r}, E') \phi(\underline{r}, E', \underline{\Omega}', t) dE' d\Omega' \tag{2.10}$$

By integration of the transport equation (2.8) over the direction $\underline{\Omega}$ one could attempt to obtain an equation for the scalar flux $\phi(\underline{r}, E, t)$. The flow term with $\underline{\Omega} \cdot \nabla \phi$ can, however, not be expressed in $\phi(\underline{r}, E, t)$. To this end, we have to introduce the vector quantity $\underline{J}(\underline{r}, E, t)$ according to

$$\underline{J}(\underline{r}, E, t) = \int_{4\pi} \underline{\Omega} \, \phi(\underline{r}, E, \underline{\Omega}, t) d\Omega \tag{2.11}$$

This is called the net neutron flux density because $\underline{n} \cdot \underline{J} \, dS$ indicates the net number of neutrons that flows through a (fixed) surface dS per unit time. Here 'net' means the difference between the number that passes through dS to the side to which the normal vector points and the number that flows to the other side.

Now integration of (2.8) over the direction $\underline{\Omega}$ gives

$$\frac{1}{v} \frac{\partial \phi}{\partial t}(\underline{r}, E, t) + \underline{\nabla} \cdot \underline{J}(\underline{r}, E, t) + \Sigma_t(\underline{r}, E) \phi(\underline{r}, E, t)$$
$$= S(\underline{r}, E, t) + \int_0^\infty \Sigma_s(\underline{r}, E' \to E) \phi(\underline{r}, E', t) dE' \tag{2.12}$$

This balance equation is sometimes called the continuity equation.

2.2. The diffusion equation

In order to arrive at a more convenient equation than (2.8), we look at the case of mono-energetic neutrons. Then the energy-dependence disappears and (2.8) becomes

$$\frac{1}{v}\frac{\partial}{\partial t}\phi(\underline{r},\underline{\Omega},t) + \underline{\Omega}\cdot\underline{\nabla}\phi(\underline{r},\underline{\Omega},t) + \Sigma_t(\underline{r})\phi(\underline{r},\underline{\Omega},t)$$
$$= S(\underline{r},\underline{\Omega},t) + \int_{4\pi}\Sigma_s(\underline{r},\underline{\Omega}'\rightarrow\underline{\Omega})\phi(\underline{r},\underline{\Omega}',t)d\Omega' \qquad (2.13)$$

By integration over $\underline{\Omega}$ we get the mono-energetic form of the continuity equation

$$\frac{1}{v}\frac{\partial}{\partial t}\phi(\underline{r},t) + \underline{\nabla}\cdot\underline{J}(\underline{r},t) + \Sigma_a(\underline{r})\phi(\underline{r},t) = S(\underline{r},t) \qquad (2.14)$$

in which use has been made of $\Sigma_a = \Sigma_t - \Sigma_s$.

Subsequently, we introduce an approximation. We expand the angle-dependent flux $\phi(\underline{r},\underline{\Omega},t)$ to the direction $\underline{\Omega}$ in a series (compare with series expansion in Legendre polynomials; see Appendix) and truncate the series expansion after the second term:

$$\phi(\underline{r},\underline{\Omega},t) = \frac{1}{4\pi}\{\phi(\underline{r},t) + 3\underline{\Omega}\cdot\underline{J}(\underline{r},t)\} \qquad (2.15)$$

By integration over $\underline{\Omega}$ for the left term of this equation one gets $\phi(\underline{r},t)$ and by first multiplying with $\underline{\Omega}$ and subsequently integrating over $\underline{\Omega}$ one obtains $\underline{J}(\underline{r},t)$, which by performing these operations appears to match the right term, so that the series expansion is correct (see Appendix for the integrations).

Multiplication of (2.13) with $\underline{\Omega}$ and integration over $\underline{\Omega}$ now yields

$$\frac{1}{v}\frac{\partial \underline{J}(r,t)}{\partial t} = -\int\underline{\Omega}\left[\underline{\Omega}\cdot\underline{\nabla}\phi(\underline{r},\underline{\Omega},t)\right]d\Omega - \Sigma_t(\underline{r})\underline{J}(\underline{r},t) + \int\underline{\Omega}S(\underline{r},\underline{\Omega},t)d\Omega$$
$$+ \iint\underline{\Omega}\Sigma_s(\underline{r},\underline{\Omega}'\rightarrow\underline{\Omega})\phi(\underline{r},\underline{\Omega}',t)d\Omega'd\Omega \qquad (2.16)$$

By applying the series expansion (2.15), we can write (see also the Appendix)

$$-\int \underline{\Omega}[\underline{\Omega}\cdot\underline{\nabla}\phi(\underline{r},\underline{\Omega},t)]d\Omega = -\frac{1}{4\pi}\int \underline{\Omega}[\underline{\Omega}\cdot\underline{\nabla}\phi(\underline{r},t)]d\Omega - \frac{3}{4\pi}\int \underline{\Omega}[\underline{\Omega}\cdot\underline{\nabla}(\underline{\Omega}\cdot\underline{J})]d\Omega$$

$$= -\frac{1}{3}\underline{\nabla}\phi(\underline{r},t) - \frac{3}{4\pi}\int \underline{\Omega}(\underline{\Omega}\cdot\underline{\Omega}\,\underline{\nabla}\cdot\underline{J})d\Omega \qquad (2.17)$$

$$= -\frac{1}{3}\underline{\nabla}\phi(\underline{r},t) - \frac{3}{4\pi}\underline{\nabla}\cdot\underline{J}\int \underline{\Omega}d\Omega = -\frac{1}{3}\underline{\nabla}\phi(\underline{r},t)$$

for the first term in the right part of (2.16).

If the source S is isotropic, which usually will be the case, the integral over the source strength does not contribute. The term that is determined by scattering of neutrons can, via a laborous derivation, be written as

$$\iint \underline{\Omega}\Sigma_s(\underline{r},\underline{\Omega}'\to\underline{\Omega})\phi(\underline{r},\underline{\Omega}',t)d\Omega'd\Omega = \overline{\mu}_0\Sigma_s(\underline{r})\underline{J}(\underline{r},t) \qquad (2.18)$$

in which $\overline{\mu}_0$ is the average value of the cosine $\mu_0 = \underline{\Omega}\cdot\underline{\Omega}'$ of the scattering angle. In Section 5.2 an expression for $\overline{\mu}_0$ will be derived.

Equation (2.16) now becomes

$$\frac{1}{v}\frac{\partial \underline{J}(r,t)}{\partial t} = -\frac{1}{3}\underline{\nabla}\phi(\underline{r},t) - \Sigma_t(\underline{r})\underline{J}(\underline{r},t) + \overline{\mu}_0\Sigma_s(\underline{r})\underline{J}(\underline{r},t)$$

$$= -\frac{1}{3}\underline{\nabla}\phi(\underline{r},t) - \Sigma_{tr}(\underline{r})\underline{J}(\underline{r},t) \qquad (2.19)$$

with the macroscopic transport cross section Σ_{tr}

$$\Sigma_{tr}(\underline{r}) = \Sigma_t(\underline{r}) - \overline{\mu}_0\Sigma_s(\underline{r}) = \Sigma_a(\underline{r}) + (1-\overline{\mu}_0)\Sigma_s(\underline{r}) \qquad (2.20)$$

In the case of time-dependent problems, in practice the change of the neutron flow $\underline{J}$ appears to be negligible with respect to the other terms in (2.19), so that under the condition

$$\frac{1}{|\underline{J}|}\frac{\partial J}{\partial t} \ll v\Sigma_t$$

It follows from (2.19) that

$$\underline{J}(\underline{r},t) = -\frac{1}{3\Sigma_{tr}(\underline{r})}\underline{\nabla}\phi(\underline{r},t) = -D(\underline{r})\underline{\nabla}\phi(\underline{r},t) \qquad (2.21)$$

29

with which we have found a relationship between the neutron flow $\underline{J}$ and the scalar flux ϕ. At the same time the diffusion coefficient

$$D(\underline{r}) = \frac{1}{3\Sigma_{tr}(\underline{r})} \tag{2.22}$$

has now been defined. Then equation (2.21) has a form that can also be found in particle-diffusion problems. (N.B. The reactor-physical diffusion coefficient has the dimension of length. In other disciplines of physics it is customary to work with particle densities instead of with the flux density, so that in those disciplines a diffusion coefficient has the dimension area per time).

Substitution of (2.21) into (2.14) yields the *diffusion equation*

$$\frac{1}{v}\frac{\partial \phi(r,t)}{\partial t} = \underline{\nabla} \cdot D(\underline{r})\underline{\nabla}\phi(\underline{r},t) - \Sigma_a(\underline{r})\phi(\underline{r},t) + S(\underline{r},t) \tag{2.23}$$

The approximation assumed in order to obtain this result, was that of the limited series expansion of the angle-dependent flux. The diffusion equation can, therefore, not be valid at places with strongly differing properties or in strongly absorbing media. It is apparent that the flux is not allowed to vary sharply over distances in the order of magnitude of a free path length $\lambda_t = 1/\Sigma_t$ of the neutrons. This implies that the diffusion theory may show deviations from a more accurate solution of the transport equation in the proximity of external neutron sources and interfaces.

As an application of the diffusion theory we consider the stationary case of a point source emitting Q neutrons/s in an infinite homogeneous medium. As a result of the spherical symmetry of the system, the diffusion equation gets the form

$$D\left\{\frac{d^2\phi}{dr^2} + \frac{2}{r}\frac{d\phi}{dr}\right\} - \Sigma_a \phi = 0 \qquad r > 0 \tag{2.24}$$

or:

$$\frac{d^2}{dr^2}[r\phi] - \frac{1}{L^2}[r\phi] = 0 \tag{2.25}$$

in which

$$L = \sqrt{D / \Sigma_a} \tag{2.26}$$

is the diffusion length of the neutrons.

The general solution is:

$$\phi(r) = A \frac{e^{-r/L}}{r} + B \frac{e^{r/L}}{r} \tag{2.27}$$

Because that the neutron flux cannot become infinitely large for r → ∞, it follows that B = 0. The remaining constant A can be found by the boundary condition that the neutron flow from a very small sphere around the source must be equal to the source strength:

$$\lim_{r \to 0} \ 4\pi r^2 J(r) = Q \tag{2.28}$$

From this it follows that:

$$\phi(r) = \frac{Q}{4\pi D} \frac{e^{-r/L}}{r} \tag{2.29}$$

On the ground of the physical consideration that all source neutrons must be absorbed in the infinitely large system, it must hold that

$$\int_0^\infty \Sigma_a \ \phi(r)dV = \int_0^\infty \Sigma_a \ \phi(r)4\pi r^2 dr = Q \tag{2.30}$$

Verify this with the found solution ϕ(r).

The physical meaning of the diffusion length can be seen by calculation of the average distance covered by the neutrons, measured in a straight line, until they are absorbed:

$$\bar{r} = \frac{1}{Q} \int_0^\infty r\Sigma_a \ \phi(r)4\pi r^2 dr = 2L \tag{2.31}$$

For thermal neutrons with an energy of 0.025 eV a few values of L are given in Table 2.1.

Table 2.1. Transport quantities for thermal neutrons of 0.025 eV in some materials

Material	Σ_a (cm^{-1})	λ_a (cm)	D (cm)	L (cm)
H_2O	0.022	45.5	0.142	2.54
D_2O	3.3×10^{-5}	30300	0.840	160
Be	1.24×10^{-3}	806	0.416	18.3
C	3.2×10^{-4}	3120	0.916	53.5

The average quadratic distance until absorption is:

$$\overline{r^2} = \frac{1}{Q} \int_0^\infty r^2 \Sigma_a \, \phi(r) 4\pi r^2 dr = 6L^2 \tag{2.32}$$

Therefore, the diffusion length is a measure for the average distance between the place where neutrons are produced and where they are absorbed. This distance must not be confused with the average distance traveled by the neutrons. The latter is equal to the mean free path for absorption $\lambda_a = 1/\Sigma_a$ and is much larger than the distance measured in a straight line, as a result of the 'zigzag' movement of the neutrons.

2.3. Boundary condition

In the diffusion theory. the boundary condition $\phi(\underline{r}_s, \underline{\Omega})=0$ for $\underline{n}\cdot\underline{\Omega} < 0$ cannot be used. A reasonable approximation is to demand that the inwardly directed neutron flow at the surface is zero.

For a one-dimensional rectangular (plate-)geometry there is symmetry about the x-axis. The neutron flow vector $\underline{J}$ will thus always be directed along this axis. so that we can limit ourselves to its magnitude.

The neutron flow in the positive x-direction J_+ is

$$
\begin{aligned}
J_+(x) &= \int_{\underline{n}\cdot\underline{\Omega}>0} \underline{n}\cdot\underline{\Omega}\phi(x,\underline{\Omega})d\Omega \\
&= \frac{1}{4\pi} \int_{\underline{n}\cdot\underline{\Omega}>0} \underline{n}\cdot\underline{\Omega}\phi(x)d\Omega + \frac{3}{4\pi} \int_{\underline{n}\cdot\underline{\Omega}>0} \underline{n}\cdot\underline{\Omega}(\underline{\Omega}\cdot\underline{J})d\Omega \\
&= \frac{1}{4\pi}\phi(x)\int_0^1\int_0^{2\pi} \mu \, d\mu \, d\psi + \frac{3}{4\pi}J(x)\int_0^1\int_0^{2\pi} \mu^2 \, d\mu \, d\psi = \frac{1}{4}\phi(x) + \frac{1}{2}J(x)
\end{aligned}
\tag{2.33}
$$

Similarly, the neutron flow in the negative x-direction (defined as positive quantity!) is

32

$$J_-(x) = \int_{\underline{n}\cdot\underline{\Omega}\langle\langle\rangle 0} |\underline{n}\cdot\underline{\Omega}|\phi(x,\underline{\Omega})d\Omega = \frac{1}{4}\phi(x) - \frac{1}{2}J(x) \qquad (2.34)$$

If we set this equal to zero at an interface x_S with vacuum, then with $J(x) = -D\dfrac{d\phi}{dx}$ we obtain

$$d = \frac{\phi(x)}{-\dfrac{d\phi}{dx}} = 2D = \frac{2}{3\Sigma_{tr}} = \frac{2}{3}\lambda_{tr} \qquad (2.35)$$

for the so-called extrapolation distance (see Figure 2.2) with λ_{tr} the so-called transport free path.
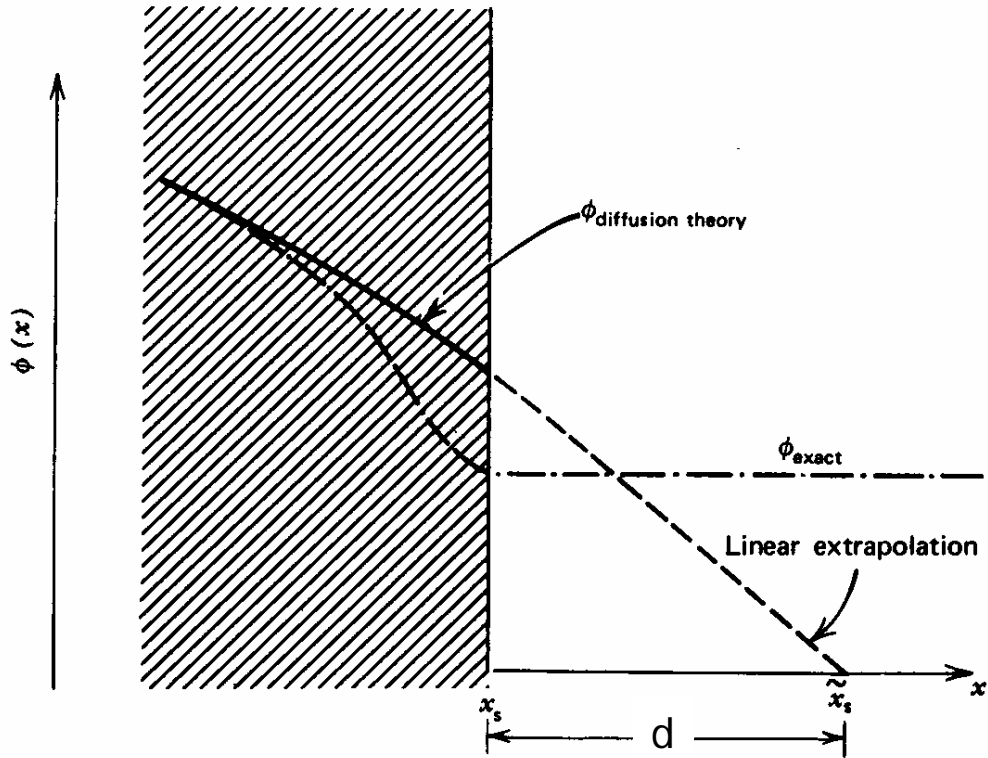
Figure 2.2. Determination of the extrapolation distance

For homogeneous, weakly absorbing media, an exact solution of the mono-energetic transport equation in this case yields

$$d = 0.7104\ \lambda_{tr}$$

so that the result of the diffusion theory is rather good.

Therefore, as practical boundary condition one often uses

$\phi\,(\mathrm{x_S} + 0.71\ \lambda_{\mathrm{tr}}) = 0$

At *interfaces* between two different media, on physical grounds the neutron flux and net neutron flow density must be continuous. In other words, ϕ and J are not allowed to show a 'jump'. As J must be continuous, the flux gradient will show a jump if the diffusion coefficients in both media differ from each other.

Finally, it can be remarked that according to (2.33) and (2.34) it holds that:

$$\text{net flow density} = \mathrm{J_+(x)} - \mathrm{J_-(x)} = \mathrm{J(x)} \tag{2.36}$$

$$\text{total flow density} = \mathrm{J_+(x)} + \mathrm{J_-(x)} = 1/2\ \phi\,(\mathrm{x}) \tag{2.37}$$

This latter quantity gives the number of neutrons flowing through a surface per unit time irrespective the side the neutrons come from. The scalar flux is sometimes confused with the total flux density, but equation (2.37) shows that these quantities differ by a factor two in the case of isotropic or linearly anisotropic fluxes.

Chapter 3

Reactor analysis with diffusion theory

In this chapter we will inspect how the neutron distribution is in a nuclear reactor and which conclusions we can draw about sustaining the chain reaction in the reactor. We will confine ourselves to mono-energetic neutrons or a one-group approximation, whereby one can consider all neutrons to belong to one (energy) group.

3.1. One-group diffusion theory

The one-group diffusion equation (2.23) with a source as a result of fissions

$$S(\underline{r},t) = v\Sigma_f(\underline{r})\phi(\underline{r},t) \tag{3.1}$$

reads

$$\underline{\nabla} \cdot D(\underline{r})\underline{\nabla}\phi(\underline{r},t) + v\Sigma_f(\underline{r})\phi(\underline{r},t) - \Sigma_a(\underline{r})\phi(\underline{r},t) = \frac{1}{v}\frac{\partial\phi}{\partial t} \tag{3.2}$$

with associated boundary and initial conditions.

The time-dependent behaviour of a neutron population in a multiplying system (*i.e.* a system in which fissions take place) will depend on the ratio between the production term on the one hand and the absorption and leakage terms on the other hand in the left hand side of (3.2). If the production term predominates, the neutron population will increase, and in the reversed case it will decrease. When production and losses exactly balance, the neutron flux will be constant in time; in that case one speaks of a critical reactor. Only then one may set the time derivative in (3.2) equal to zero.

Also for a non-critical reactor one wants to have a measure for the production, absorption and leakage of neutrons from the reactor being out of balance, without having to solve a time-dependent diffusion equation, because the exact time-dependent behaviour is the result instead of the cause for this balance. One can obtain a steady-state equation artificially by adjusting the source term in (3.2). Physically this means that one makes the system seemingly critical by a (fictive) change in neutron production per fission. Mathematically this yields an eigenvalue equation with eigenvalue k:

$$\underline{\nabla} \cdot D(\underline{r}) \underline{\nabla} \phi(\underline{r}) + \frac{\nu}{k} \Sigma_f(\underline{r}) \phi(\underline{r}) - \Sigma_a(\underline{r}) \phi(\underline{r}) = 0 \tag{3.3}$$

The eigenvalue has been placed in the denominator of the production term, because by that it gets an important physical meaning, which can be seen as follows. Integration over the volume of the reactor gives

$$k = \frac{\int\limits_V \nu \Sigma_f(\underline{r}) \phi(\underline{r}) dV}{-\int\limits_V \underline{\nabla} \cdot D(\underline{r}) \underline{\nabla} \phi(\underline{r}) dV + \int\limits_V \Sigma_a(\underline{r}) \phi(\underline{r}) dV} \tag{3.4}$$

With the aid of the divergence theorem of Gauss, the first integral in the denominator can be transformed into:

$$-\int\limits_V \underline{\nabla} \cdot D(\underline{r}) \nabla \phi(\underline{r}) dV = -\int\limits_S D(\underline{r}) \underline{n} \cdot \underline{\nabla} \phi(\underline{r}) dS = \int\limits_S \underline{n} \cdot \underline{J}(\underline{r}) dS \tag{3.5}$$

in which S is the outer surface of the reactor and $\underline{n}$ the local unit normal vector to the surface. The integral thus equals the total neutron leakage from the reactor. Equation (3.4) now has a simple physical meaning; in words:

$$k = \frac{total\ neutron\ production\ rate\ by\ fissions}{total\ neutron\ loss\ rate\ by\ leakage\ and\ absorption} \tag{3.6}$$

This factor, which is important in reactor physics, is called the effective multiplication factor k_{eff}.

The physical events in a reactor can be considered as a coming and going of successive neutron generations, whereby the fission processes are considered as moments of birth. The multiplication factor k_{eff} then gives the ratio of the neutron population size in two successive generations. if the flux is spatially distributed according to the eigenvalue distribution that is the solution of (3.3).

In order to arrive at an analytically solvable equation, we will assume that the reactor is homogeneous, *i.e.* that the macroscopic cross sections are space independent. This is the case if the materials are homogeneously mixed or in the trivial case that only one material is present. In general, reactors will have a heterogeneous structure, *i.e.* contain regions of different composition (nuclear fuel, construction material, moderator, coolant, control rods, etc.). If the dimensions of the regions of different compositions are small in comparison with the mean free

path of the neutrons, the reactor can neutron-physically be considered approximately homogeneous.

For homogeneous systems (3.3) can be written as:

$$\nabla^2 \phi(\underline{r}) + B^2 \phi(\underline{r}) = 0 \tag{3.7}$$

with

$$B^2 = \frac{\nu\Sigma_f / k - \Sigma_a}{D} \tag{3.8}$$

One can thus see this quantity, defined as the eigenvalue of (3.7), as a type of eigenvalue different from the multiplication factor k, with which a direct correlation exists according to (3.8).
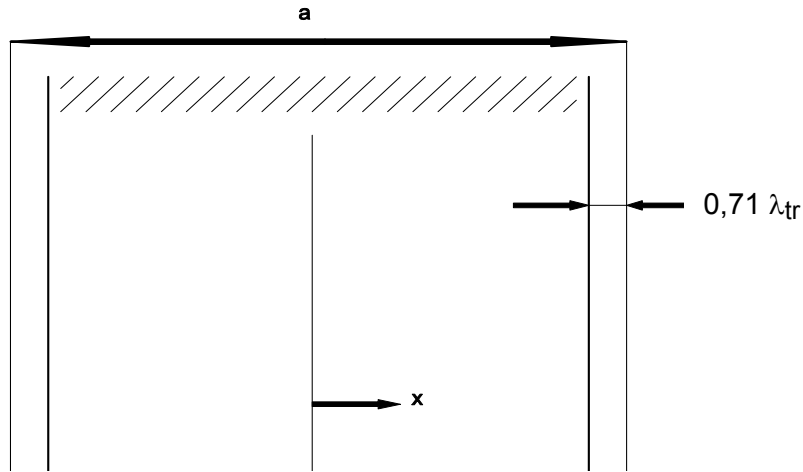
Figure 3.1. Infinite-plate reactor

For the geometrically most simple case, a slab reactor with extrapolated width a and infinite in both other directions (Figure 3.1), the equation becomes:

$$\frac{d^2\phi}{dx^2} + B^2 \phi(x) = 0 \tag{3.9}$$

The solution satisfying the symmetry condition with respect to x = 0 is:

$$\phi(x) = A \cos Bx \tag{3.10}$$

In order to satisfy the boundary condition ($\phi = 0$ at the extrapolated edge x = ± a/2), the following must hold

$$B^2 = \left(\frac{\pi}{a}\right)^2 \tag{3.11}$$

We see that the eigenvalue B^2 is exclusively dependent on the geometry (shape + dimensions) of the reactor. According to (3.7):

$$B^2 = -\frac{\nabla^2 \phi(\underline{r})}{\phi(\underline{r})} \tag{3.12}$$

so B^2 indicates the curvature or buckling of the flux in the reactor. Therefore, B^2 is also called the geometric buckling factor B_g^2. Table 3.1 gives the solution of equation (3.7) for a number of geometries; the associated flux distributions are shown in Figure 3.2. The eigenfunctions have been normalized to the value 1 at the origin. Notice that the coefficient A from (3.10) is undetermined, because the solution of (3.7) or (3.9) can be multiplied by an arbitrary factor.

Table 3.1. Buckling factors for various geometries
(the dimensions are extrapolated dimensions)

Geometry	B^2	$\varphi(\underline{r})$	(minimum) volume at given B^2
infinite plate (thickness a)	$\left(\frac{\pi}{a}\right)^2$	$\cos \pi \frac{x}{a}$	–
rectangular parallel-epipedum (edges a,b,c)	$\left(\frac{\pi}{a}\right)^2 + \left(\frac{\pi}{b}\right)^2 + \left(\frac{\pi}{c}\right)^2$	$\cos \pi \frac{x}{a} \cos \pi \frac{y}{b} \cos \pi \frac{z}{c}$	$\dfrac{161}{B^3}$
sphere (radius R)	$\left(\frac{\pi}{R}\right)^2$	$\dfrac{\sin \pi \frac{r}{R}}{\pi \frac{r}{R}}$	$\dfrac{130}{B^3}$
cylinder	$\left(\frac{\pi}{H}\right)^2 + \left(\frac{2.405}{R}\right)^2$	$J_0\left(2.405 \frac{r}{R}\right) \cos \pi \frac{z}{H}$	$\dfrac{148}{B^3}$

With the aid of (3.7) for a homogeneous reactor it can be derived from (3.4) that:

$$k_{eff} = \frac{\nu \Sigma_f}{\Sigma_a + DB_g^2} = \frac{\nu \Sigma_f}{\Sigma_a} \frac{1}{1 + DB_g^2 / \Sigma_a} = \frac{k_\infty}{1 + B_g^2 L^2} \tag{3.13}$$
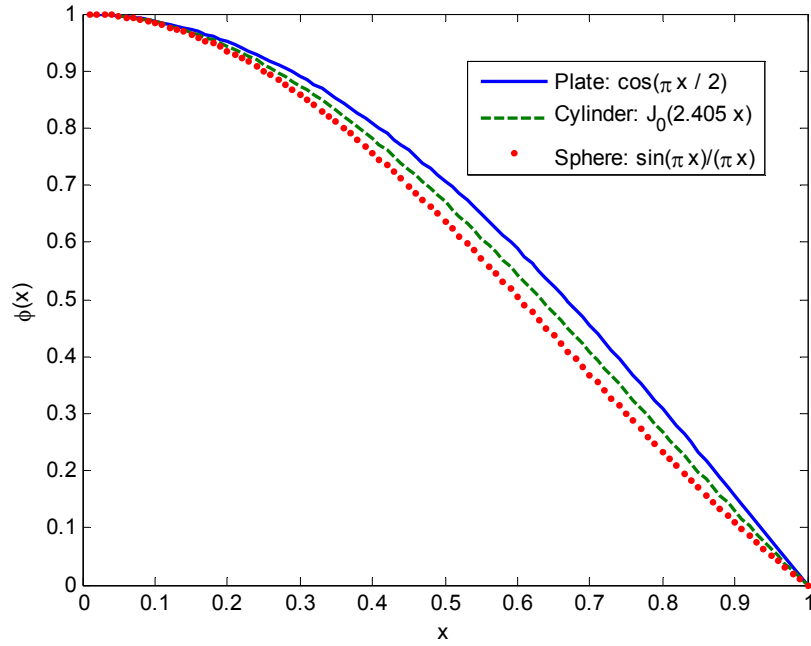
Figure 3.2. Flux distribution in systems of three different geometries

in which

$$k_\infty = \nu \frac{\Sigma_f}{\Sigma_a} \qquad (3.14)$$

is the multiplication factor of an infinitely large, so leakage free, reactor and

$$L = \sqrt{D/\Sigma_a} \qquad (3.15)$$

is the diffusion length of the neutrons. The result (3.13) could also have been derived directly from (3.8).

The difference between k_∞ and k_{eff} is the leakage of neutrons from the reactor, so that according to (3.13)

$$P_{n1} = \frac{1}{1 + B_g^2 L^2} \qquad (3.16)$$

is the non-leakage probability or retention factor, *i.e.* the probability that neutrons produced during fission do not leak from the reactor but are absorbed in it.

In addition to the geometric buckling factor B_g^2, one also has defined the material buckling factor B_m^2, which exclusively depends on the material composition of the reactor core:

$$B_m^2 = \frac{\nu\Sigma_f - \Sigma_a}{D} = \frac{k_\infty - 1}{L^2} \tag{3.17}$$

From (3.3) one sees that only for a critical reactor (or a subcritical reactor with source, but for positions outside the source region) it holds that

$$\Delta^2\phi(\underline{r}) + B_m^2\,\phi(\underline{r}) = 0 \quad k = 1 \tag{3.18}$$

One also sees that for a critical reactor it must hold that

$$B_g^2 = B_m^2 \tag{3.19}$$

After calculation of k_∞ and L^2 one can thus simply calculate the critical dimensions for a given shape of the reactor core.

For illustration of the foregoing we will perform some calculations on a sphere of highly enriched (*circa* 93%) uranium. The atomic number densities for this case are:

$$N(^{235}U) = 0.04545 \cdot 10^{24} \text{ cm}^{-3}$$
$$N(^{238}U) = 0.00256 \cdot 10^{24} \text{ cm}^{-3}$$

As the fission neutrons in the uranium only lose a little energy as a result of collisions, this will be a so-called fast reactor, in which also fission by ^{238}U occurs. The parameters for the one-group calculation are given in Table 3.2.

Table 3.2. Parameters for one-group calculation

Nuclide	ν	σ_f (b)	σ_c (b)	σ_{tr} (b)
^{235}U	2.6	1.34	0.159	6.8
^{238}U	2.6	0.215	0.112	6.9

The multiplication factor k_∞ amounts to:

$$k_\infty = \frac{N_5 v_5 \sigma_{f5} + N_8 v_8 \sigma_{f8}}{N_5 \sigma_{a5} + N_8 \sigma_{a8}} = 2.317$$

while the diffusion length is:

$$L = \sqrt{D/\Sigma_a} = \frac{1}{\sqrt{3\Sigma_{tr}\Sigma_a}} = 3.846 \text{ cm}$$

so that for the material buckling factor we find:

$$B_m^2 = \frac{k_\infty - 1}{L^2} = 0.0890 \text{ cm}^{-2}$$

For a critical system this factor must be equal to the geometric buckling factor, as indicated in Table 3.1. The extrapolated radius of a critical sphere is thus:

$$R_{extr} = \frac{\pi}{B_g} = \frac{\pi}{B_m} = 10.53 \text{ cm}$$

Then the real radius, making use of the extrapolation distance $0.71\lambda_{tr}$ amounts to:

$$R_{crit} = R_{extr} - 0.71\lambda_{tr} = 8.361 \text{ cm}$$

which for a density of metallic uranium of 18.75 g/cm^3 corresponds with a critical mass of 45.8 kg.

The measured critical mass of such a system amounts to 48.8 kg, so that our result is rather accurate. As the one-group model used here is a rough approximation, this accuracy is owing to the fact that the parameters given in Table 3.2 have been calculated accurately with the aid of a multi-group model, which we will go further into later.

There exist more solutions than (3.11) of the eigenvalue problem (3.9) that satisfy the boundary conditions, *viz.*

$$B_n^2 = \left(\frac{n\pi}{a}\right)^2 \qquad n = 1,3,5,... \tag{3.20}$$

with associated eigenfunctions

$$\phi_n(x) = A_n \cos n\pi \frac{x}{a} \qquad n = 1, 3, 5, \ldots \tag{3.21}$$

A series of eigenvalues k_i (i=1.2.…) corresponds with these solutions. The eigenfunction ϕ_1 is called the fundamental mode and the associated eigenvalue $k_1 = k_{eff}$. Further, $B_g^2 = B_1^2$, so that we can define the geometric buckling factor more precisely as the smallest eigenvalue of (3.7) and k_{eff} as the largest eigenvalue of (3.3). As the higher eigenfunctions for certain values of x are negative, these flux shapes do not have a meaning of their own. As the eigenfunctions are mutually orthogonal, *i.e.*

$$\int \phi_n(x)\phi_m(x)dx = 0 \quad for\ m \neq n \tag{3.22}$$

the flux in the reactor as a result of an arbitrary source distribution can be written as a series of these eigenfunctions. Also in transition phenomena in time-dependent processes the higher eigenfunctions and eigenvalues play a part (due to the smaller values of the corresponding multiplication factor they die out fast and they will not be further discussed here).

3.2. Multi-zone systems

A reactor core may consist of various zones of different composition. The consequence of this is that the material buckling factor, and therefore, the flux curvature, will vary per zone.
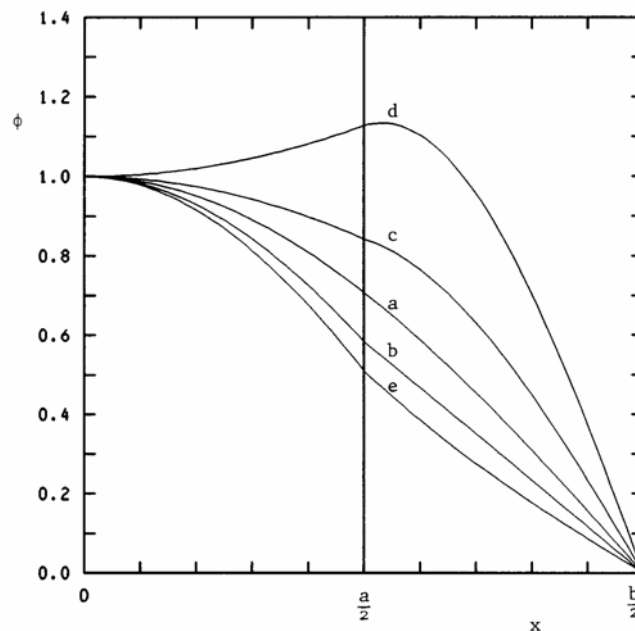
Figure 3.3. Flux as a function of x in a two-zone reactor;
material buckling factors as in Table 3.3

Figure 3.3 illustrates this for a slab reactor with two zones. From this figure one sees that by variation of B_m^2 flux flattening can be obtained with respect to a single-zone system. To this end, the B_m^2 in the centre of the core is made lower (for example by a lower degree of enrichment and by that a lower k_∞) than in the exterior zones. Such flattening gives a more uniform power density distribution, by which a higher total power can be supplied without exceeding certain temperature limits.

Table 3.3. Material buckling factors for a two-zone system

	B_{m1}^2	B_{m2}^2
a	$\dfrac{9.870}{b^2}$	$\left(\dfrac{\pi}{b}\right)^2 = \dfrac{9.870}{b^2}$
b	$\dfrac{14.40}{b^2}$	$\left(0.2\dfrac{\pi}{b}\right)^2 = \dfrac{0.395}{b^2}$
c	$\dfrac{5.19}{b^2}$	$\left(1.75\dfrac{\pi}{b}\right)^2 = \dfrac{30.23}{b^2}$
d	$-\dfrac{4.00}{b^2}$	$\dfrac{44.83}{b^2}$
e	$\dfrac{17.18}{b^2}$	$-\dfrac{16.00}{b^2}$

For the determination of the flux distribution in both zones of a critical reactor, the diffusion equations in zone 1 and zone 2 need to be solved:

$$D_1\nabla^2\phi_1 - \Sigma_{a1}\phi_1 + \nu\Sigma_{f1}\phi_1 = 0 \qquad |x|\le\frac{a}{2} \tag{3.23}$$

$$D_2\nabla^2\phi_2 - \Sigma_{a2}\phi_2 + \nu\Sigma_{f2}\phi_2 = 0 \qquad \frac{a}{2}\le|x|\le\frac{b}{2} \tag{3.24}$$

with a the real width of zone 1 and b the outer dimension of the reactor including the extrapolation distance (see Figure 3.4).
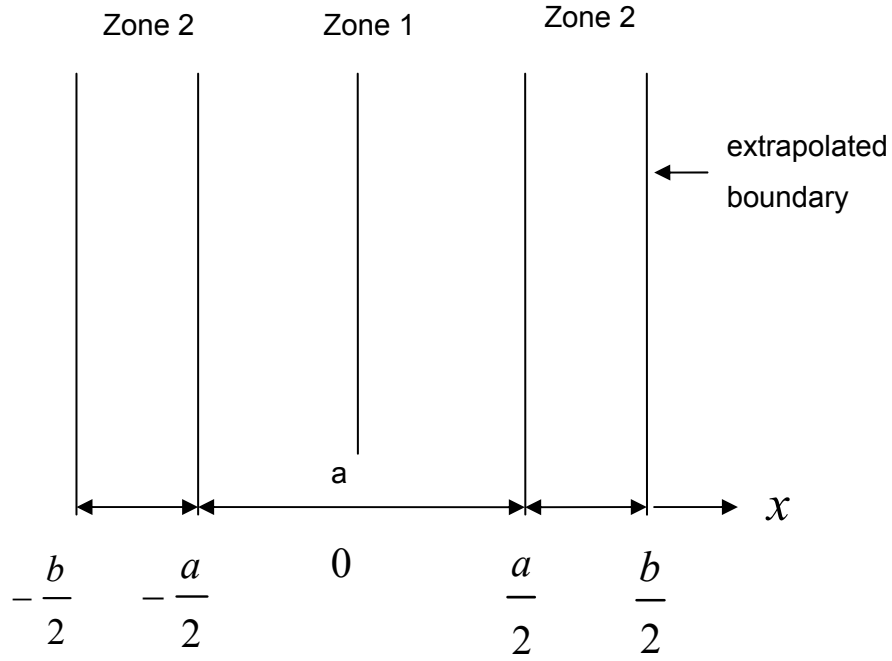
Figure 3.4. Geometry for plate-shaped two-zone reactor

.

The boundary and interface conditions are

$$\frac{d\phi_1(0)}{dx} = 0 \qquad\qquad \text{due to symmetry} \qquad\qquad (3.25)$$

$$\phi_1\left(\frac{a}{2}\right) = \phi_2\left(\frac{a}{2}\right) \qquad\qquad \text{due to continuity of the flux} \qquad\qquad (3.26)$$

$$J_1\left(\frac{a}{2}\right) = J_2\left(\frac{a}{2}\right) \qquad\qquad \text{due to continuity of the neutron current} \qquad (3.27)$$

$$\phi_2\left(\frac{b}{2}\right) = 0 \qquad\qquad \text{boundary condition for vacuum edge} \qquad (3.28)$$

The diffusion equations for zones 1 and 2, with the material buckling factors B_{m1}^2 and B_{m2}^2 according to (3.17), can also be written as

$$\nabla^2\phi_1(x) + B_{m1}^1\phi_1(x) = 0 \qquad\qquad (3.29)$$

$$\nabla^2\phi_2(x) + B_{m2}^2\phi_2(x) = 0$$

44

with solutions

$$\phi_1(x) = A_1 \cos B_{m1}x + C_1 \sin B_{m1}x \tag{3.31}$$

$$\phi_2(x) = A_2 \cos B_{m2}x + C_2 \sin B_{m2}x \tag{3.32}$$

As the flux in a reactor without external source can only be determined to within an arbitrary factor, we choose $A_1 = 1$. Because of the symmetry condition $C_1 = 0$, so that

$$\phi_1(x) = \cos B_{m1}x \tag{3.33}$$

From boundary condition (3.28), after some rewriting it follows that ϕ_2 can be written as

$$\phi_2(x) = C_2' \; \sin B_{m2}\left(\frac{b}{2} - x\right) \tag{3.34}$$

From condition (3.26) C'_2 can be determined:

$$\phi_2(x) = \frac{\cos B_{m1}\dfrac{a}{2}}{\sin B_{m2}\left(\dfrac{b-a}{2}\right)} \sin B_{m2}\left(\frac{b}{2} - x\right) \tag{3.35}$$

With condition (3.27) no other coefficient can be determined (even A_1 could not have been determined with this condition). Application of this condition and some manipulation leads to

$$D_1 B_{m1} \tan B_{m1} \frac{a}{2} = D_2 B_{m2} \cotg B_{m2}\left(\frac{b-a}{2}\right) \tag{3.36}$$

This is the condition that must be satisfied for a critical reactor, in which dimensions of the reactor are coupled to the material properties. For the two-zone reactor, this critical equation replaces condition (3.19) for the single-zone reactor. For the situations depicted in Figure 3.3 it has been assumed that $b = 2a$. Situation a, with $B_{m1}^2 = B_{m2}^2$ and $D_1 = D_2$, is the transition into a single-zone reactor. For the remaining situations $D_1 = 0.75\ D_2$ has been chosen, so that the

derivative of the flux is discontinuous at the interface. For situations b and c, B_{m2}^2 was chosen and B_{m1}^2 was calculated from (3.36).

For situation d, B_{m2}^2 was chosen negative. This case occurs if $k_\infty < 1$. Notice that the flux in zone 1 then is concave. This can also be described mathematically with (3.35) by setting $B_{m1} = iB'_{m1}$ and applying the relations $\sin(iy) = i\sinh(y)$ and $\cos(iy) = \cosh(y)$. The critical equation then becomes

$$-D_1 B'_{m1} \tanh B'_{m1} \frac{a}{2} = D_2 B_{m2} \, cotg \, B_{m2}\left(\frac{b-a}{2}\right) \tag{3.37}$$

Finally, in situation e the reactor core in zone 1 is surrounded by a non-multiplying medium, a so-called reflector. For this case, according to one-group diffusion theory the following holds:

$$B_{m2}^2 = -\frac{1}{L_2^2} = -\kappa_2^2 \tag{3.38}$$

with $\kappa_2 = 1/L_2$, by which the flux in zone 2 is concave. By placing such a neutron reflector around the core, one decreases the critical mass. The critical equation becomes

$$D_1 B_{m1} \tan B_{m1} \frac{a}{2} = D_2 \kappa_2 \, coth \, \kappa_2\left(\frac{b-a}{2}\right) = D_2 \kappa_2 \, coth \, \kappa_2 T \tag{3.39}$$

with T the thickness of the reflector. In order to give a measure for the savings as a result of the use of a reflector, one introduces the concept of reflector savings δ:

$$\delta = \frac{1}{2}a_0 - \frac{1}{2}a \tag{3.40}$$

in which a_0 is the extrapolated dimension of a critical slab reactor for a non-reflected core, so that

$$\delta = \frac{\pi}{2B_{m1}} - \frac{1}{2}a \tag{3.41}$$

Now

46

$$\tan B_{m1}\,\delta = \tan\left(\frac{\pi}{2} - \frac{1}{2}B_{m1}a\right) = \cotg\frac{1}{2}B_{m1}a = \frac{D_1 B_{m1}}{D_2\kappa_2}\tanh\kappa_2 T \qquad (3.42)$$

so that

$$\delta = \frac{1}{B_{m1}}\arctan\left(\frac{D_1 B_{m1}}{D_2\kappa_2}\tanh\kappa_2 T\right) \qquad (3.43)$$

With this equation one can calculate the reflector savings as a function of the reflector thickness T. Figure 3.5 shows the relation between δ and T.
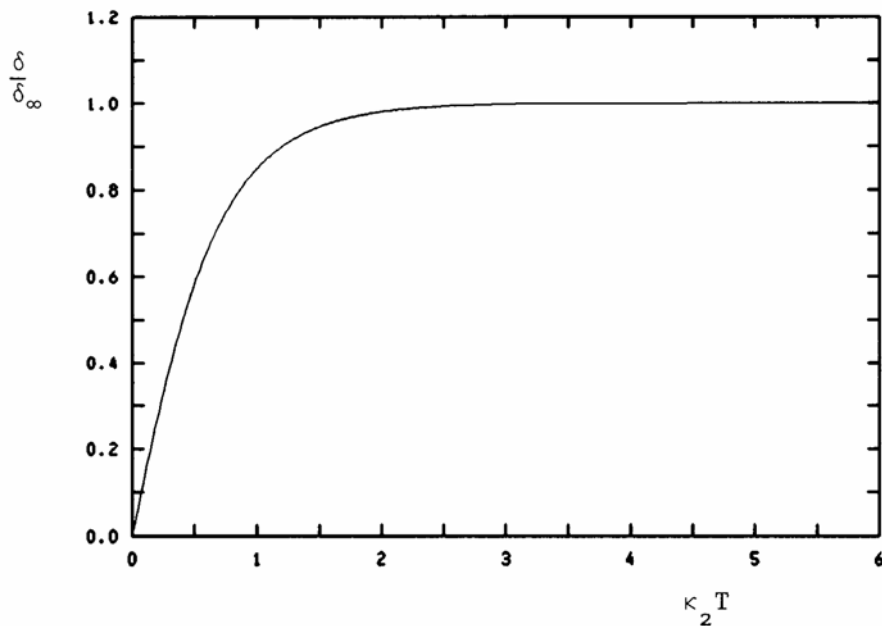
Figure 3.5. Reflector savings as a function of reflector thickness

One sees that the reflector savings has a finite value for $\kappa_2 T \to \infty$ equal to

$$\delta_\infty = \frac{1}{B_{m1}}\arctan\frac{D_1 B_{m1}}{D_2\kappa_2} \qquad (3.44)$$

Physically this can be understood as follows: when the reflector has a thickness of a few diffusion lengths, the probability that neutrons that have come into the outer shell of the reflector are scattered back to the core is very small, so that an even thicker reflector hardly yields extra savings. For a good reflector one will select material with a large scattering cross section and a small absorption cross section.

3.3. Perturbation theory

The purpose of perturbation theory is to calculate the influence of small changes in the macroscopic cross sections on the multiplication factor of a reactor. Our starting point is a critical reactor, for which holds that:

$$\underline{\nabla} \cdot D(\underline{r})\underline{\nabla}\phi(\underline{r}) + \nu\Sigma_f(\underline{r})\phi(\underline{r}) - \Sigma_a(\underline{r})\phi(\underline{r}) = 0 \tag{3.45}$$

in which the macroscopic cross sections may be space dependent. A change of the macroscopic cross sections gives a diffusion equation for a non-critical reactor with multiplication factor k:

$$\underline{\nabla} \cdot (D + \delta D)\underline{\nabla}\phi' + \frac{\nu}{k}(\Sigma_f + \delta\Sigma_f)\phi' - (\Sigma_a + \delta\Sigma_a)\phi' = 0 \tag{3.46}$$

in which the indication of spatial dependence has been omitted for the sake of brevity. We multiply (3.45) by ϕ' and (3.46) by ϕ, integrate over the reactor volume and subtract the resulting equations from each other, and then calculate the **reactivity** ρ:

$$\rho = \frac{k-1}{k} = \frac{\int\{\phi\underline{\nabla}(D + \delta D)\underline{\nabla}\phi' - \phi'\underline{\nabla} \cdot D\underline{\nabla}\phi + \nu\delta\Sigma_f\,\phi\phi' - \delta\Sigma_a\phi\phi'\}dV}{\int \nu(\Sigma_f + \delta\Sigma_f)\phi\phi'dV} \tag{3.47}$$

The first two terms in the numerator of the right hand side of (3.47) can be reduced to

$$\int\phi\underline{\nabla}\cdot(D+\delta D)\underline{\nabla}\phi'\,dV - \int\phi'\underline{\nabla}\cdot D\underline{\nabla}\phi\,dV =$$

$$\int\underline{\nabla}\cdot(D+\delta D)\phi\underline{\nabla}\phi'\,dV - \int(D+\delta D)\underline{\nabla}\phi\cdot\underline{\nabla}\phi'\,dV -$$

$$\int\underline{\nabla}\cdot D\phi'\underline{\nabla}\phi\,dV + \int D\underline{\nabla}\phi'\cdot\underline{\nabla}\phi\,dV =$$

$$\int\underline{n}\cdot(D+\delta D)\phi\underline{\nabla}\phi'dS - \int\underline{n}\cdot D\phi'\underline{\nabla}\phi dS - \int\delta D\underline{\nabla}\phi\cdot\underline{\nabla}\phi'dV =$$

$$-\int\delta D\underline{\nabla}\phi\cdot\underline{\nabla}\phi'dV$$

because of the boundary condition $\phi = \phi' = 0$ at the boundary of the system, by which the surface integrals do not contribute. The reactivity can now be written as

$$\rho = \frac{\int \left\{ -\delta D \underline{\nabla}\phi \cdot \underline{\nabla}\phi' + \nu\delta\Sigma_f \,\phi\phi' - \delta\Sigma_a \phi\phi' \right\} dV}{\int \nu \left(\Sigma_f + \delta\Sigma_f \right) \phi\phi' dV} \tag{3.48}$$

As a first-order approximation, for small disturbances one may assume $\phi' = \phi$, while $\delta\Sigma_f$ in the denominator then also can be neglected with respect to Σ_f (notice that in the numerator only perturbation terms are present so that $\delta\Sigma_f$ cannot be neglected there), with which the reactivity according to first-order perturbation theory becomes

$$\rho = \frac{\int \left\{ -\delta D \left(\underline{\nabla}\phi \right)^2 + \left(\nu\delta\Sigma_f - \delta\Sigma_a \right)\phi^2 \right\} dV}{\int \nu\Sigma_f \,\phi^2 dV} \tag{3.49}$$

From (3.49) we see that the reactivity change by a small change in Σ_a or Σ_f is proportional to the square of the flux at the position of the change; a small change in D is weighted with $(\underline{\nabla}\phi)^2$.
For a cosine-shaped flux we obtain the clock-shaped curves in Figure 3.6 as the importance function for perturbations. As is to be expected physically, changes in Σ_a have the largest effect in the core centre, whereas changes in the diffusion coefficient have a large influence at the edge of the core.
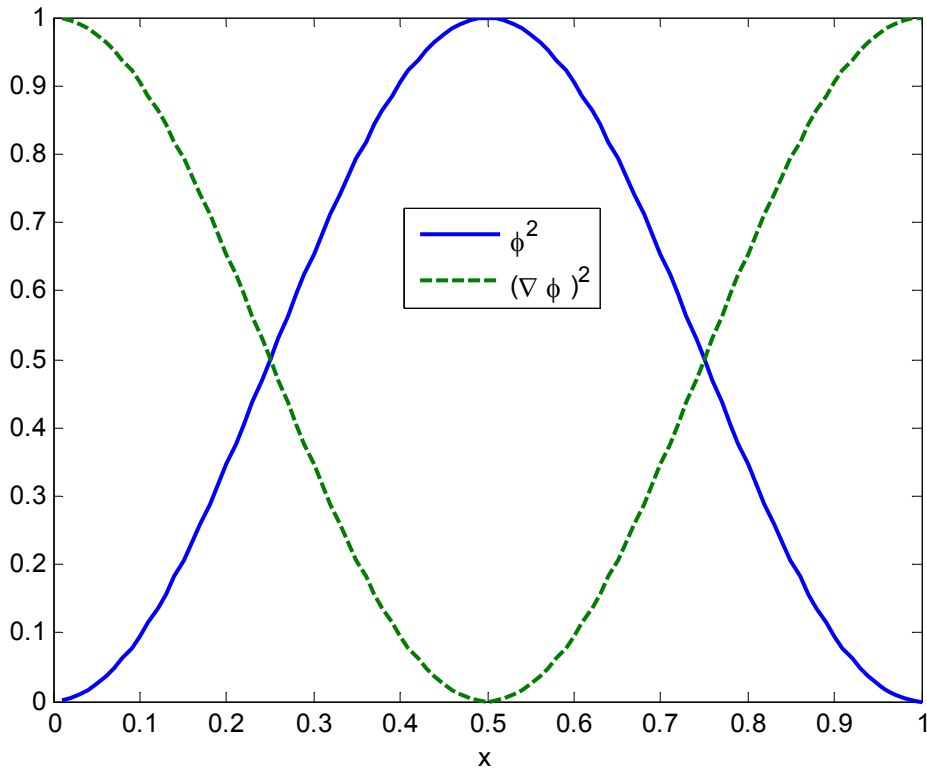
Figure 3.6. Space-dependent importance function in a reactor

Chapter 4

Time-dependent behaviour of reactors

4.1. Introduction

In the preceding chapter, reactors have been analysed by introducing the multiplication factor as eigenvalue and with that forcing a steady-state equation. In this chapter, amongst other things it will be investigated how the neutron flux changes if k_{eff} is not equal to one. The value of k_{eff} can be changed, for example, by moving control rods into or out of the reactor core. When starting up a reactor, one uses this for increasing the flux and with that the power. Hereby we speak of reactor kinetics in the 'seconds domain'. When the reactor generates sufficient power, the temperature in the reactor will change as a function of the power. The effects thereof will be treated qualitatively. During operation of the reactor the composition of the nuclear fuel will gradually change as a result of:

1. consumption of nuclear fuel (burnup)
2. formation of new nuclear fuel by conversion of fertile material
3. formation of fission products

If one wants to maintain a stationary energy production, it will be necessary to compensate for the influence of these effects by, for example, adjusting the control rods. The first two effects take place at a time scale of months/years. The influence of the fission products, which lead to extra absorption of neutrons, can be split into:

1. the effects of xenon and samarium poisoning, which manifest themselves on a time scale of hours/days
2. the gradual build-up of long-lived or stable fission products on a time scale of months/years.

4.2. Simple description of reactor kinetics

We can obtain a simplified solution of the time-dependent diffusion equation (3.2) by assuming that the reactor has a homogeneous composition and that the spatial and time dependence can be separated:

$$\phi(\underline{r},t) = \phi(t)\psi(\underline{r}) \tag{4.1}$$

By substitution into (3.2), the space dependent part $\psi(\underline{r})$ satisfies the eigenvalue equation (3.7)

$$\nabla^2\psi(\underline{r}) + B_g^2\psi(\underline{r}) = 0 \tag{4.2}$$

For the time-dependent part then follows that

$$\frac{1}{v}\frac{d\phi}{dt} = v\Sigma_f\,\phi(t) - \Sigma_a\phi(t) - DB_g^2\phi(t) \tag{4.3}$$

We now define the neutron lifetime ℓ as the average time between the appearance of the free neutron and its disappearance by absorption or leakage. For an infinitely large, so leakage-free, reactor the lifetime ℓ_∞ becomes the ratio of the absorption mean free path and the velocity:

$$\ell_\infty = \frac{\lambda_a}{v} = \frac{1}{v\Sigma_a} \tag{4.4}$$

For a reactor of finite dimensions leakage will occur, so that the lifetime ℓ_∞ must be multiplied by the non-leakage probability P_{nl}, given by (3.16):

$$\ell = \ell_\infty P_{nl} = \frac{1}{v\Sigma_a\left(1 + B_g^2 L^2\right)} \tag{4.5}$$

We can now rewrite the time-dependent equation (4.3) as

$$\begin{aligned}
\frac{d\phi}{dt} &= v\Sigma_a\left\{v\Sigma_f/\Sigma_a - \left(1 + B_g^2 L^2\right)\right\}\phi(t) \\
&= v\Sigma_a\left(1 + B_g^2 L^2\right)\left(k_{eff} - 1\right)\phi(t) = \frac{k_{eff} - 1}{\ell}\phi(t)
\end{aligned} \tag{4.6}$$

One obtains an even simpler derivation of this equation by introducing the concept of neutron generation. A neutron generation 'lives' a lifetime ℓ, after which it disappears and produces a new generation. One can now interpret k_{eff} as the ratio of the number of neutrons in two successive generations. If at a certain moment N neutrons are present, then in the next generation there will be k_{eff}·N neutrons, while all neutrons of the previous generation have disappeared. As this happens in lifetime ℓ, the following holds for the net change of the number of neutrons per unit time:

52

$$\frac{dN}{dt} = \frac{k_{eff}\, N - N}{\ell} = \frac{k_{eff} - 1}{\ell}\, N(t)$$ (4.7)

As the flux is proportional to the number of neutrons, this equation corresponds with (4.6). Its solution is

$$N(t) = N_0 \exp\left\{\frac{k_{eff} - 1}{\ell}\, t\right\}$$ (4.8)

with N_0 the number of neutrons at t = 0. For k_{eff} = 1 one obtains a stationary number of neutrons. If $k_{eff} \neq 1$ the number of neutrons will increase or decrease exponentially with time.

A representative value for the lifetime ℓ in a thermal reactor is 10^{-4} to 10^{-3} s. In a fast reactor, the lifetime of neutrons will be considerably shorter, because although Σ_a is smaller, the average velocity v is much larger than in a thermal reactor. In this type of reactor ℓ will amount to 10^{-7} to 10^{-6} s. One can easily verify that in a thermal reactor with k_{eff} = 1.001 and ℓ equal to 10^{-4} s, per second a power increase by a factor e^{10} = 22000 would occur. A reactor with such a response to a small change in k_{eff} would be difficult to control, but fortunately nature comes to aid. In the major part of the fissions the fission neutrons will directly (promptly) be emitted. However, almost 1 % only is released during the decay of certain fission products. These are so-called *delayed neutrons*. An example of this is given in Figure 4.1.
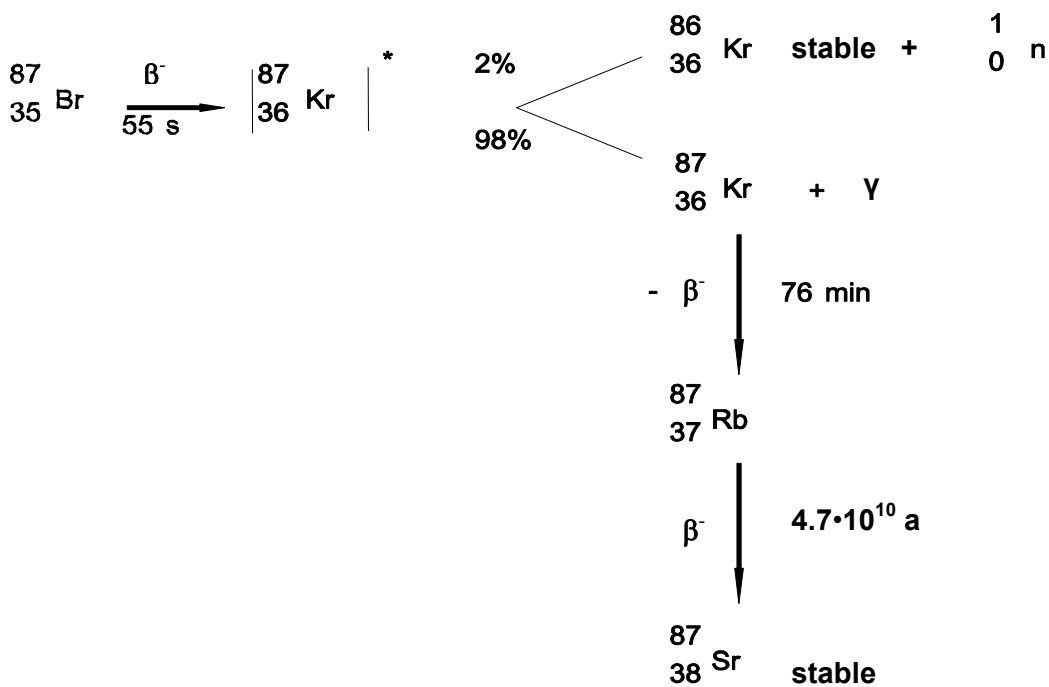
Figure 4.1. Decay scheme with emission of a delayed neutron

As the delayed neutrons will immediately be emitted by the highly excited nuclei, they will be released with a half-life that is equal to the half-life for β decay of the so-called precursors or parent nuclei (^{87}Br in the example of Figure 4.1). On the whole, there are some tens of precursors of delayed neutrons among the fission products. Their half-lifes can be grouped into six so-called delayed-neutron groups, each with a characteristic half-life $T_{1/2}$ and yield β_i, which denotes the fraction of the total neutron production per fission in which a precursor from the group concerned is formed.

Table 4.1. Data of delayed neutrons (yields are for thermal fission)

Group i	$T_{1/2}$ (s)	λ (s^{-1})	β_i (%)		
			^{233}U	^{235}U	^{239}Pu
1	55	0.0127	0.0255	0.0260	0.0081
2	22	0.0317	0.0811	0.1459	0.0594
3	6.0	0.115	0.0672	0.1288	0.0458
4	2.2	0.311	0.0938	0.2788	0.0695
5	0.50	1.40	0.0216	0.0877	0.0218
6	0.18	3.87	0.0068	0.0178	0.0074
		β	0.296	0.685	0.212
		$\overline{\lambda} = \beta / \sum_i \dfrac{\beta_i}{\lambda_i}$	0.0839	0.0784	0.0652 s^{-1}

The total fraction of delayed neutrons $\beta = \Sigma \beta_i$ varies from nuclide to nuclide (Table 4.1) and is also somewhat dependent on the energy of the neutrons causing the fissions. The average energy of the delayed neutrons amounts to about 0.5 MeV and is thus considerably lower than that of the prompt neutrons. For not too large values of k_{eff} these delayed neutrons cause the 'effective lifetime' of the neutrons to be considerably larger than their real lifetime as a result of the 'birth delay' of part of the neutrons. A first approximation for the effective lifetime is

$$\ell_{eff} = \sum_i \beta_i t_i + \ell \tag{4.9}$$

in which β_i = fraction of delayed neutrons of group i

        t_i = average time between fission and release of the neutrons of group i,

          for which thus holds that:

$$t_i = \frac{\int_0^\infty t \cdot e^{-\lambda_i t} \, dt}{\int_0^\infty e^{-\lambda_i t} \, dt} = \frac{1}{\lambda_i} \tag{4.10}$$

From Table 4.1 it follows that $\sum_i \beta_i t_i \approx 0.1\,\mathrm{s}$ for ^{235}U; as ℓ is much smaller, ℓ_{eff} is completely determined by the delayed neutrons. Using the same calculation example as before, now for the reactor period (*i.e.* the time in which the reactor power increases by a factor e) it thus holds that $T = 10^{-1}/10^{-3} = 100$ s. This makes the reactor much more attractive for the control technician. In general, reactors are started up with a period of 30 s or more. When the period becomes much smaller (by making k_{eff} larger) the power increases too fast to guarantee a reliable start-up from a technical and safety point of view.

4.3. Reactor kinetics with delayed neutrons

For a more accurate description of the time-dependent behaviour of a reactor, the production of neutrons by decay of precursors must be included in the description. For the neutron balance equation this means that in (3.2) the production term $\nu\Sigma_f\phi$ must be replaced by the production of prompt neutrons, which is a factor $1-\beta$ smaller, while the neutrons released by decay of precursors must be added. If the concentration of precursors of group i of delayed neutrons is denoted by C_i, the equation becomes

$$\frac{1}{v}\frac{\partial \phi}{\partial t} = \underline{\nabla} \cdot D\underline{\nabla}\phi(\underline{r},t) - \Sigma_a \phi(\underline{r},t) + (1-\beta)\nu\Sigma_f \phi(\underline{r},t) + \sum_i \lambda_i C_i(\underline{r},t) + S \tag{4.11}$$

The balance equation for the precursors is determined by the formation of these nuclei by fission and by their decay

$$\frac{\partial C_i}{\partial t} = \beta_i \nu\Sigma_f \, \phi(\underline{r},t) - \lambda_i C_i(\underline{r},t) \quad i = 1,...,6 \tag{4.12}$$

Again with the assumption of separation of spatial and time dependence, also for the precursor concentration, we can reduce (4.11) to:

$$\frac{l}{v}\frac{d\phi}{dt} = \frac{k(1-\beta)-1}{\ell}\frac{1}{v}\phi(t) + \sum_i \lambda_i C_i(\underline{r},t) + S \tag{4.13}$$

55

By transition to the neutron density $n = \phi / v$ and introduction of the neutron generation time Λ

$$\Lambda = \frac{\ell}{k} = \frac{1}{vv\Sigma_f}$$

(4.14)

and using the reactivity $\rho = (k-1)/k$ we obtain the kinetic equations

$$\frac{dn}{dt} = \frac{\rho - \beta}{\Lambda} n(t) + \sum_i \lambda_i C_i(t) + S$$

(4.15)

$$\frac{dC_i}{dt} = \frac{\beta_i}{\Lambda} n(t) - \lambda_i C_i(t) \quad i = 1, ..., 6$$

(4.16)

We now consider a reactor without external source. The system of coupled first-order differential equations can be solved with Laplace transformation or by trying the solution

$$n(t) = n_0 \, e^{\omega t}$$

(4.17)

$$C_i(t) = C_{i0} e^{\omega t}$$

(4.18)

with ω to be determined. Substitution in (4.16) gives the relation between the coefficients of the neutron density and the precursors

$$C_{i0} = \frac{1}{\Lambda} \frac{\beta_i}{\omega + \lambda_i} n_0$$

(4.19)

Substitution in (4.15) subsequently yields an equation for ω, which after some manipulation can be written as

$$\rho = \omega \Lambda + \sum_i \frac{\omega \beta_i}{\omega + \lambda_i}$$

(4.20)

This equation is known as the inhour equation, because ω was originally determined in inverse hours. For a given value of the reactivity ρ the associated values of ω are determined with this equation. Figure 4.2 shows the relation between ρ and ω graphically. From this figure it is seen that for a given value of ρ seven solutions exist for ω.

56
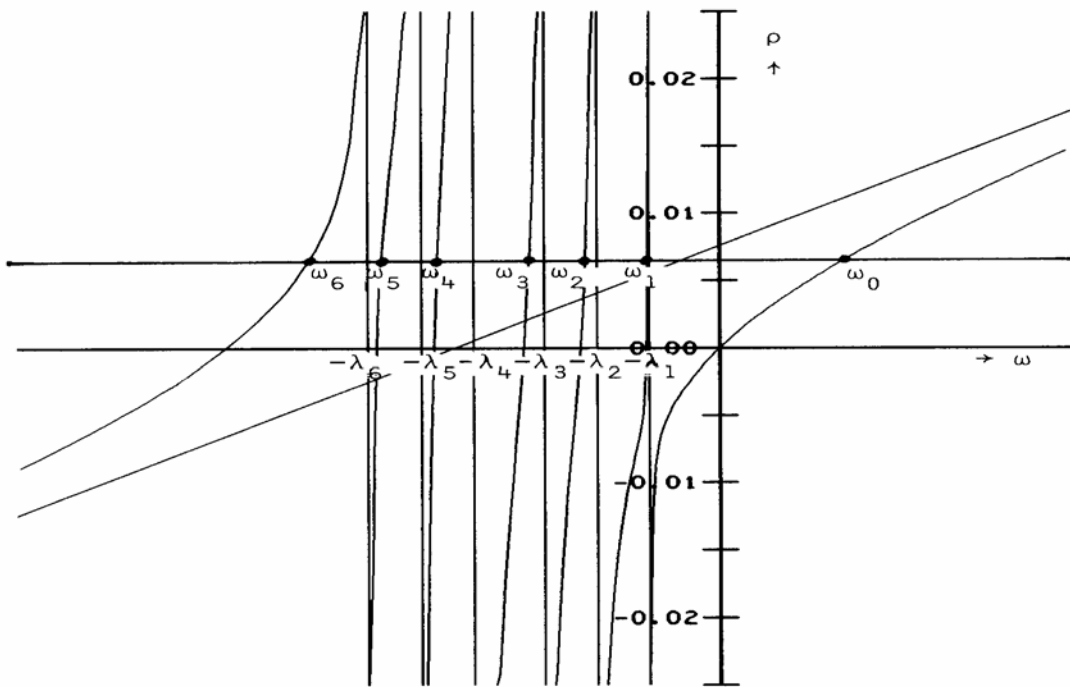
Figure 4.2. Graphical representation of the inhour equation

The fact that there exists more than one solution for ω means that the neutron density as solution of the kinetic equations can be written as

$$n(t) = A_0 e^{\omega_0 t} + A_1 e^{\omega_1 t} + ... + A_6 e^{\omega_6 t} \tag{4.21}$$

and an analogous solution for the precursor concentration. The coefficients A_i are determined by the initial conditions.

Of the seven roots for ω, six are always negative; these thus describe a transition phenomenon. The root with the algebraically largest value (ω_0) is positive for $\rho > 0$ and negative for $\rho < 0$; this root thus describes the reactor response, which is lasting after the transition phenomena have died out. The reactor power then increases or decreases with the so-called stable reactor period, for which holds that

$$T = \frac{1}{\omega_0} \tag{4.22}$$

The reactivity of a reactor is sometimes expressed in dollars, whereby $\rho(\$) = \rho / \beta$. When the reactivity is larger than one dollar (the absolute value of which depends on the nuclear fuel applied!), the prompt neutrons alone already cause a supercritical state; the reactor then is prompt-supercritical and the stable reactor period is very short; a situation that must be avoided.
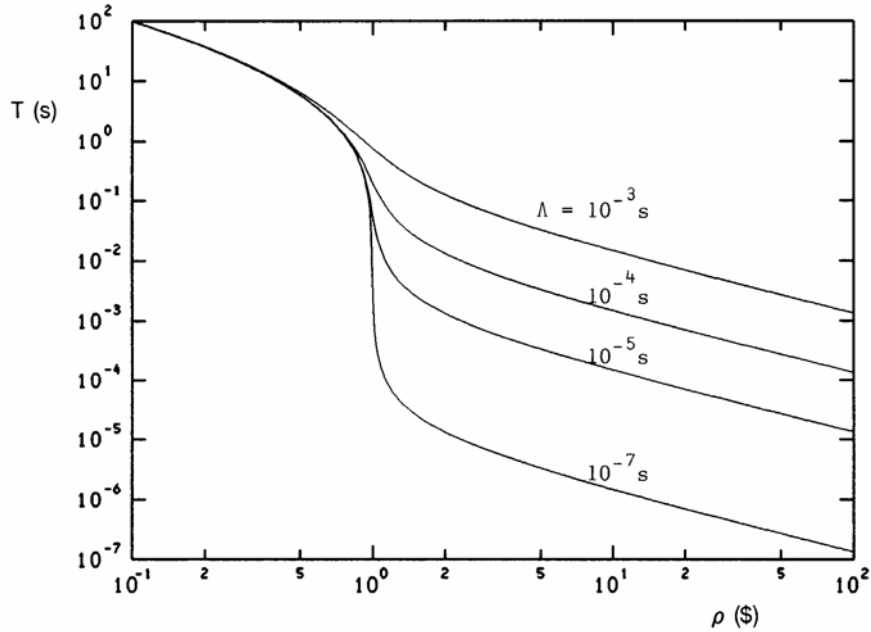
Figure 4.3. Stable reactor period as a function of the reactivity for a number of values of the generation time

Figure 4.3 depicts the stable reactor period as a function of ρ for a number of values of the generation time Λ. One sees that for reactivity values below $ 0.5 the stable period is independent of the generation time.

In order to obtain further insight in the reactor-kinetic behaviour, one can simplify the kinetic equations by assuming that all delayed neutrons belong to one group with a suitably chosen half-life λ. The inhour equation (4.20) then becomes:

$$\rho = \omega\Lambda + \frac{\omega\beta}{\omega + \lambda} \tag{4.23}$$

in which λ is chosen in such a way that for small values of ω (*i.e.* $|\omega| < \lambda_i$ for all i) the solution of (4.23) approximates the solution of (4.20). For small ω (4.20) becomes:

$$\rho \approx \omega\Lambda + \omega \sum_i \frac{\beta_i}{\lambda_i} \tag{4.24}$$

from which upon comparison with (4.23) for small ω it follows that:

$$\frac{1}{\lambda} = \frac{1}{\beta} \sum_i \frac{\beta_i}{\lambda_i} \tag{4.25}$$

The values of λ calculated in this way are also given in Table 4.1 for a number of nuclear fuels. The inhour equation now becomes a second-order equation

$$\Lambda\,\omega^2 + (\beta - \rho + \lambda\Lambda)\,\omega - \rho\lambda = 0 \tag{4.26}$$

Except in the case that $\rho \approx \beta$, the term $\lambda\Lambda$ can be neglected with respect to $\beta - \rho$. If we limit ourselves to small values of ρ, then we can expect a small and a large (negative) value of ω as solutions, which can be approximated by

$$\omega_0 \approx \frac{\rho\,\lambda}{\beta - \rho} \tag{4.27}$$

$$\omega_1 \approx -\frac{\beta - \rho}{\Lambda} \tag{4.28}$$

so that the general solution of the kinetic equations becomes:

$$n(t) = A_0 e^{\frac{\rho\,\lambda}{\beta - \rho}t} + A_1\,e^{-\frac{\beta - \rho}{\Lambda}t} \tag{4.29}$$

For a critical reactor in which at t=0 a step-shaped reactivity insertion takes place, one must set the following initial conditions:

$$n(0) = n_0 = A_0 + A_1 \tag{4.30}$$

$$\lim_{t \downarrow 0} \frac{dn}{dt} = \frac{\rho}{\Lambda}\,n_0 \tag{4.31}$$

This latter condition follows from (4.15), in which n(t) and C(t) must be continuous at t=0. The steady-state value of C_i for t<0 follows from (4.16) by equating the derivative to zero, so that

$$C_{i0} = \frac{\beta_i}{\Lambda \lambda_i} n_0 \qquad (4.32)$$

Applying the same approximation leading to (4.27) and (4.28), it follows that

$$n(t) = n_0 \left\{ \frac{\beta}{\beta - \rho} e^{\frac{\rho \lambda}{\beta - \rho} t} - \frac{\rho}{\beta - \rho} e^{-\frac{\beta - \rho}{\Lambda} t} \right\} \qquad (4.33)$$

After a positive reactivity insertion the power thus increases almost immediately with a factor $\beta/(\beta - \rho)$ (the so-called prompt jump), because the second term dies out very rapidly, after which it gradually increases further with the reactor period $(\beta - \rho)/\rho\lambda$. Therefore, the stable reactor period is determined by the delayed neutrons, while the slope of the prompt jump is determined by the generation time of the prompt neutrons.

Figures 4.4 and 4.5 depict the flux as a function of time for positive and negative reactivity steps. For example, one sees that after a reactivity addition of $ 0.3 the flux almost immediately increases with *circa* 40 % and then increases further with a relatively long period ($\approx$ 30 s).

For $\rho > \beta$, the second term in the right hand side of (4.33) yields a positive contribution that increases very rapidly in consequence of the short generation time Λ: the reactor is prompt-supercritical.

Physically, the prompt jump can be understood by thinking in terms of multiplication of neutrons. The multiplication M of a multiplying system is understood to mean the average of the total number of neutrons in successive generations after introducing one neutron into the system, *i.e.*

$$M = 1 + k_{eff} + k_{eff}^2 + ... = \frac{1}{1 - k_{eff}} \qquad (4.34)$$

Of course this quantity only has meaning if $k_{eff} < 1$, so for subcritical systems. For a reactor that is not prompt-supercritical, one can define the *prompt multiplication*, *i.e.* the multiplication via prompt neutrons only:

$$M = 1 + k_{eff} (1 - \beta) + k_{eff}^2 (1 - \beta)^2 + ...$$
$$= \frac{1}{1 - k_{eff} (1 - \beta)} = \frac{1}{k_{eff}} \frac{1}{\beta - \rho} \approx \frac{1}{\beta - \rho} \qquad (4.35)$$

For a critical reactor ($\rho = 0$) the prompt multiplication is $1/\beta$, which for a reactor with ^{235}U as nuclear fuel results in a value of *circa* 150, *i.e.* on average each neutron produces a chain of 150

neutrons. After dying out of such a chain, which happens in a short time because of the short generation time Λ, the emission of a delayed neutron is necessary in order to initiate a new chain.
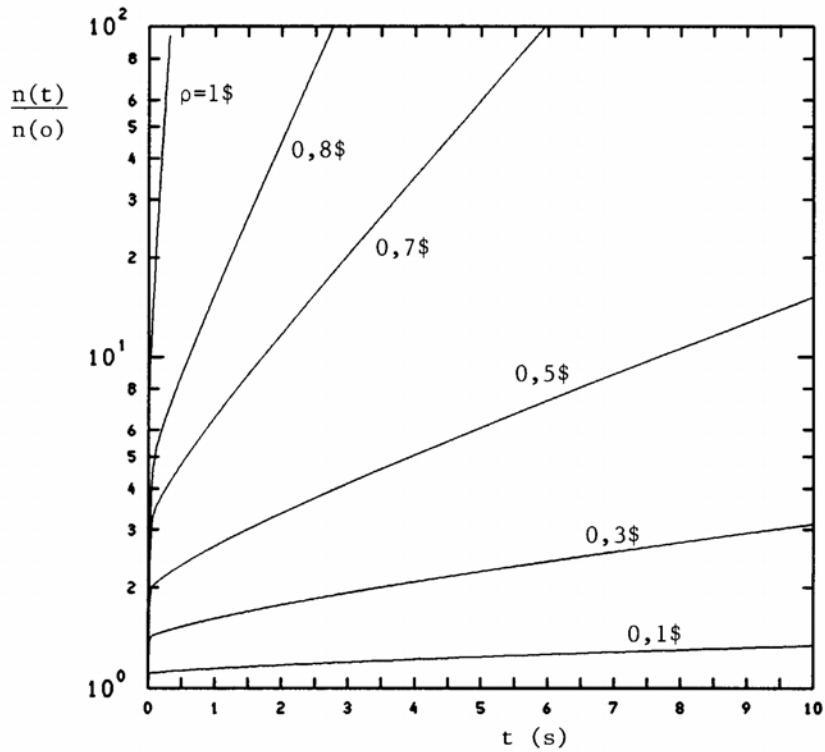
Figure 4.4. Reactor response after a positive reactivity step
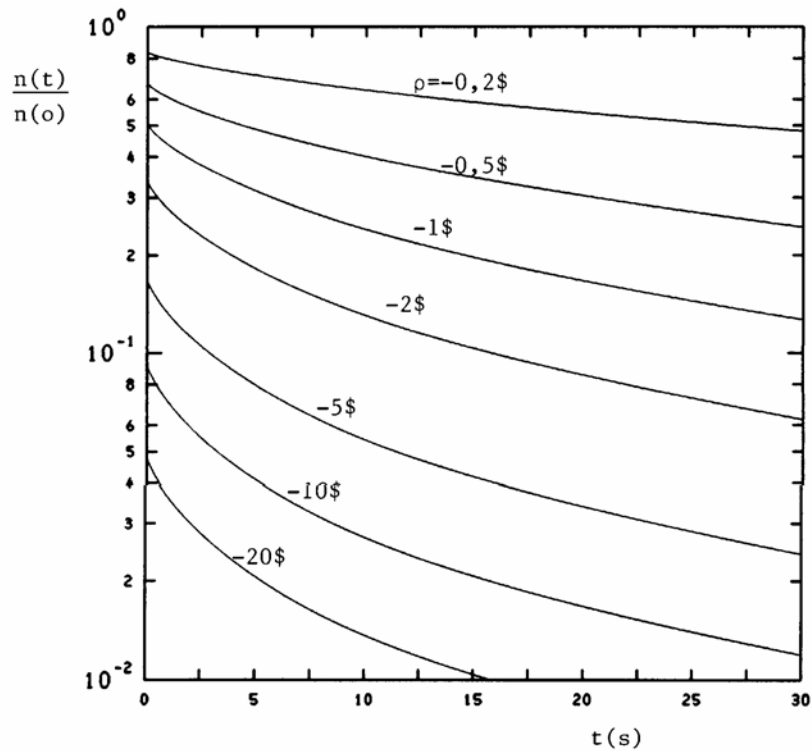
Figure 4.5. Reactor response after a negative reactivity step

After the reactivity change, the prompt multiplication is given by (4.35), so that the prompt multiplication increases or decreases by a factor $\beta / (\beta - \rho)$.

When introducing a large negative reactivity, as in the case of stopping a reactor by inserting all of the control rods into the core, the stable reactor period is almost equal to the inverse decay constant of the longest-living group of delayed neutrons, *i.e.* about 80 s, as can also be deduced from Figure 4.2.

With regard to the fraction β of delayed neutrons, it must be remarked that in practical cases one should not use the values of Table 4.1. The reason for this is that the delayed neutrons on average have a lower energy than the prompt neutrons (0.5 MeV and 2 MeV, respectively). Because of this, their probability of leaking out of the reactor is smaller, so that their contribution to the chain reaction is larger in terms of percentage. Therefore, one should use an effective value β_{eff}, which can be up to 15 % larger than the actual fraction β.

4.4. Temperature effects

In preceding considerations about the reactor kinetics in the seconds domain it was assumed that k_{eff} does not depend on the reactor power. In reality a power increase will result in a temperature increase, by which k_{eff} is affected. The physical mechanisms that occur can be depicted schematically as follows:

schematically as follows:
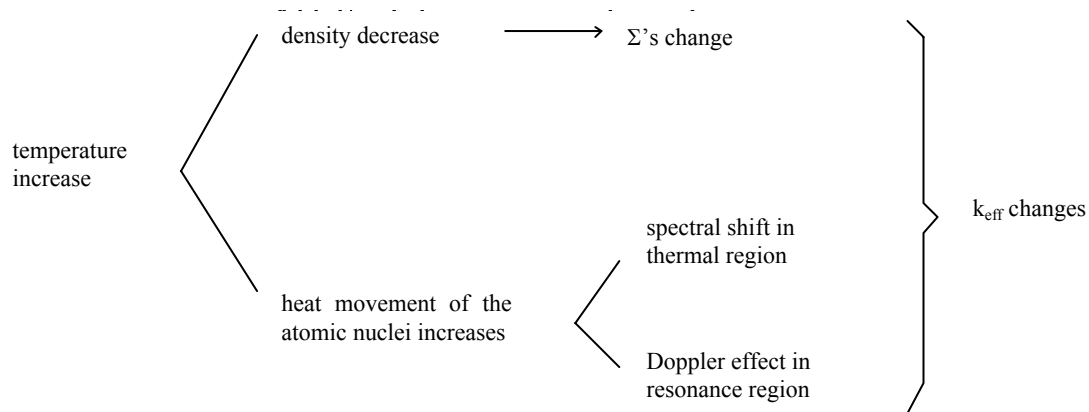
In order to describe the influence of all these processes on the reactivity, one defines the temperature coefficient α:

$$\alpha = \frac{d\rho}{dT} \tag{4.36}$$

so that a temperature increase ΔT results in a reactivity increase $\Delta\rho = \alpha\Delta T$.

If a reactor has been designed in such a way that the temperature coefficient is positive, in the case of a temperature increase in the reactor by whichever cause the reactivity will increase, by which the power increases and the temperature rises further. This implies an unstable system, which must be avoided. If the temperature coefficient is negative, then a temperature increase will be counteracted by a negative reactivity and thus a power decrease.

In a simple description of the heat balance of the reactor with thermal power P(t), the heat is transferred to a reservoir of constant temperature T_r by means of an overall heat-transfer coefficient K. The difference in heating power is used for heating of the reactor, so that

$$\rho_m C_p V \frac{dT}{dt} = P(t) - K\left\{ T(t) - T_r \right\}$$ (4.37)

in which ρ_m is the density, C_p the specific heat capacity and V the volume of the reactor. For a critical reactor with power P_0, it follows for the steady-state temperature that

$$T_0 = T_r + \frac{P_0}{K}$$ (4.38)

If, for the sake of simplicity, we consider the reactor kinetics without delayed neutrons but with an effective generation time Λ_{eff}, in which the influence of the delayed neutrons has been taken into account, then the equation for the power, analogous to (4.7), reads

$$\frac{dP}{dt} = \frac{\rho(t)}{\Lambda_{eff}} P(t)$$ (4.39)

in which the reactivity ρ is the sum of the externally imposed reactivity (for example by moving the control rods) and the reactivity as a result of the temperature effect

$$\rho(t) = \rho_{ext} + \alpha\left\{ T(t) - T_0 \right\}$$ (4.40)

These equations can be solved for a constant reactivity insertion ρ_{ext} by considering the power and temperature changes, $p(t) = P(t) - P_0$ and $\theta(t) = T(t) - T_0$, respectively, and linearising the equations by neglecting the second-order term $\theta(t) p(t)$. For a positive reactivity step and positive α, the power will keep increasing and faster than according to the kinetics discussed in Section 4.2. For a negative temperature coefficient, the reactivity increase ρ_{ext} at a temperature

$T_1 = T_0 - \rho_{ext}/\alpha$ will be compensated by the temperature feedback. The power will then stabilize at a value P_1, for which follows from (4.37) that

$$P_1 = K\left(T_1 - T_r\right) \tag{4.41}$$

For the stationary power we thus find

$$P_1 = P_0 - \frac{K\,\rho_{ext}}{\alpha} \tag{4.42}$$

As the temperature in the reactor is not uniform, it is better to distinguish between the nuclear fuel with average temperature T_f and the moderator/coolant with average temperature T_m, for which separate temperature coefficients α_f and α_m are defined

$$\alpha_f = \left(\frac{\partial \rho}{\partial T_f}\right)_{T_m} \tag{4.43}$$

$$\alpha_m = \left(\frac{\partial \rho}{\partial T_m}\right)_{T_f} \tag{4.44}$$

so that the reactivity change by temperature changes ΔT_f of the nuclear fuel and ΔT_m of the moderator are given by

$$\Delta \rho = \alpha_f\,\Delta T_f + \alpha_m \Delta T_m \tag{4.45}$$

Of course, the temperature coefficients may themselves depend on the temperatures. One can set up separate heat balances for the nuclear fuel and the moderator, analogous to (4.37). However, working those out carries too far.

The temperature coefficient of the nuclear fuel is determined by the nuclear Doppler effect (see also Section 1.4). A temperature increase in the nuclear fuel is accompanied by an increase of the velocity of the atoms by their lattice vibrations. The lattice vibrations are the cause of the fact that mono-energetic neutrons have a certain energy spread with respect to the atomic nuclei (analogy with the acoustic Doppler effect). This spread becomes larger as the temperature increases and results in a broadening and lowering ('spreading') of the resonance peaks. This leads to an increase of the resonance absorption. The area below each resonance peak remains

64

the same, but the absorption in the flanks of the peak increases, while the absorption in the vicinity of the peak maximum hardly decreases, because in practical cases the absorption here is almost 100 %. When the absorption in the resonance region in ^{238}U dominates the fission in ^{235}U, so for not too high a degree of enrichment, α_f will be negative and the reactivity will decrease with increasing temperature of the nuclear fuel.

The temperature coefficient of the moderator is determined by the density change of the water with temperature (for boiling-water reactors also by the change of the steam fraction) and the change of the moderation of the fast neutrons. We will return to this in Section 6.6.

As the Doppler coefficient is determined by the temperature increase of the nuclear fuel, this takes effect much faster than the moderator temperature and the void coefficient, for these have a delayed effect as a result of the necessary heat transfer. The time scales of the various temperature effects, which depend on the thermohydraulic circumstances, thus have an important influence on the stability of the reactor.

4.5. Burn-up and conversion

Longer-term reactivity effects in a working reactor are the nuclear fuel consumption and the conversion of non-fissile nuclides (fertile material) in the nuclear fuel. The most important example of such a conversion reaction is

$$^{238}U + n \rightarrow \; ^{239}U \xrightarrow[23.5\,\text{min}]{\beta^-} \; ^{239}Np \xrightarrow[2.3d]{\beta^-} \; ^{239}Pu \left(T_{1/2} = 24000 \, a \right)$$
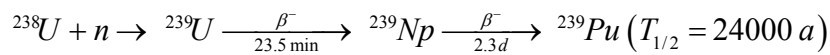
On the basis of such reactions one can define the conversion ratio C

$$C = \frac{production \; rate \; of \; fissile \; nuclides}{consumption \; rate \; of \; fissile \; nuclides}$$

The larger this ratio, the more one uses the nuclides that were non-fissile in the beginning, such as ^{238}U. When the total amount of fissile nuclides increases with time (C > 1), one speaks of a breeder reactor; this can only be realized in fast reactors, because then the number of neutrons that is released per absorbed neutron is amply above the value 2.

For a ^{235}U–^{238}U reactor the 'burn-up' equations can be established easily. For example, for the concentrations of ^{235}U, ^{238}U and ^{239}Pu the following equations hold:

$$\frac{dN_5}{dt} = - \sigma_{a5} N_5 \phi \tag{4.46}$$

$$\frac{dN_8}{dt} = -\sigma_{c8} N_8 \phi \tag{4.47}$$

$$\frac{dN_9}{dt} = \sigma_{c8} N_8 \phi - \sigma_{a9} N_9 \phi \tag{4.48}$$

In these equations, the indices indicate the nuclides. In (4.48) the average lifetime of the intermediate products ^{239}U and ^{239}Np has been neglected. The equations can easily be extended to higher plutonium isotopes (^{240}Pu, ^{241}Pu, ^{242}Pu), for the absorption in ^{239}Pu partly (capture) gives rise to formation of ^{240}Pu, etc. Gradually the fissile plutonium isotopes will also start to contribute to the power production, so that the ^{235}U inventory will not decrease linearly with time in a reactor operating at constant power. Figure 4.6 shows the change in concentration of the most important nuclear fuel nuclides in a light-water reactor. Along the horizontal axis the fluence is marked out, *i.e.* the time integral of the flux density. Usually the burn-up of nuclear fuel is expressed in MWd/t (megawatt days per tonne of nuclear fuel). As burn-up of 1 g of nuclear fuel yields about 1 MWd (Section 1.2), a burn-up of, for example, 10.000 MWd/t implies that about 1 % of the nuclear fuel present (all nuclides included!) has been burnt up. The highest fluence value in Figure 4.6 thus corresponds with a burn-up of almost 40,000 MWd/ton. As the burn-up increases, more fission products are formed, which swell the nuclear fuel. Because of this there are technological limits to the achievable burn-up.
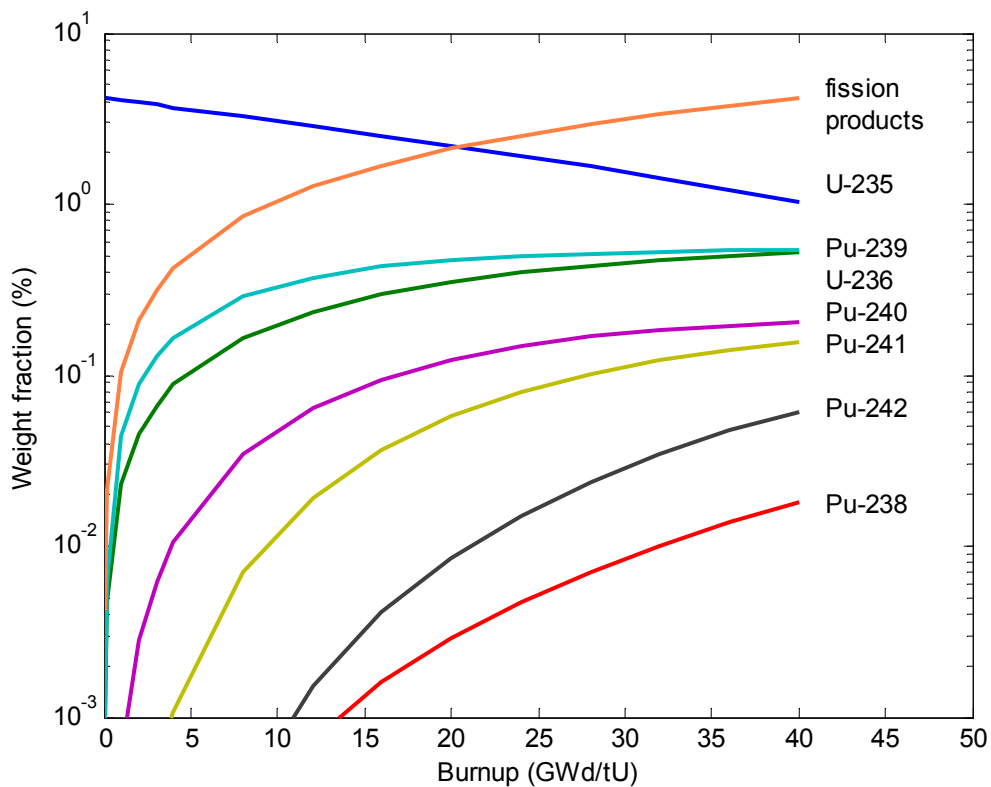
Figure 4.6. Change in nuclear fuel composition as a function burnup in a light-water reactor

4.6. Fission products

Of the many nuclides that are formed as fission products in a reactor, two are of special importance, because they have very high absorption cross sections, so that their presence has a large influence on the reactivity. These two nuclides, $^{135}_{54}Xe$ (xenon) and $^{149}_{62}Sm$ (samarium), are known as reactor poisons, ^{135}Xe is the most important reactor poison with $\sigma_a = 2.65 \cdot 10^6$ barn. It is partly formed directly during fission, but for a more important part as decay product of ^{135}Te (tellurium) and ^{135}I:

^{135}Te (tellurium) en ^{135}I

$$^{135}_{52}Te \xrightarrow[19.2s]{\beta^-} {}^{135}_{53}I \xrightarrow[6.6h]{\beta^-} {}^{135}_{54}Xe \xrightarrow[9.2h]{\beta^-} {}^{135}_{55}Cs \xrightarrow[2.10^6 a]{\beta^-} {}^{135}_{56}Ba \, (stable)$$
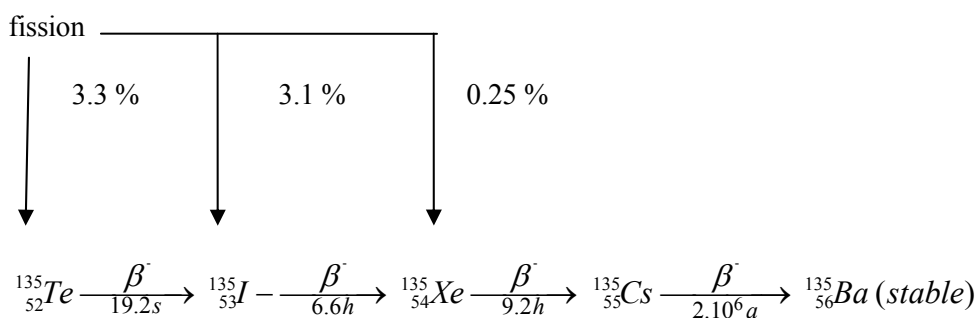
The half-life of tellurium-135 is so short, that iodine-135 can be considered as the primary fission product.
The effect of xenon-135 on the reactivity depends on its concentration during reactor operation and after shutdown of the reactor. The equation for the iodine concentration I is:

$$\frac{dI}{dt} = \gamma_I \Sigma_f \phi - \lambda_I I \tag{4.49}$$

in which γ_I is the fission yield of ^{135}I including that of ^{135}Te ($\gamma_I = 0.064$) and λ_I the decay constant. A term for neutron capture is lacking, because this is negligible for ^{135}I. For the xenon concentration X the following holds:

$$\frac{dX}{dt} = \lambda_I \, I + \gamma_X \Sigma_f \, \phi - \lambda_X \, X - \sigma_{aX} \, X\phi \tag{4.50}$$

In view of the half-lifes in the tellurium decay chain, the equilibrium concentration of ^{135}Xe in a reactor operating at constant power will be reached after *circa* two days:

$$X_0 = \frac{(\gamma_I + \gamma_X)\Sigma_f \phi}{\lambda_X + \sigma_{aX}\phi} \qquad (4.51)$$
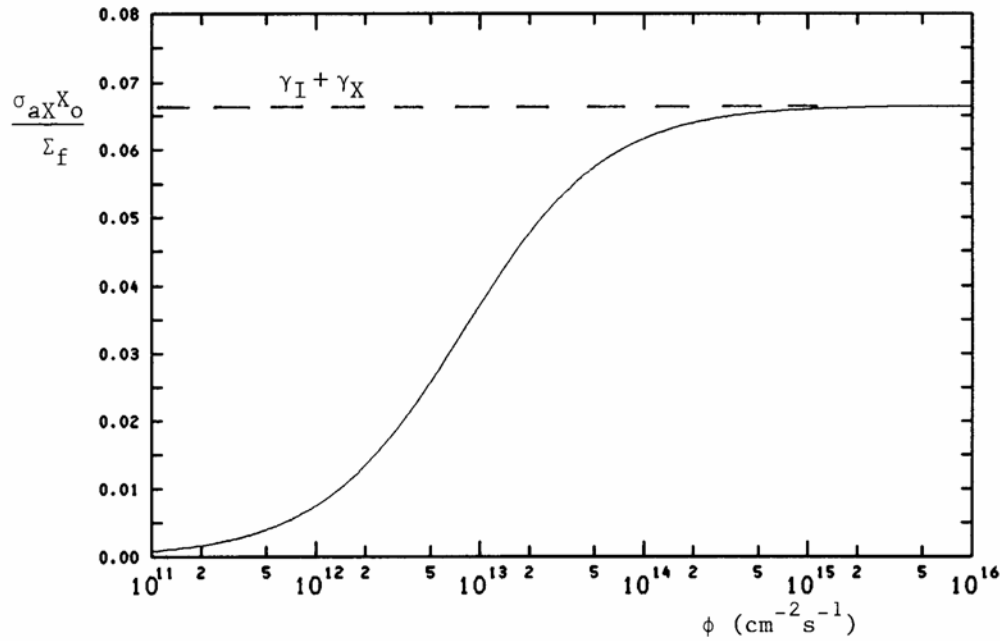
Figure 4.7. Equilibrium xenon poisoning as a function of the neutron flux

Figure 4.7 shows $\sigma_{aX}X_0/\Sigma_f$ as a function of the flux ϕ. The effect of the xenon concentration on the reactivity can easily be determined if we consider a homogeneous reactor and assume that the presence of ^{135}Xe does not influence the leakage of neutrons from the reactor. The change in reactivity can then be described as:

$$\rho_X = \frac{k_X - 1}{k_X} = \frac{k_X - k}{k_X} = 1 - \frac{k}{k_X} = 1 - \frac{k_\infty}{k_{\infty X}}$$
$$= 1 - \frac{\nu\Sigma_f/\Sigma_a}{\nu\Sigma_f/(\Sigma_a + \Sigma_{aX})} = -\frac{\Sigma_{aX}}{\Sigma_a} = -\frac{k_\infty}{\nu}\frac{\sigma_{aX}X}{\Sigma_f} \qquad (4.52)$$

in which k_X and $k_{\infty X}$ are the multiplication factors of the 'poisoned' reactor. According to Figure 4.7, ρ_X will increase with increasing ϕ and reach an asymptotic value if $\phi \gg \lambda_X/\sigma_{aX} = 7.5 \cdot 10^{12}$ cm^{-2}s^{-1}.

For example, for the 'Higher Education Reactor' at Delft with 93 % enriched uranium, in the equilibrium situation $\phi = 10^{13}$ cm^{-2}s^{-1} and $k_\infty = 1.4$, so that $\rho_X = -2.1$ %. Therefore, in order to compensate for the xenon effect during continuous operation an additional reactivity of over 2 % must be available. (It is noted that the reactor in Delft now uses Low Enriched Uranium).

68

By solving equations (4.49) and (4.50) at constant flux, one can calculate how the xenon concentration accumulates with time after start-up of the reactor.

Another important aspect of xenon poisoning is the behaviour after a reactor shutdown; we thereby assume that before shutdown xenon equilibrium is present. Immediately after shutting down the reactor, the terms containing ϕ are dropped from the right part of (4.50), while the concentration of I is still determined by the steady-state solution of (4.49): $I_0 = \gamma_I \Sigma_f \phi / \lambda_I$. The production rate of xenon directly after shutdown is given by $\lambda_I I_0$, while the rate of disappearance is given by $\lambda_X X_0$. If now $\lambda_I I_0 > \lambda_X X_0$ or

$$\phi > \frac{\gamma_X}{\gamma_I} \frac{\lambda_X}{\sigma_{aX}} = 3 \cdot 10^{11} \ cm^{-2} s^{-1} \tag{4.53}$$

the rate of production is larger than the rate of disappearance and at first the xenon concentration increases. The rate of the increase depends on the original neutron flux and increases with increasing flux. The xenon concentration will reach a maximum as a result of the decay of ^{135}I, after which all xenon will disappear by radioactive decay. This behaviour is depicted in Figure 4.8. For large values of ϕ a maximum occurs at $\ln(\lambda_I/\lambda_X)/(\lambda_I - \lambda_X) \approx 11.2$ h after shutdown of the reactor. An important consequence of this 'xenon peak' after a reactor shutdown is that, unless sufficient additional reactivity is present, it cannot be possible to start up the reactor again before many hours have passed. Also in the case of a varying reactor power xenon transients will continually occur, whereby, analogous to the increase of the xenon concentration after a reactor shutdown, the concentration can at first increase after a power
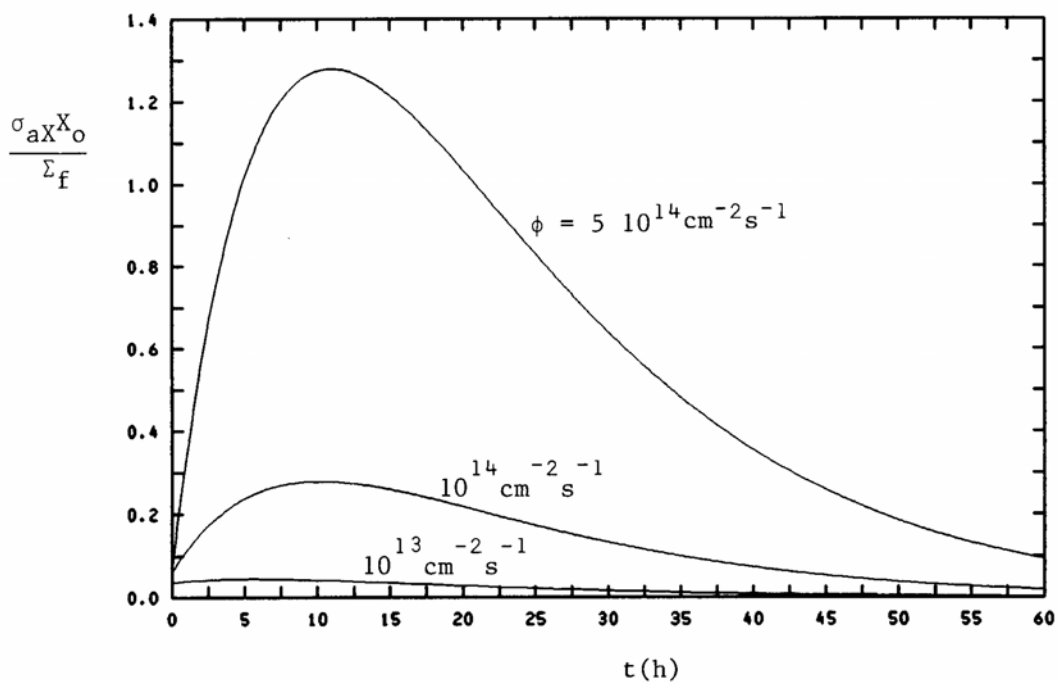
Figure 4.8. Xenon poisoning as a function of time after shutdown of a reactor
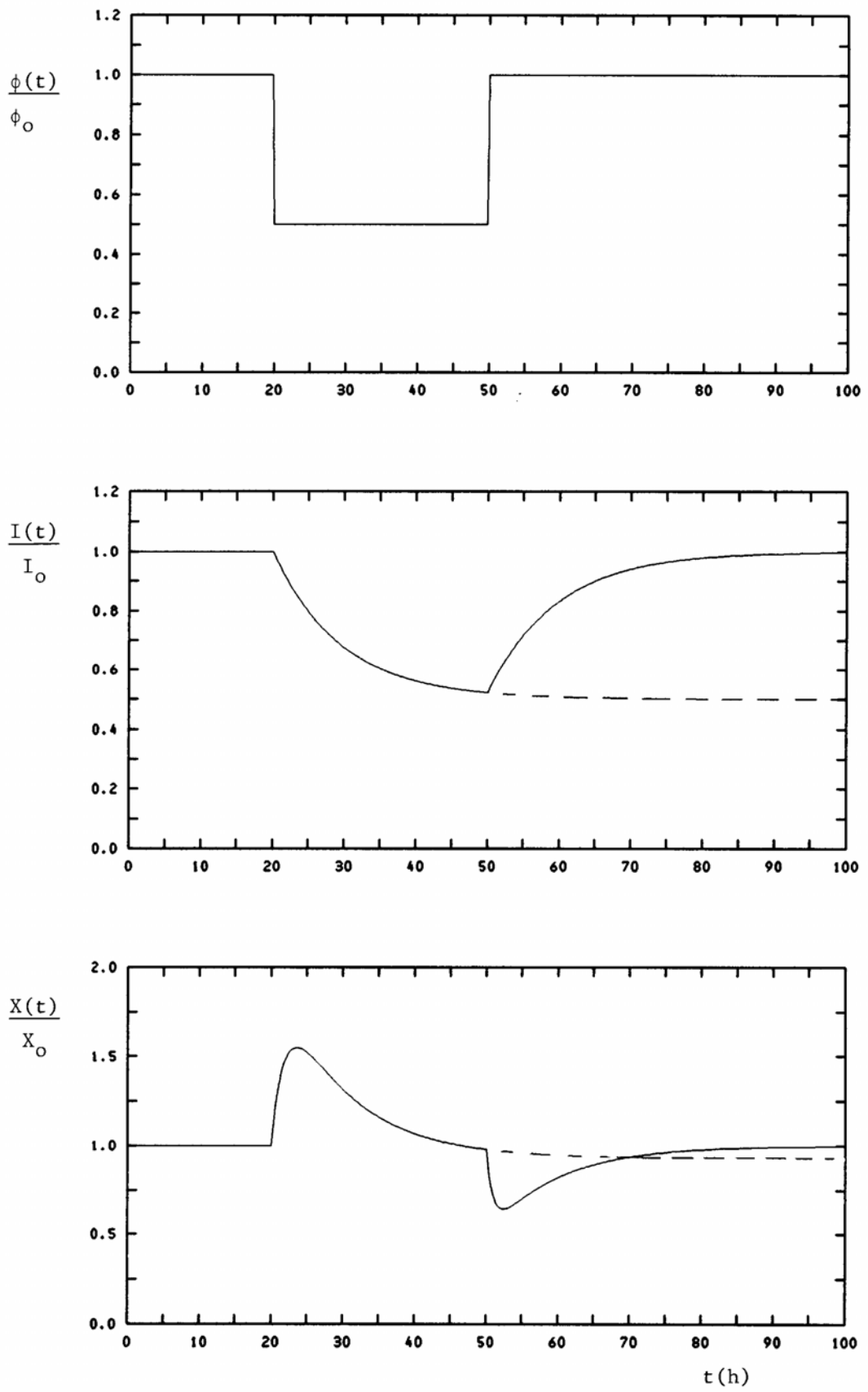
Figure 4.9. Xenon transients for varying power

reduction. Vice versa, in the case of a power increase, the xenon concentration at first can decrease. Figure 4.9 illustrates such a transient.

The fission product ^{149}Sm ($\sigma_a = 4.1 \cdot 10^4$ b) is formed in the following chain of fission products (short-lived nuclides in the start of the chain have been omitted):

fission

$$\downarrow \quad 1.09\,\%$$

$$^{149}_{60}Nd \xrightarrow[1.73\,h]{\beta^-} \, ^{149}_{61}Pm \xrightarrow[53.1h]{\beta^-} \, ^{149}_{62}Sm \,(stable)$$
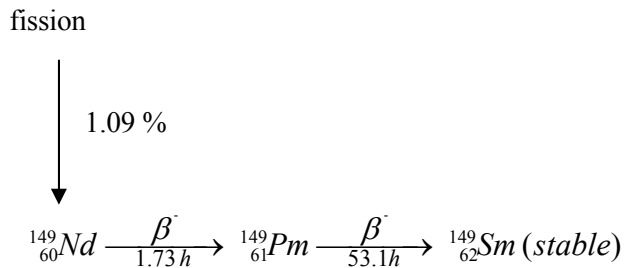
In the same manner as indicated above for xenon, one finds for the equilibrium concentration of ^{149}Sm:

$$S_0 = \frac{\gamma_{Nd}\Sigma_f}{\sigma_{aS}} \tag{4.54}$$

This concentration is independent of the neutron flux, because ^{149}Sm is stable.
For the reactivity effect one finds:

$$\rho_{S_0} = -\frac{k_\infty}{\nu}\gamma_{Nd} \tag{4.55}$$

For the example of the 'Higher Education Reactor' thus holds that $\rho_{S0} = -0.6\,\%$.
It is left to the reader to check how fast the accumulation of the samarium concentration occurs after start-up of a reactor and how the samarium concentration changes after a reactor shutdown.

4.7. Reactivity and reactor control

When putting a reactor into operation, a certain 'overreactivity' must have been invested in the core, which must be controlled by neutron capture in control components. This overreactivity is the reactivity of the core in the imaginary case that all control components have been removed. By gradually reducing the neutron capture in the control components, one can compensate the decrease in reactivity that occurs during reactor operation and maintain the desired power.

Table 4.2. Reactivity effects in a pressurized-water reactor and a boiling-water reactor

Reactor type	PWR Borssele	BWR Gundremmingen
Average nuclear fuel enrichment in new core (% ^{235}U)	2.8	2.22
k_{eff} of new core	1.28	1.26
Reactivity effects during operation (Δk in %)		
poisoning (Xe + Sm)	4	4.0
temperature effect	7	1.4
bubble formation	-	1.6
burn-up	16	18.0
Reactivity value of neutron absorbers for control (Δk in %)		
control rods	9	20
absorber plates	-	10
boric acid	23	-
boron salt injection for emergencies	-	18

Table 4.2 shows the values of the different reactivity effects for a pressurized-water reactor and a boiling-water reactor. The total reactivity value of the neutron absorbers used for reactor control is chosen in such a way that the reactor is sufficiently subcritical in the case of control rods that are completely driven in. The so-called 'shutdown margin' is usually expressed in percentage negative reactivity value and for the reactors in Table 4.2 amounts to 4 % in the case of a cold 'clean' core (no fission products and burn-up).

Three kinds of neutron absorbers can be distinguished:

- controllable absorbers (control rods);
- liquid absorbers, homogeneously mixed with the moderator (boric acid in PWRs);
- solid absorbers that have been built in the nuclear fuel and gradually disappear during reactor operation ('burnable poison' such as boron and gadolinium).

The control rods serve for the normal start up and shutdown of the reactor, changes in power and emergency shutdowns; boric acid and burnable poison mainly serve as compensation of the burn-up.

Adding boric acid to the coolant of pressurized-water reactors enables reactor operation with the control rods almost completely withdrawn, which has the advantage of a more uniform power density distribution in the reactor core than in the case of partially inserted control rods.

In boiling-water reactors often a device is present for injecting boric acid or a boron salt, which can serve as an emergency shutdown system should difficulties occur with the control rod drive mechanisms. The quantity k_∞ is sketched in Figure 4.10 as a function of the specific energy produced in the nuclear fuel, expressed in MWd/ton.
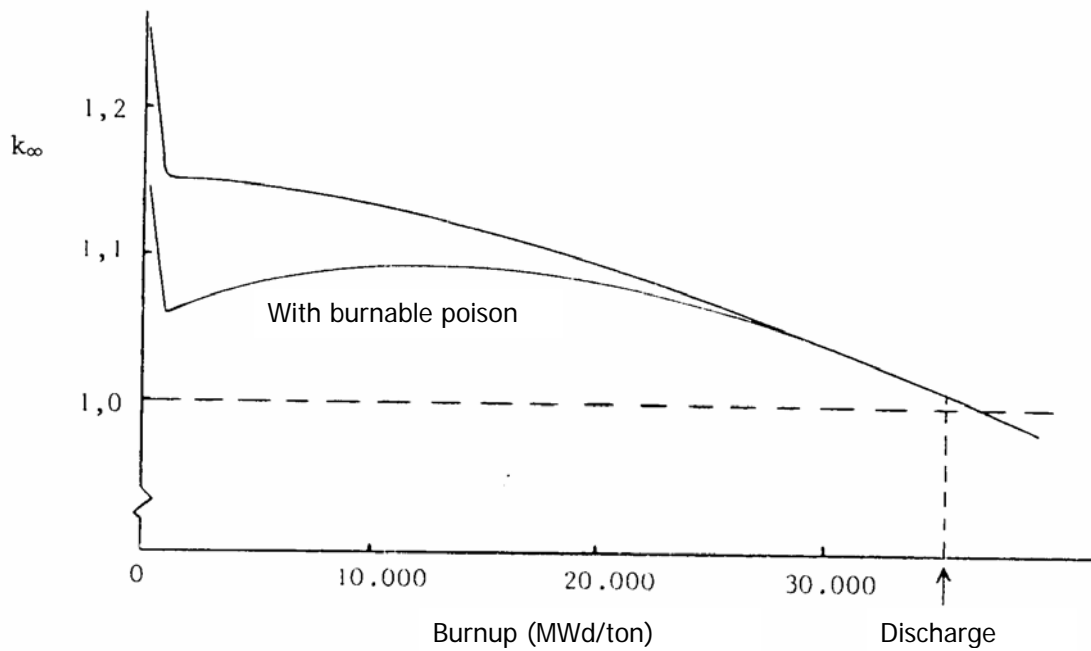
Figure 4.10. k_∞ as a function of the degree of burn-up (numbers are characteristic of light-water reactors)

This pattern is the resultant of the effects discussed in the preceding paragraphs:

1. a rather rapid build-up of the xenon and samarium poisoning to an equilibrium value;

2. a gradual decrease of the reactivity by nuclear fuel consumption;

3. an increase of the reactivity by formation of plutonium (conversion); in light-water reactors. at the end of the life of the core the formed plutonium takes part in the energy production for about 50%;

4. in the presence of a burnable poison, the disappearance of this poison can at first cause a reactivity increase. Here 'disappear' means: conversion into nuclides with low capture cross sections, for example:

$$_{5}^{10}B\left(\sigma_c = 3800\,b\right) + n \rightarrow {}_{3}^{7}Li\left(\sigma_c \approx 0\right) + {}_{2}^{4}He\left(\sigma_c = 0\right)$$
$$_{64}^{155}Gd\left(\sigma_c = 61000\,b\right) + n \rightarrow {}_{64}^{156}Gd\left(\sigma_c = 8\,b\right)$$
$$_{64}^{157}Gd\left(\sigma_c = 254000\,b\right) + n \rightarrow {}_{64}^{158}Gd\left(\sigma_c = 3.5\,b\right)$$
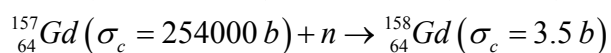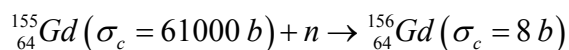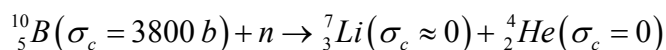
By applying burnable poisons the reactivity change during the life of the core is limited, which simplifies the reactivity control with the aid of the control rods.

Control rods, of course, influence the spatial flux distribution in a reactor core and thus the power density distribution. This should be taken into account when designing and operating a reactor, because the temperature distribution, which is connected with the power density distribution, is decisive for the maximum power that can be produced in a safe manner.

The reactivity effect of a control rod depends, amongst other things, on the insertion depth into the core. Figure 3.6 includes the importance function for a change in the macroscopic absorption cross section, which occurs if a control rod is moved over a small distance. Although the perturbation theory of Section 3.3 is not valid for such heavy disturbances as a control rod, it does give an indication for the effect that is to be expected. The differential reactivity of the control rod is thus approximately proportional to

$$\frac{d\rho}{dz} \div \phi^2(z) \tag{4.56}$$

A reactor core will generally be surrounded by a reflector, so that the flux at the edge of the core will not yet go to zero. The characteristic shape of a differential and an integral reactivity curve are shown in Figure 4.11.

In general, these curves are asymmetric due to 'shadow effects' of other control rods, which give an asymmetric flux distribution along the path of the control rod considered. Such curves can be determined experimentally by measuring the reactor response, for example the stable reactor period, to a movement of the control rod.
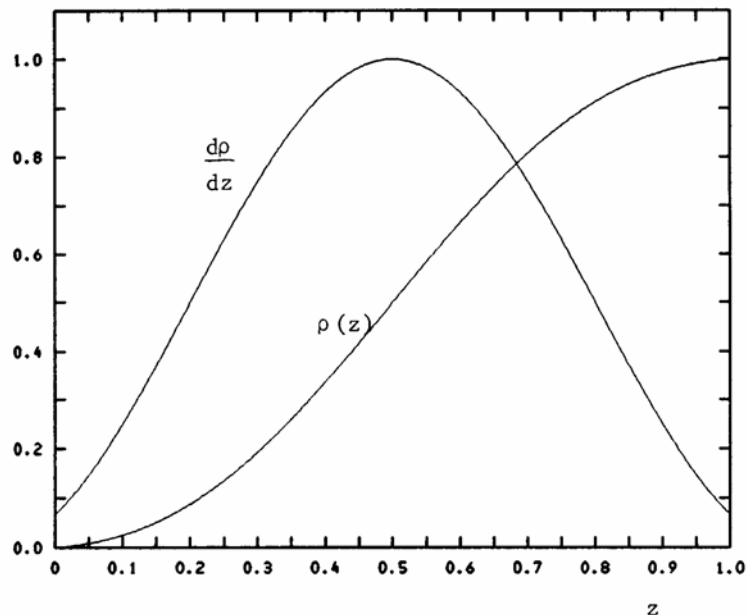
Figure 4.11. Differential and integral reactivity curve of a control rod

Chapter 5

Energy dependence of the neutron flux

In the preceding chapters we have treated the steady-state and time-dependent behaviour of reactors using the diffusion theory for mono-energetic neutrons or the one-group theory.

In this chapter we will pay attention to the energy dependence of the neutron spectrum in the reactor. Seeing that obtaining an analytical solution of the energy-dependent diffusion equation is almost impossible, we must resort to an approximating description.

5.1. Multi-group diffusion theory

We obtain the energy-dependent diffusion equation by integrating the transport equation (2.8) over $\underline{\Omega}$ and replacing the flow term $-\int \underline{\Omega} \cdot \underline{\nabla} \phi(\underline{r},E,\underline{\Omega},t)d\Omega = -\underline{\nabla} \cdot J(\underline{r},E,t)$ by $\underline{\nabla} \cdot D(\underline{r},E)\underline{\nabla}\phi(\underline{r},E,t)$, analogous to the one-group diffusion theory

$$
\frac{1}{v}\frac{\partial\phi(\underline{r},E,t)}{\partial t} = \underline{\nabla}\cdot D(\underline{r},E)\underline{\nabla}\phi(\underline{r},E,t) - \Sigma_t(\underline{r},E)\phi(\underline{r},E,t)
$$
$$
+ S(\underline{r},E,t) + \int_0^\infty \Sigma_s(\underline{r},E'\rightarrow E)\phi(\underline{r},E',t)dE'
$$

(5.1)

As the energy range comprises many decades (e.g. 10^{-4} eV to 10 MeV) and the microscopic cross sections may show very sharp resonance peaks (see Section 1.4), a solution by fine discretisation of the energy range is doomed to failure. Therefore, we divide the whole energy range in (a limited number of) energy groups (see Figure 5.1). Seeing that the neutrons are released with high energy during fission and lose energy by moderation, the groups are generally numbered from high to low energy.
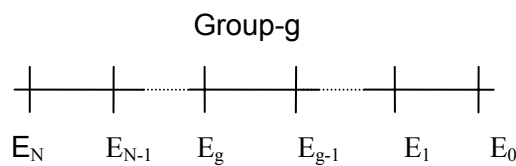
Figure 5.1. Division into energy groups

We define the so-called group flux ϕ_g for energy group g as

$$\phi_g(\underline{r},t) = \int\limits_{E_g}^{E_{g-1}} \phi(\underline{r},E,t)dE = \int\limits_g \phi(\underline{r},E,t)dE \qquad (5.2)$$

By integration of equation (5.1) over the energy interval of group g, we obtain the coupled multi-group diffusion equations

$$\frac{1}{v_g}\frac{\partial \phi_g(\underline{r},t)}{\partial t} = \underline{\nabla} \cdot D_g(\underline{r})\underline{\nabla}\phi_g(\underline{r},t) - \Sigma_{tg}(\underline{r})\phi_g(\underline{r},t)$$
$$+ \sum_{g'}\Sigma_{g'g}(\underline{r})\phi_{g'}(\underline{r},t) + S_g(\underline{r},t) \qquad (5.3)$$

If fission occurs in the system, the source of group g is given by

$$S_g(\underline{r},t) = \chi_g\sum_{g'}v_{g'}\Sigma_{fg'}(\underline{r})\phi_{g'}(\underline{r},t) + S_{g,ext}(\underline{r},t) \qquad (5.4)$$

Here χ_g is the fraction of neutrons with an energy in group g that is released during fission and $S_{g,ext}$ is an external source. In fact, in (5.3) the following definitions have been introduced

$$\Sigma_{tg} = \frac{1}{\phi_g}\int\limits_g \Sigma_t(E)\phi(\underline{r},E,t)dE \qquad (5.5)$$

$$D_g = \frac{\int D(E)\underline{\nabla}\phi(\underline{r},E,t)dE}{\int \underline{\nabla}\phi(\underline{r},E,t)dE} \qquad (5.6)$$

$$\Sigma_{g'g} = \frac{1}{\phi_{g'}}\int\limits_g\int\limits_{g'} \Sigma_s(E' \to E)\phi(\underline{r},E',t)dE'dE \qquad (5.7)$$

$$\frac{1}{v_g} = \frac{1}{\phi_g}\int\limits_g \frac{1}{v}\phi(\underline{r},E,t)dE \qquad (5.8)$$

These definitions of the so-called group cross sections are only formal, as for their application the flux $\phi(\underline{r},E,t)$ within group g must be known. In order to still be able to use the group cross sections, an approximation is sought for this flux, whereby moreover it is assumed that this flux

can be separated into a position- and time-dependent part on the one side and an energy-dependent part on the other side. Notice that without this last approximation even for a homogeneous system these group constants are position and time dependent.

In order to get an approximated description for the energy dependence $\phi(E)$ of the flux, we will first study the moderation process of the neutrons and to this end derive the form of the macroscopic scattering cross section $\Sigma_s\left(E' \rightarrow E\right)$ by analysis of the collision process of a neutron with a nucleus.

5.2. Energy transfer in elastic collisions

The neutrons released during fission with an average energy of 2 MeV, in a reactor on average undergo a number of collisions before they are absorbed. As a result of these collisions (elastic and inelastic) they lose energy, so that the reactor spectrum is always 'softer' than the fission spectrum. In thermal reactors, use is made of this moderation of neutrons in order to profit from the larger cross sections at lower energies. In these reactors, the neutrons are predominantly absorbed only when they are in kinetic equilibrium with the thermal movement of the atomic nuclei. The energy distribution of the thermal neutrons is treated in Section 5.4.

Elastic collisions form the most important mechanism for slowing down neutrons, because inelastic collisions only play a part in the case of heavy nuclei and only at high energies (see Section 1.4).

Elastic scattering can be considered as a collision of two hard spheres and can be described with the aid of classical mechanics. The neutron with mass m has a vector velocity $\underline{v}'$ before collision and a velocity $\underline{v}$ after collision. The energy of the neutron $E'=\tfrac{1}{2}\,m\,v'^2$ is much larger than that of the nucleus, so that the nucleus can be considered as motionless. After collision, the nucleus has a velocity $\underline{V}$. The velocity of the neutron after collision can be calculated with the laws of conservation of momentum and energy. However, this is easier by transformation to the centre-of-mass system, the origin of which is in the centre-of-mass of the colliding particles (see Figure 5.2). This is thus a moving co-ordinate system with velocity

$$\underline{v}_{cm} = \frac{m\underline{v}' + M\underline{V}'}{m+M} = \frac{m\underline{v}'}{m+Am} = \frac{1}{A+1}\underline{v}' \tag{5.9}$$

with A = M/m the mass of the nucleus with respect to the mass of the neutron. If we indicate the velocities in the centre-of-mass system with u and U for the neutron and the nucleus, respectively, the following holds

$$\underline{u}' = \underline{v}' - \underline{v}_{cm} = \frac{A}{A+1}\underline{v}' \qquad (5.10)$$

`

$$\underline{U}' = \underline{V}' - \underline{v}_{cm} = -\frac{1}{A+1}\underline{v}' \qquad (5.11)$$
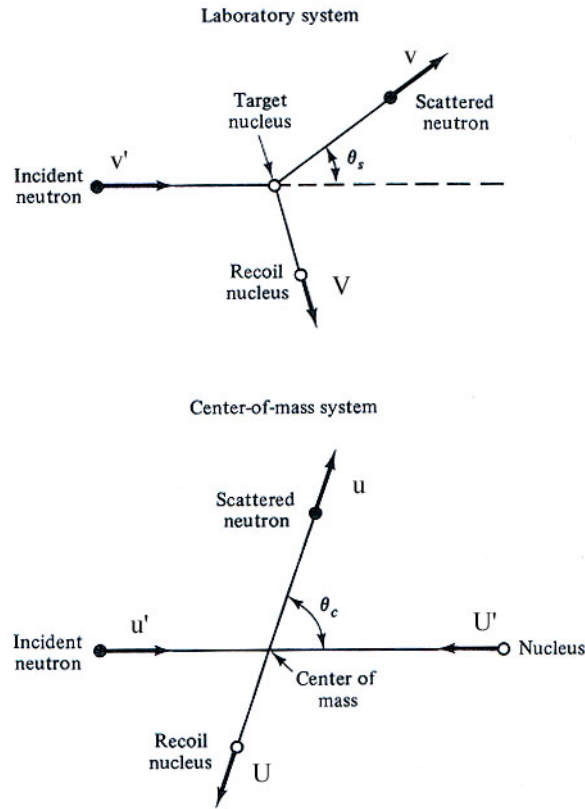
Figure 5.2. Collision in laboratory and centre-of-mass system

The momentum in the centre-of-mass (cm) system is equal to zero both before and after the collision, so that for the velocities after the collision holds that

$$\underline{U} = -\frac{1}{A}\underline{u} \qquad (5.12)$$

The law of conservation of kinetic energy, applied to the centre-of-mass system, yields

$$\tfrac{1}{2}m\left(\frac{A}{A+1}v'\right)^2 + \tfrac{1}{2}mA\left(\frac{1}{A+1}v'\right)^2 = \tfrac{1}{2}mu^2 + \tfrac{1}{2}mA\left(\frac{1}{A}u\right)^2 \qquad (5.13)$$

For the magnitude of the velocities after the collision in the centre-of-mass system it follows from (5.13) that

$$u = \frac{A}{A+1}v'$$

(5.14)

$$U = \frac{1}{A+1}v'$$

(5.15)

with which it has been demonstrated again that the magnitude of the velocities in the centre-of-mass system does not change upon collision. One gets the velocity of the neutron in the laboratory system by the transformation

$$\underline{v} = \underline{u} + \underline{v}_{cm}$$

(5.16)
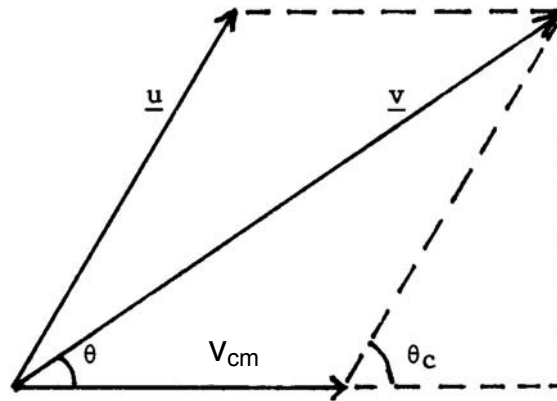
Figure 5.3. Back-transformation to the laboratory system

In the centre-of-mass system, the neutron is scattered over an angle θ_c (see Figure 5.3), so that with the aid of the cosine rule we find:

$$v^2 = \left(\frac{A}{A+1}\right)^2 v'^2 + \left(\frac{1}{A+1}\right)^2 v'^2 + 2\frac{A}{(A+1)^2}v'^2\mu_c$$

(5.17)

with $\mu_c = \cos\theta_c$. So that finally

$$\frac{E}{E'} = \frac{v^2}{v'^2} = \frac{A^2 + 2A\mu_c + 1}{(A+1)^2} \tag{5.18}$$

with which the energy after the collision has been expressed in the energy before the collision and the scattering angle in the centre-of-mass system.

The maximum energy transfer takes place if $\theta_c = 180^\circ$ or $\mu_c = -1$, so in the case of a frontal collision:

$$\left(\frac{E}{E'}\right)_{min} = \left(\frac{A-1}{A+1}\right)^2 = \alpha \tag{5.19}$$

For ^{1}H (with small rounding) A = 1, so that $\alpha = 0$. In the case of a frontal collision, the neutron will therefore transfer all of its energy to the hydrogen nucleus. For ^{12}C the maximum energy loss is 28.4 % and for ^{235}U only 1.7 %. For effective moderation of neutrons in thermal reactors, one will thus have to choose materials with low A values.

Of course, frontal collisions do not always occur, so we have to look at the probability distribution for a certain energy transfer. It appears that for energies below *circa* 1 MeV, scattering in the centre-of-mass system is isotropic, *i.e.* all directions have an equal probability of occurring. For the probability distribution for a direction $\underline{\Omega}_c$ in the centre-of-mass system it then holds that

$$p(\underline{\Omega}_c)d\Omega_c = \frac{d\Omega_c}{4\pi} \tag{5.20}$$

From this, by integration of the azimuthal angle ψ_c it follows for the probability distribution of the cosine of the scattering angle μ_c in the centre-of-mass system that

$$p(\mu_c) = \int_0^{2\pi} p(\underline{\Omega}_c)d\psi_c = \tfrac{1}{2} \tag{5.21}$$

As the energy E after the collision unambiguously depends on μ_c, we finally obtain

$$p(E' \to E) = p(\mu_c)\frac{d\mu_c}{dE} = \frac{p(\mu_c)}{\dfrac{dE}{d\mu_c}} = \frac{\tfrac{1}{2}}{\dfrac{2A}{(A+1)^2}E'} = \frac{1}{E'(1-\alpha)} \qquad \alpha E' < E < E' \tag{5.22}$$

for the probability distribution of the energy after scattering. Hereby the derivative of (5.18) has been determined. As the probability distribution does not depend on E, all energies between $\alpha E'$ and E' are equally probable. We can write the differential scattering cross section $\Sigma_s\left(E'\rightarrow E\right)$, which appears in (5.1) and in the definition of the group scattering cross section (5.7), as

$$\Sigma_s(E'\rightarrow E)=\frac{\Sigma_s(E')}{E'(1-\alpha)}\qquad \alpha E'<E<E' \tag{5.23}$$

From Figure 5.3 we can also determine the relation between the scattering angles in the centre-of-mass system and the normal (laboratory) system. If we call $\mu_0 = \cos\theta$ the cosine of the scattering angle in the laboratory system, then

$$v\mu_0 = v_{mmp}+u\mu_c \tag{5.24}$$

or

$$\mu_0 = \frac{1}{A+1}\frac{v'}{v}+\frac{A}{A+1}\frac{v'}{v}\mu_c = \frac{A\mu_c+1}{\sqrt{A^2+2A\mu_c+1}} \tag{5.25}$$
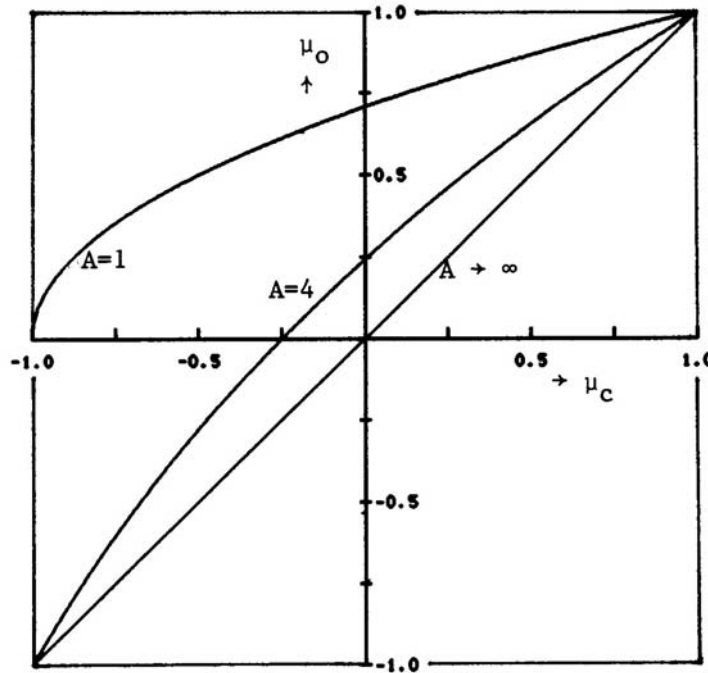
Figure 5.4. Relation between cosine of scattering angle
in centre-of-mass and laboratory system

This relation is shown in Figure 5.4. The isotropy in the centre-of-mass system thus gives a preference for forward scattering in the laboratory system, which is stronger according as the nucleus with which the neutron collides is lighter. At high neutron energies, a forward preference occurs in the centre-of-mass system also, which results in strongly forwardly directed scattering in the laboratory system and thus a preference for smaller energy transfer.

With the aid of (5.25) we can now also calculate the average value of the cosine of the scattering angle in the laboratory system $\bar{\mu}_0$, which quantity appears in the definition of the macroscopic transport cross section (2.20) and with that in the definition of the diffusion coefficient

$$\overline{\mu_0} = \int_{-1}^{1} \mu_0 p(\mu_0) d\mu_0 = \int_{-1}^{1} \mu_0(\mu_c) p(\mu_c) d\mu_c = \frac{2}{3A} \tag{5.26}$$

As in elastic collisions on average a constant fractional energy loss occurs per collision, it is also useful to work with logarithmic quantities. For example, one defines an average logarithmic energy decrement per collision:

$$\xi = \overline{\ln E' - \ln E} = \int_{\alpha E'}^{E'} \ln \frac{E'}{E} p(E' \to E) dE = 1 + \frac{\alpha}{1-\alpha} \ln \alpha \tag{5.27}$$

With the aid of this quantity it is easy to calculate the average number of collisions that a neutron must undergo in order to slow down from, for example 2 MeV to 1 eV:

$$N(2 \text{ MeV} \to 1 \text{eV}) = \ln 2 \cdot 10^6 / \xi = 14.5 / \xi \tag{5.28}$$

Table 5.1 gives a number of values.

Table 5.1. Moderation data for some elements

Element	A	ξ	N (2 MeV → 1 eV)
H	1	1.000	15
D	2	0.725	20
He	4	0.425	34
Be	9	0.207	70
C	12	0.158	92
O	16	0.120	121

In connection with the logarithmic character of the moderation process, one also sometimes uses the concept of 'lethargy' u ('laziness') instead of energy, defined as

$$u(E) = \ln \frac{E_0}{E} \qquad (5.29)$$

in which E_0 is a suitably chosen reference energy. For example, if one chooses $E_0 = 2$ MeV, then the lethargy of neutrons with the average fission energy is equal to zero, while $u(1$ eV$) = 14.5$. The average number of collisions in order to reach a lethargy u then is:

$$n(u) = u / \xi \qquad (5.30)$$

Now it is easy to make a list of requirements for a good moderator material:

a) Σ_s large

b) ξ large

c) Σ_a small

The product $\xi\Sigma_s$ is called the slowing-down power and indicates the average logarithmic energy loss per unit path length covered by a neutron. The quotient $\xi\Sigma_s/\Sigma_a$ is sometimes called the moderation ratio or moderator quality. Table 5.2 gives some values for moderator materials.

Table 5.2. Slowing-down power and moderator quality of some often applied moderators

Moderator	slowing-down power (cm^{-1})	moderator quality
H_2O	1.35	71
D_2O	0.176	6000
Be	0.158	43
C	0.060	192

From this table it appears that normal water slows down the neutrons faster than heavy water. However, seeing that light hydrogen absorbs quite a lot of neutrons, heavy water is still a better moderator material. One of the consequences is that in light-water reactors enriched uranium (*i.e.* with over 0.71 % ^{235}U) must be applied, whereas in heavy-water reactors natural uranium can be used.

5.3. The epithermal spectrum for moderation

The position and energy dependent neutron field in a reactor can be determined by solving the energy-dependent diffusion equation. In general, this requires the use of a computer. However, with a few simplified assumptions we can get insight in the energy distribution of neutrons during the moderation process along an analytical path. Firstly, we limit ourselves to such an

energy range that the source neutrons (coming from fissions and external sources) have already undergone a number of collisions before passing the upper limit of this range. In addition, the lower limit of the range is above the range where the thermal movement of the nuclei starts to play a part and the nuclei can no longer be considered motionless with respect to the neutrons. The range chosen in this way roughly extends from 1 eV to 100 keV and is called the epithermal range. In this range, the differential scattering cross section (5.23) is valid, if we limit ourselves to elastic collisions. The energy-dependent diffusion equation (5.1) for the steady-state situation reads

$$\underline{\nabla} \cdot D(\underline{r}, E)\underline{\nabla}\phi(\underline{r}, E) - \Sigma_t(\underline{r}, E)\phi(\underline{r}, E) + \int_E^{E/\alpha} \Sigma_s(\underline{r}, E' \to E)\phi(\underline{r}, E')\, dE' = 0 \qquad (5.31)$$

If we now consider an infinite homogeneous medium, in which absorption during moderation can be neglected, (5.31) reduces to

$$\Sigma_s(E)\phi(E) + \int_E^{E/\alpha} \frac{\Sigma_s(E')}{E'(1-\alpha)}\phi(E')\, dE' \qquad (5.32)$$

By substitution one can easily verify that this equation has the solution

$$F(E) = \Sigma_s(E)\phi(E) = \frac{C}{E} \qquad (5.33)$$

The constant C can be determined by considering the slowing-down density q(E), *i.e.* the number of neutrons that 'passes' the energy E per cm^3 and per second. As we assume that no absorption or leakage occurs, q is energy-independent and equal to the source strength per cm^3 as a result of fissions. For the slowing-down density it holds that (see Figure 5.5)

$$q = \int_{E'=E}^{E/\alpha} \int_{E''=\alpha E'}^{E} \Sigma_s(E' \to E'')\, dE''\phi(E')\, dE' = \int_E^{E/\alpha} \Sigma_s(E')\phi(E')\frac{E - \alpha E'}{E'(1-\alpha)}\, dE'$$
$$= C\left(1 + \frac{\alpha}{1-\alpha}\ln\alpha\right) = C\xi \qquad (5.34)$$

84
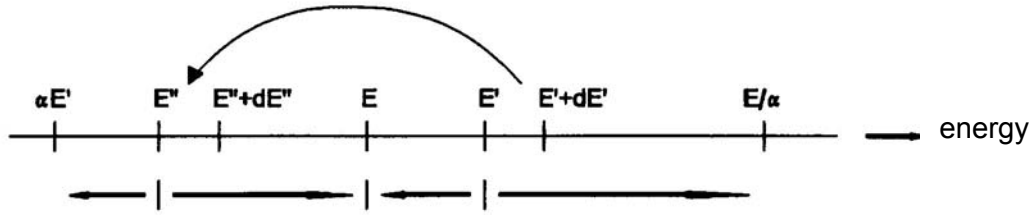
Figure 5.5. Energy diagram for calculation of the slowing-down density

so that for the epithermal spectrum follows

$$\phi(E) = \frac{q}{\xi \Sigma_s(E)E} \tag{5.35}$$

As $\Sigma_s(E)$ varies little over a large part of the epithermal range (potential scattering), under the assumptions made there is a so-called '1/E spectrum'. In thermal reactors this spectrum is approximated rather closely (except in the resonances). In systems without moderator (fast reactors), neglecting the epithermal absorption is not justified.

5.4. Fermi age theory

Equation (5.1) is the general diffusion equation for the space- and energy dependent neutron field. In section 5.3 this equation was solved for the simplified case of an infinite homogeneous medium without neutron absorption. In section 5.6 the influence of resonance absorption in an infinite homogeneous medium will be studied. In this section space dependence of the moderation process will be analyzed. In order to arrive at simple analytical expressions, neutron absorption during moderation will be neglected. The theory to be presented is known as *Fermi age theory*.

The neutron balance for a unit volume and energy interval dE for a homogeneous and absorption free medium can be written as:

$$D(E)\nabla^2 \phi(\underline{r}, E) dE = q(\underline{r}, E) - q(\underline{r}, E + dE) \tag{5.36}$$

so

$$D(E)\nabla^2 \phi(\underline{r}, E) = -\frac{\partial q}{\partial E} \tag{5.37}$$

By inserting the relation between slowing density q and neutron flux, equation (5.37) can be transformed into an equation for the slowing down density.

In the previous section we deduced for the slowing down density:

$$q(\underline{r},E) = \int\limits_{E}^{E/\alpha} \frac{E-\alpha E'}{E'(1-\alpha)} \Sigma_s(E')\phi(\underline{r},E')dE' \tag{5.38}$$

which for the case without neutron leakage is solved by:

$$E \cdot \Sigma_s(E) \cdot \phi(E) = constant \tag{5.39}$$

In case of a space dependent neutron flux, (5.39) will not be valid exactly because of neutron leakage from a volume element. However, assuming that the scattering nuclei are relatively heavy, the integration interval in (5.38) will be small ($\alpha \approx 1$) so (5.39) is a good approximation within the interval. The assumption is exact if the the interval width approaches zero, in other words in case the energy decrement per collision is so small that the moderation is effectively a continuous process. This approach is therefore known as the continuous slowing down model. In that case we can write for (5.38):

$$q(\underline{r},E) = E \cdot \Sigma_s(E) \cdot \phi(\underline{r},E) \cdot \int\limits_{E}^{E/\alpha} \frac{E-\alpha E'}{E'^2(1-\alpha)}dE' = \xi\Sigma_s(E) \cdot E \cdot \phi(\underline{r},E) \tag{5.40}$$

Combining (5.37) and (5.40) gives:

$$\nabla^2 q(\underline{r},E) = -\frac{\xi\Sigma_s(E)E}{D(E)} \cdot \frac{\partial q(\underline{r},E)}{\partial E} \tag{5.41}$$

By introducing a new variable:

$$d\tau = -\frac{D(E)}{\xi\Sigma_s(E)} \cdot \frac{dE}{E} \tag{5.42}$$

equation (5.41) can be written as:

$$\nabla^2 q(\underline{r},\tau) = \frac{\partial q(\underline{r},\tau)}{\partial \tau} \tag{5.43}$$

where τ is the so-called *Fermi age,* defined as:

$$\tau(E) = \int_E^{E_0} \frac{D(E')}{\xi \Sigma_s(E')} \frac{dE'}{E'} \tag{5.44}$$

where E_0 denotes the (mean) energy of the source neutrons.

The Fermi age has the dimension of (length)^2 and for this reason is also called *moderation area*. The term *age* has a historical origin because equation (5.43) is analogous to the Fourier equation for non-stationary heat transport, in which the time t replaces the τ in (5.43). The solutions of (5.43) for several geometries can therefore be found in text books on heat transport.

In order to illustrate the physical meaning of τ we take the case of a monoenergetic point source with a strength of S neutrons/s in an infinite medium. The solution of (5.43) is then given by (see fig. 5.6):

$$q(\underline{r}, \tau) = \frac{S \cdot e^{-r^2/4\tau}}{(4\pi\tau)^{3/2}} \tag{5.45}$$

Completely analogous to the way in which the diffusion length L was related to the distance travelled 'as the crow flies' by mono-energetic neutrons before being absorbed (section 2.2), we now calculate the mean quadratic distance travelled by neutrons before passing an energy E or, in other words, reaching the Fermi age $\tau(E)$:

$$\overline{r^2(\tau)} = \frac{1}{S} \int_0^\infty r^2 \cdot 4\pi r^2 q(r, \tau) dr = 6\tau \tag{5.46}$$

which is completely analogous to equation (2.32). The Fermi age or moderation area can thus be considered as 1/6th of the mean squared distance referred to.
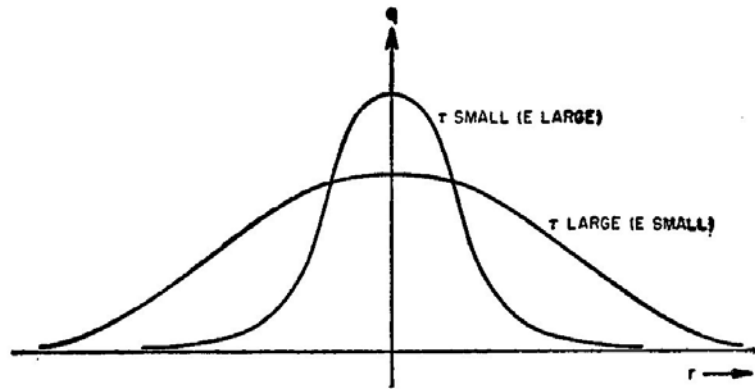
Figure 5.6. Slowing down density for a monoenergetic point source in an infinite homogeneous medium according to Fermi age theory

In fact there is a difference between the moderation area given by (5.44) and a moderation area based on the definition of 1/6th of the mean squared moderation distance 'as the crow flies'. The equation is based on the assumption of continuous slowing down, whereas the latter definition can also be applied to realistic systems in which moderation occurs in discrete steps which can be rather large like in low-A moderators. For this reason, the values given in literature for the Fermi age in moderators are based on measurements or on accurate transport calculations. In Table 5.3 values are given for experimentally determined moderation areas for fission neutrons to reach thermal energy (usually referred to as 'the' Fermi age in a moderator, although more general this quantity depends on both initial and final energies considered).

Table 5.3. Fermi age for fission neutrons in some moderators

Moderator	Age in cm^2
water	33
heavy water	120
beryllium	98
graphite	350

5.5. The thermal neutron spectrum

When fission neutrons are brought into an infinite medium that is free of absorption, after moderation they will become in 'thermal' equilibrium with the moderator nuclei, *i.e.* the neutrons behave as a strongly diluted gas in thermal equilibrium. Their energy distribution is thus given by the Maxwell-Boltzmann distribution for particles of an ideal gas at temperature T

$$M(E) = \frac{2\pi}{(\pi kT)^{3/2}} \sqrt{E} \exp\left(-\frac{E}{kT}\right) \tag{5.47}$$

in which k is the Boltzmann constant (k = 8.52·10^{-5} eV/K). The distribution function M(E) is normalised, so that the energy integral is equal to 1.

For the thermal flux density it thus holds that

$$\phi_M(E) = n_0 v M(E) = \frac{2\pi n_0}{(\pi kT)^{3/2}} \sqrt{2/m} E \exp\left(-\frac{E}{kT}\right)$$ (5.48)

in which n_0 is the total thermal neutron density. This distribution is shown in Figure 5.7.

The most probable energy (for which the spectrum is maximum) is E = kT. At room temperature this is 0.025 eV. The velocity corresponding with this energy is 2200 m/s. Therefore, tables of 'thermal cross sections' usually give the value for this velocity. At a reactor temperature of 590 K, a value characteristic of water-moderated reactors, the most probable velocity is 3100 m/s and the corresponding energy is 0.051 eV.

The distribution (5.48) only holds for complete thermal equilibrium. In a nuclear reactor this equilibrium will never be complete because of absorption of neutrons and continuous 'supply' of neutrons from the epithermal range by moderation. As most absorption cross sections at low energy show $1/\sqrt{E}$ behaviour (Section 1.4), low-energy neutrons are absorbed preferentially, which leads to a shift of the spectrum to higher energies. The continuous supply of slowing-
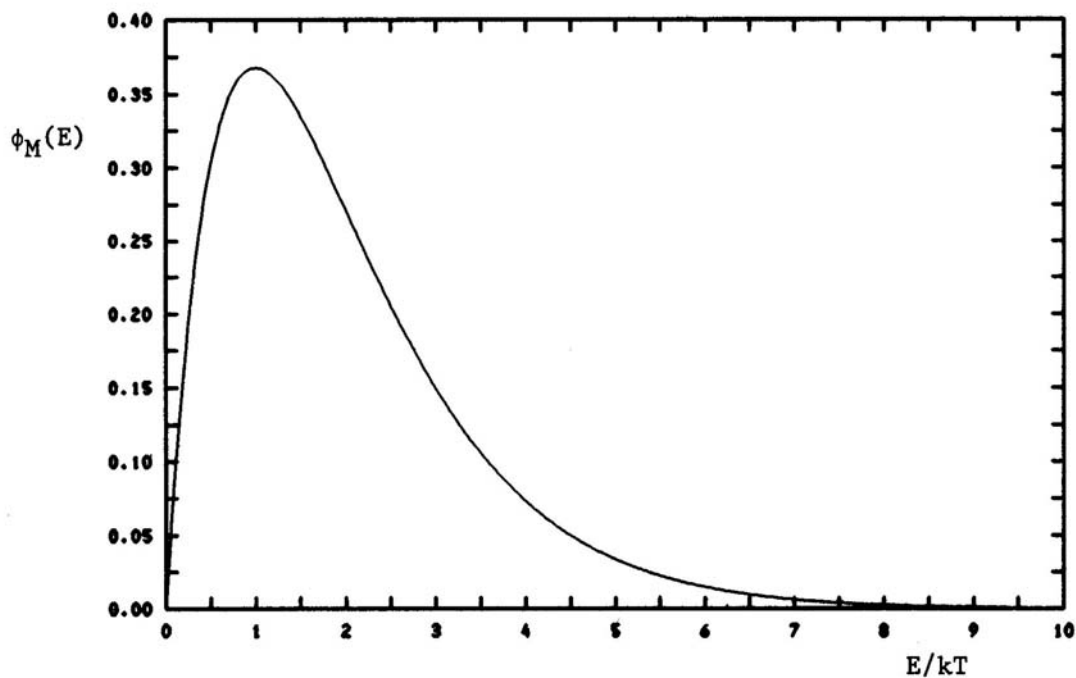
Figure 5.7. Thermal flux density based on the Maxwell-Boltzmann equation

down neutrons has a comparable effect, because at the high-energy side the thermal spectrum has a '1/E tail'.

Although neutron leakage has an opposite effect, because with decreasing energy the diffusion coefficient D decreases as a result of the increasing cross sections and the leakage preferentially removes neutrons with higher energies, this effect is much less important. In order that the spectrum can still be described well with (5.48), one can introduce a neutron temperature T_n, which will be higher than the actual temperature.

For global reactor calculations the thermal neutrons are treated as one group. For calculating the group thermal cross sections with (5.5) – (5.8), the thermal spectrum must be taken into account. In this way the thermal average absorption cross section with a 1/v dependence becomes

$$\sigma_{a,th} = \frac{\int_0^\infty \sigma_a(E)\phi_M(E,T_n)dE}{\int_0^\infty \phi_M(E,T_n)dE} = \tfrac{1}{2}\sqrt{\pi}\,\sigma_{a0}\sqrt{293/T_n} \qquad (5.49)$$

in which σ_{a0} is the microscopic absorption cross section for 2200 m/s neutrons and T_n the effective neutron temperature of the thermal spectrum in K.

Table 5.4 gives microscopic and macroscopic cross sections of all elements for 2200 m/s neutrons. As this table has reference to elements nature with their natural isotopic composition, the cross sections of, for example, enriched uranium cannot be read from this table.

5.6. Calculation of group cross sections

On the ground of the considerations in the previous sections, we can now make a global representation of the neutron spectrum in a thermal reactor for all energies. In the fast region (roughly above 100 keV) it will have the shape of a fission spectrum according to (1.2). In the epithermal region the spectrum will show a 1/E behaviour (except for the resonances) and in the thermal region (roughly down to 0.5 eV) a Maxwell-Boltzmann distribution according to (5.48). Such a spectrum is shown schematically in Figure 5.8.
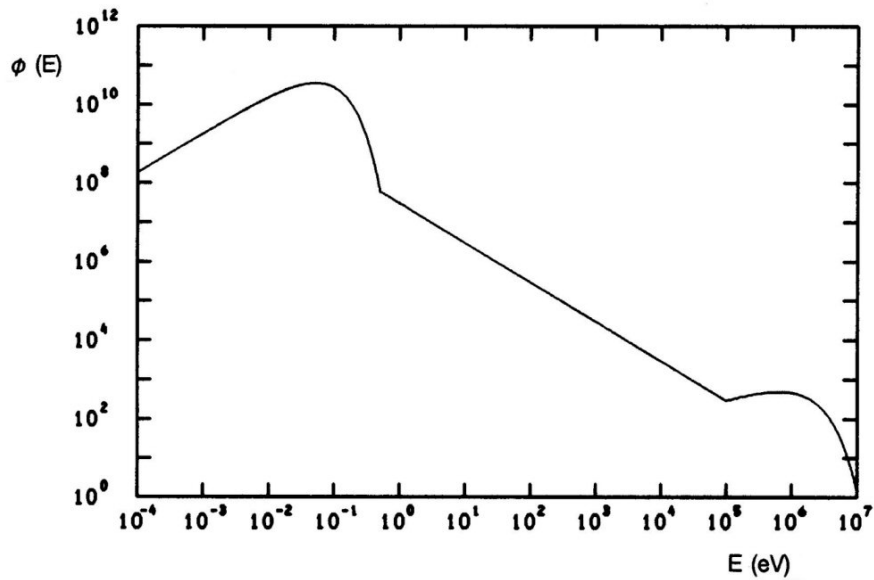
Figure 5.8. Schematic flux spectrum in a thermal reactor

This schematic spectrum is often used as averaging spectrum for the calculation of group cross sections according to (5.5) – (5.8). If this is done for a large number of small groups (*circa* 200) the deviation of the actual spectrum within a group will be small.

After that, one could do a multi-group diffusion calculation with the actual reactor geometry. With a large number of energy groups this is hardly feasible. Therefore, one first applies *condensation* of energy groups, *i.e.* combining energy groups into a limited number of broad groups. The cross sections for the broad groups are then calculated using the neutron spectrum that is obtained from a calculation with the fine groups, but with much simplified representation of the geometry, for example a one-dimensional representation.

Table 5.4. Neutron cross sections of the elements for 2200 m/s neutrons

Atomic No.	Element or Compound	Atomic or Mol. Wt.	Density, gm/cm^3	Nuclei per Unit Vol. $\times 10^{-24}$	$1-\bar{\mu}_0$	ξ	Microscopic Cross Section, barn			Macroscopic Cross Section, cm^{-1}		
							σ_a	σ_s	σ_t	Σ_a	Σ_s	Σ_t
1	H	1.008	8.9^a	5.3^a	0.3386	1.000	0.33	38	38	1.7^a	0.002	0.002
	H$_2$O	18.016	1	0.0335^b	0.676	0.948	0.66	103	103	0.022	3.45	3.45
	D$_2$O	20.030	1.10	0.0331^b	0.884	0.570	0.001	13.6	13.6	3.3^a	0.449	0.449
2	He	4.003	17.8^a	2.6^a	0.8334	0.425	0.007	0.8	0.807	0.02^a	2.1^a	2.1^a
3	Li	6.940	0.534	0.0463	0.9047	0.268	71	1.4	72.4	3.29	0.065	3.35
4	Be	9.013	1.85	0.1236	0.9259	0.209	0.010	7.0	7.01	124^a	0.865	0.865
	BeO	25.02	3.025	0.0728^b	0.939	0.173	0.010	6.8	6.8	73^a	0.501	0.501
5	B	10.82	2.45	0.1364	0.9394	0.171	755	4	759	103	0.346	104
6	C	12.011	1.60	0.0803	0.9444	0.158	0.004	4.8	4.80	32^a	0.385	0.385
7	N	14.008	0.0013	5.3^a	0.9524	0.136	1.88	10	11.9	9.9^a	50^a	60^a
8	O	16.000	0.0014	5.3^a	0.9583	0.120	20^a	4.2	4.2	0.000	21^a	21^a
9	F '	19.00	0.0017	5.3^a	0.9649	0.102	0.001	3.9	3.90	0.01^a	20^a	20^a
10	Ne	20.183	0.0009	2.6^a	0.9667	0.0968	<2.8	2.4	5.2	7.3^a	6.2^a	13.5^a
11	Na	22.991	0.971	0.0254	0.9710	0.0845	0.525	4	4.53	0.013	0.102	0.115
12	Mg	24.32	1.74	0.0431	0.9722	0.0811	0.069	3.6	3.67	0.003	0.155	0.158
13	Al	26.98	2.699	0.0602	0.9754	0.0723	0.241	1.4	1.64	0.015	0.084	0.099
14	Si	28.09	2.42	0.0522	0.9762	0.0698	0.16	1.7	1.86	0.008	0.089	0.097
15	P	30.975	1.82	0.0354	0.9785	0.0632	0.20	5	5.20	0.007	0.177	0.184
16	S	32.066	2.07	0.0389	0.9792	0.0612	0.52	1.1	1.62	0.020	0.043	0.063
17	Cl	35.457	0.0032	5.3^a	0.9810	0.0561	33.8	16	49.8	0.002	80^a	0.003
18	A	39.944	0.0018	2.6^a	0.9833	0.0492	0.66	1.5	2.16	1.7^a	3.9^a	5.6^a
19	K	39.100	0.87	0.0134	0.9829	0.0504	2.07	1.5	3.57	0.028	0.020	0.048
20	Ca	40.08	1.55	0.0233	0.9633	0.0492	0.44	3.0	3.44	0.010	0.070	0.080
21	Sc	44.96	2.5	0.0335	0.9852	0.0438	24	24	48	0.804	0.804	1.61
22	Ti	47.90	4.5	0.0566	0.9861	0.0411	5.8	4	9.8	0.328	0.226	0.555
23	V	50.95	5.96	0.0704	0.9869	0.0387	5	5	10.0	0.352	0.352	0.704
24	Cr	52.01	7.1	0.0822	0.9872	0.0385	3.1	3	6.1	0.255	0.247	0.501
25	Mn	54.94	7.2	0.0789	0.9878	0.0359	13.2	2.3	15.5	1.04	0.181	1.22
26	Fe	55.85	7.86	0.0848	0.9881	0.0353	2.62	11	13.6	0.222	0.933	1.15
27	Co	58.94	8.9	0.0910	0.9887	0.0335	38	7	45	3.46	0.637	4.10
28	Ni	58.71	8.90	0.0913	0.9887	0.0335	4.6	17.5	22.1	0.420	1.60	2.02
29	Cu	63.54	8.94	0.0848	0.9896	0.0309	3.85	7.2	11.05	0.326	0.611	0.937
30	Zn	65.38	7.14	0.0658	0.9897	0.0304	1.10	3.6	4.70	0.072	0.237	0.309
31	Ga	69.72	5.91	0.0511	0.9925	0.0283	2.80	4	6.80	0.143	0.204	0.347
32	Ge	72.60	5.36	0.0445	0.9909	0.0271	2.45	3	5.45	0.109	0.134	0.243
33	As	74.91	5.73	0.0461	0.9911	0.0264	4.3	6	10.3	0.198	0.277	0.475
34	Se	78.96	4.8	0.0366	0.9916	0.0251	12.3	11	23.3	0.450	0.403	0.853
35	Br	79.916	3.12	0.0235	0.9917	0.0247	6.7	6	12.7	0.157	0.141	0.298
36	Kr	83.80	0.0037	2.6^a	0.9921	0.0236	31	7.2	38.2	81^a	19^a	99^a
37	Rb	85.48	1.53	0.0108	0.9922	0.0233	0.73	12	12.7	0.008	0.130	0.138
38	Sr	87.63	2.54	0.0175	0.9925	0.0226	1.21	10	11.2	0.021	0.175	0.195
39	Yt	88.92	5.51	0.0373	0.9925	0.0223	1.31	3	4.3	0.049	0.112	0.160
40	Zr	91.22	6.4	0.0423	0.9927	0.0218	0.185	8	8.2	0.008	0.338	0.347
41	Nb	92.91	8.4	0.0545	0.9928	0.0214	1.16	5	6.16	0.063	0.273	0.336
42	Mo	95.95	10.2	0.0640	0.9931	0.0207	2.70	7	9.70	0.173	0.448	0.621
43	Tc	98	—	—	0.9932	0.0203	22	—	—	—	—	—
44	Ru	101.1	12.2	0.0727	0.9934	0.0197	2.56	6	8.56	0.186	0.436	0.622
45	Rh	102.91	12.5	0.0732	0.9935	0.0193	149	5	154	10.9	0.366	11.3
46	Pd	106.4	12.16	0.0689	0.9937	0.0187	8	3.6	11.6	0.551	0.248	0.799
47	Ag	107.88	10.5	0.0586	0.9938	0.0184	63	6	69	3.69	0.352	4.04
48	Cd	112.41	8.65	0.0464	0.9940	0.0178	2,450	7	2,457	114	0.325	114
49	In	114.82	7.28	0.0382	0.9942	0.0173	191	2.2	193	7.30	0.084	7.37
50	Sn	118.70	6.5	0.0330	0.9944	0.0167	0.625	4	4.6	0.021	0.132	0.152
51	Sb	121.76	6.69	0.0331	0.9945	0.0163	5.7	4.3	10.0	0.189	0.142	0.331
52	Te	127.61	6.24	0.0295	0.9948	0.0155	4.7	5	9.7	0.139	0.148	0.286
53	I	126.91	4.93	0.0234	0.9948	0.0157	7.0	3.6	10.6	0.164	0.084	0.248
54	Xe	131.30	0.0059	2.7^a	0.9949	0.0152	35	4.3	39.3	95^a	12^a	0.001
55	Cs	132.91	1.873	0.0085	0.9950	0.0150	28	20	48	0.238	0.170	0.408
56	Ba	137.36	3.5	0.0154	0.9951	0.0145	1.2	8	9.2	0.018	0.123	0.142
57	La	138.92	6.19	0.0268	0.9952	0.0143	8.9	15	24	0.239	0.403	0.642
58	Ce	140.13	6.78	0.0292	0.9952	0.0142	0.73	9	9.7	0.021	0.263	0.283
59	Pr	140.92	6.78	0.0290	0.9953	0.0141	11.3	4	15.3	0.328	0.116	0.444
60	Nd	144.27	6.95	0.0290	0.9954	0.0138	46	16	62	1.33	0.464	1.79

Atomic No.	Element or Compound	Atomic or Mol. Wt.	Density, gm/cm³	Nuclei per Unit Vol. × 10⁻²⁴	$1-\bar{\mu}_0$	ξ	Microscopic Cross Section, barn			Macroscopic Cross Section, cm⁻¹		
							σ_a	σ_s	σ_t	Σ_a	Σ_s	Σ_t
61	Pm	145	—	—	0.9954	0.0137	60	—	—	—	—	—
62	Sm	150.35	7.7	0.0309	0.9956	0.0133	5,600	5	5,605	173	0.155	173
	Sm₂O₃	348.70	7.43	0.0128ᵇ	0.974	0.076	16,500	22.6	16,500	211	0.289	211
63	Eu	152	5.22	0.0207	0.9956	0.0131	4,300	8	4,308	89.0	0.166	89.2
	Eu₂O₃	352.00	7.42	0.0127ᵇ	0.978	0.063	8,740	30.2	8,770	111	0.383	111
64	Gd	157.26	7.95	0.0305	0.9958	0.0127	46,000	—	—	1,403	—	—
65	Tb	158.93	8.33	0.0316	0.9958	0.0125	46	—	—	1.45	—	—
66	Dy	162.51	8.56	0.0317	0.9959	0.0122	950	100	1,050	30.1	3.17	33.3
	Dy₂O₃	372.92	7.81	0.0126ᵇ	0.993	0.019	2,200	214	2,414	27.7	2.7	30.4
67	Ho	164.94	8.76	0.0320	0.9960	0.0121	65	—	—	2.08	—	—
68	Er	167.27	9.16	0.0330	0.9960	0.0119	173	15	188	5.71	0.495	6.20
69	Tm	168.94	9.35	0.0333	0.9961	0.0118	127	7	134	4.23	0.233	4.46
70	Yb	173.04	7.01	0.0244	0.9961	0.0115	37	12	49	0.903	0.293	1.20
71	Lu	174.99	9.74	0.0335	0.9962	0.0114	112	—	—	3.75	—	—
72	Hf	178.5	13.3	0.0449	0.9963	0.0112	105	8	113	4.71	0.359	5.07
73	Ta	180.95	16.6	0.0553	0.9963	0.0110	21	5	26	1.16	0.277	1.44
74	W	183.86	19.3	0.0632	0.9964	0.0108	19.2	5	24.2	1.21	0.316	1.53
75	Re	186.22	20.53	0.0664	0.9964	0.0107	86	14	100	5.71	0.930	6.64
76	Os	190.2	22.48	0.0712	0.9965	0.0105	15.3	11	26.3	1.09	0.783	1.87
77	Ir	192.2	22.42	0.0703	0.9965	0.0104	440	—	—	30.9	—	—
78	Pt	195.09	21.37	0.0660	0.9966	0.0102	8.8	10	18.8	0.581	0.660	1.24
79	Au	197	19.32	0.0591	0.9966	0.0101	98.8	9.3	107.3	5.79	0.550	6.34
80	Hg	200.61	13.55	0.0407	0.9967	0.0099	380	20	400	15.5	0.814	16.3
81	Tl	204.39	11.85	0.0349	0.9967	0.0098	3.4	14	17.4	0.119	0.489	0.607
82	Pb	207.21	11.35	0.0330	0.9968	0.0096	0.170	11	11.2	0.006	0.363	0.369
83	Bi	209	9.747	0.0281	0.9968	0.0095	0.034	9	9	0.001	0.253	0.256
84	Po	210	9.24	0.0265	0.9968	0.0095	—	—	—	—	—	—
85	At	211	—	—	0.9968	0.0094	—	—	—	—	—	—
86	Rn	222	0.0097	2.6ᵃ	0.9970	0.0090	0.7	—	—	—	—	—
87	Fr	223	—	—	0.9980	0.0089	—	—	—	—	—	—
88	Ra	226.05	5	0.0133	0.9971	0.0088	20	—	—	0.266	—	—
89	Ac	227	—	—	0.9971	0.0088	510	—	—	—	—	—
90	Th	232.05	11.3	0.0293	0.9971	0.0086	7.56	12.6	20.2	0.222	0.369	0.592
91	Pa	231	15.4	0.0402	0.9971	0.0086	200	—	—	8.04	—	—
92	U	238.07	18.9	0.04783	0.9972	0.0084	7.68	8.3	16.0	0.367	0.397	0.765
	UO₂	270.07	10	0.0223ᵇ	0.9887	0.036	7.6	16.7	24.3	0.169	0.372	0.542
93	Np	237	—	—	0.9972	0.0084	170	—	—	—	—	—
94	Pu	239	19.74	0.0498	0.9972	0.0083	1,026	9.6	1,036	51.1	0.478	51.6
95	Am	242	—	—	0.9973	0.0082	8.000	—	—	—	—	—
96	Cm	245	—	—	0.9973	0.0081	—	—	—	—	—	—
97	Bk	249	—	—	0.9973	0.0081	500	—	—	—	—	—
98	Cf	249	—	—	0.9973	0.0079	900	—	—	—	—	—
99	E	253	—	—	0.9974	0.0079	160	—	—	—	—	—
100	Fm	256	—	—	0.9974	0.0078	—	—	—	—	—	—
101	Mv	260	—	—	0.9974	0.0077	—	—	—	—	—	—

ᵃValue has been multiplied by 10⁵.
ᵇMolecules/cm³.

If the fine-group fluxes are given by ϕ_i, the microscopic cross section σ_{xg} for reaction type x (e.g. absorption) and for broad group g comprising the fine groups n_{g1} up to and including n_{g2} can be calculated from

$$\sigma_{xg} = \frac{\sum_{n_{g1}}^{n_{g2}} \sigma_{xi}\phi_i}{\sum_{n_{g1}}^{n_{g2}} \phi_i} \tag{5.50}$$

analogous to the integral form of (5.5).

With the broad-group cross sections obtained in this way, one can subsequently perform a reactor calculation with a more realistic representation of the geometry. However, often another intermediate step is necessary because of the very heterogeneous geometry of the reactor core: many fuel rods with cladding and surrounded by coolant / moderator, with in addition construction material and control rods.

For a large homogeneous reactor core (*i.e.* large with respect to the slowing-down and/or diffusion length of the neutrons), in which the neutron spectrum in the largest part of the core is position independent, one obtains a method that can still be applied well for calculating broad-group cross sections. The spectrum is characteristic of the composition of the core and is called the equilibrium spectrum. The spatial independence of this spectrum implies that for all (fine) groups the following equation holds

$$\nabla^2\phi + B^2\phi = 0 \tag{5.51}$$

in which B^2 is the buckling factor, which depends on the dimensions of the core (Table 3.1). As one can now replace the term $D_g\nabla^2\phi_g$ in the diffusion equation by $-D_gB^2\phi_g$ for each group, one obtains a system of linear algebraic equations that can be solved by iteration. One sometimes calls this a 'half-dimensional' calculation, because the spatial dependence is not taken into account explicitly, but neutron leakage is still taken into account.

The system of multi-group diffusion equations (5.3) for an eigenvalue problem now gets the form

$$D_g B^2\phi_g + \Sigma_{vg}\phi_g - \frac{\chi_g}{k}\sum_{g'}^{G}\nu_{g'}\Sigma_{fg'}\phi_{g'} - \sum_{g'\neq g}^{G}\Sigma_{g'g}\phi_{g'} = 0 \tag{5.52}$$

with G the number of groups and Σ_{vg} the removal cross section for group g

$$\Sigma_{vg} = \Sigma_{ag} + \sum_{g'\neq g}^{G}\Sigma_{gg'} \tag{5.53}$$

The total neutron flux can be normalised arbitrarily; a common choice is

$$\frac{1}{k}\sum_{g'}^{G}\nu_{g'}\Sigma_{fg'}\phi_{g'} = 1 \text{ cm}^{-3}\text{s}^{-1} \tag{5.54}$$

so that the system of algebraic equations to be solved becomes

$$D_g B^2 \phi_g + \Sigma_{vg}\phi_g - \sum_{g' \neq g}^{G} \Sigma_{g'g}\phi_{g'} = \chi_g \tag{5.55}$$

For a certain choice of B^2, after solution of (5.55) and substitution of the group spectrum ϕ_g' (g' = 1, …, G) in (5.54), one finds the corresponding eigenvalue k, the effective multiplication factor (for $B^2 = 0$ one finds the value of k_∞). Via iteration one can find the material buckling factor corresponding with k = 1.

As demonstration of such a half-dimensional calculation we take a three-group calculation for a fast reactor, consisting of 10 % ^{235}U and 90 % ^{238}U (atomic percents). The group parameters for the group boundaries 0, 0.4 MeV, 1.35 MeV and 10 MeV are given in Table 5.5.

Table 5.5. Parameters for three-group calculation (neutron cross sections in barn)

Nuclide	^{235}U			^{238}U		
group	1	2	3	1	2	3
ν	2.70	2.53	2.47	2.60	2.47	0
σ_f	1.29	1.27	1.77	0.524	0.01	0
σ_c	0.08	0.13	0.49	0.036	0.130	0.260
σ_{tr}	4.5	5.7	10	4.6	5.8	9.6
$\sigma_{g \rightarrow g+1}$	1.00	0.50	0	1.41	0.25	0
$\sigma_{g \rightarrow g+2}$	0.50	0	0	0.64	0	0
χ_g	0.575	0.326	0.099	0.575	0.326	0.099

The system of equations (5.55) that must be solved for the core with atomic number densities $^{235}N = 0.0048 \cdot 10^{24}$ cm^{-3} and $^{238}N = 0.0432 \cdot 10^{24}$ cm^{-3} considered here, is

$$\underset{D_1}{(1.513\,B^2 + 0.127)}\underset{\Sigma_{v1}}{\phi_1} = \underset{\chi_1}{0.575}$$

$$\underset{D_2}{(1.199\,B^2 + 0.026)}\underset{\Sigma_{v2}}{\phi_2} - \underset{\Sigma_{1 \rightarrow 2}}{0.0657\phi_1} = \underset{\chi_2}{0.326} \tag{5.56}$$

$$\underset{D_3}{(0.720\,B^2 + 0.022)}\underset{\Sigma_{v3}}{\phi_3} - \underset{\Sigma_{1 \rightarrow 3}}{0.030\phi_1} - \underset{\Sigma_{2 \rightarrow 3}}{0.0132\phi_2} = \underset{\chi_3}{0.099}$$

in which

$$D_g = \frac{1}{3\Sigma_{tr,g}} = \frac{1}{3\sum_1 N_i \sigma_{tr,g,i}} \tag{5.57}$$

Because scattering only occurs to groups of lower energy, the system can be solved easily. For $B^2 = 0$ one finds the so-called 'infinite-medium spectrum':

$\phi_1 = 4.544$ cm^{-2} s^{-1}

$\phi_2 = 24.05$ cm^{-2} s^{-1}

$\phi_3 = 25.05$ cm^{-2} s^{-1}

and by substitution in (5.54)

$$k_\infty = \sum_{g=1}^{3} v_g \Sigma_{fg} \phi_g = 0.0756\phi_1 + 0.0165\phi_2 + 0.0210\phi_3 = 1.266$$

By iteration one finds the critical buckling factor $B^2 = 0.00580$ cm^{-2} and the corresponding spectrum in the critical reactor:

$\phi_1 = 4.25$ cm^{-2} s^{-1}

$\phi_2 = 18.39$ cm^{-2} s^{-1}

$\phi_3 = 17.88$ cm^{-2} s^{-1}

By comparison with the infinite-medium spectrum, one sees that the spectrum in the critical reactor is much 'harder', *i.e.* has a higher average energy.

Incidentally, we can also determine the extrapolated radius of, for example, a spherical critical core of 10 atom percents enriched uranium. This amounts to R = π/B $\approx$ 41 cm.

With the spectrum for a critical reactor, one can subsequently determine the cross sections for a one-group calculation. The results are given in Table 5.6.

Table 5.6. Condensed one-group parameters

Nuclide	^{235}U	^{238}U
ν	2.51	2.59
σ_f	1.493	0.0595
σ_c	0.284	0.178
σ_{tr}	7.47	7.35

The transport cross sections have also been calculated according to (5.50). From this one can then determine the diffusion coefficient for the one-group calculation. However, by analogy with (5.6), one would have to average the diffusion coefficient over the fine-group fluxes. This yields a somewhat different result. If one uses the directly averaged diffusion coefficient, then the one-group calculation yields the same critical buckling factor and thus the correct critical radius. The value of k_∞ is, however, different than for the three-group calculation, because it has been determined with a different flux spectrum than for the critical sphere.

Notice that for a different enrichment percentage, different macroscopic cross sections appear in (5.56) and by that a different flux spectrum, so that the one-group parameters are also different.

5.7. Treatment of resonances

The method for calculating fine-group cross sections with an assumed flux spectrum $\phi(E)$ proportional to 1/E in the epithermal energy region as sketched above is not applicable for resonances in the microscopic cross section, because the flux then will considerably deviate from the 1/E behaviour. For a correct representation of especially the absorption as a result of resonances, a further elaboration is necessary.

In thermal reactors the nuclear fuel is present together with a moderator, If we assume the nuclear fuel and moderator to be homogeneously mixed, the equation for the flux by extension of (5.32) becomes

$$\left(\Sigma_a^F(E)+\Sigma_s^F+\Sigma_s^M\right)\phi(E)=\int\limits_{E}^{E/\alpha_F}\frac{\Sigma_s^F\phi(E')}{E'(1-\alpha_F)}dE'+\int\limits_{E}^{E/\alpha_M}\frac{\Sigma_s^M\phi(E')}{E'(1-\alpha_M)}dE' \qquad (5.58)$$

In the left part now also absorption in the nuclear fuel (superscript F) has been included, while the right part is a sum of moderation contributions of nuclear fuel and moderator. At the same time, the scattering cross sections are considered to be energy-independent (potential scattering in the nuclear fuel). If the energy E is in the resonance and the width of the resonance is small with respect to the interval over which scattering can take place ('narrow resonance' approximation), then we may set the flux in the integrals in the right part equal to the flux prevailing above the resonance, where absorption is negligible. There the flux is proportional to 1/E according to (5.35). This means that the flux per unit of lethargy, defined in (5.29), is constant outside the resonance:

$$\phi_{br}(u)=\phi_{br}(E)\left|\frac{dE}{du}\right|=E\phi_{br}(E)=\phi_u \qquad (5.59)$$

Substitution of (5.59) yields

$$\phi(E)=\frac{\phi_u\Sigma_0/E}{\Sigma_a(E)+\Sigma_0}=\frac{\phi_u}{1+\Sigma_a(E)/\Sigma_0}\frac{1}{E} \qquad (5.60)$$

for the flux in the resonance. Here $\Sigma_0 = \Sigma^F_s + \Sigma^M_s$ is the total macroscopic scattering cross section. The absorption in the resonance then becomes

$$\int \Sigma_a(E)\phi(E)dE = \int \frac{\Sigma_a(E)\phi_u}{1+\Sigma_a(E)/\Sigma_0}\frac{dE}{E} = N^F\phi_u\int \frac{\sigma_a(E)}{1+\sigma_a(E)/\sigma_0}\frac{dE}{E} \tag{5.61}$$

Here σ_0 is a fictitious microscopic cross section equal to the total (potential) scattering cross section *per nuclear fuel atom*. The integral must be taken over the width of the resonance. For the determination of the group cross section for absorption, the contributions of all resonances in that group should be summed. This means that the integral in (5.61) can be taken over the whole energy interval of the group, because the absorption cross section outside the resonances is negligibly small. Such an integral is called the resonance integral and in fact is an effective microscopic cross section, which, multiplied by the flux per unit of lethargy that would prevail without absorption, gives the correct absorption rate. The resonance integral is dependent on the "surroundings" in which the nuclear fuel is present through σ_0. The resonance integrals are usually calculated numerically for a number of values of σ_0 by substitution of the Breit-Wigner equation (1.11) for the resonance absorption cross section. If σ_0 is very large, the 1/E flux remains valid also in the resonance and one speaks of the infinitely diluted resonance integral. In other cases self-shielding occurs. The flux in the resonance is lowered by the presence of the absorber and less absorption occurs.

Chapter 6

The neutron cycle in a thermal reactor

6.1. The four-factor equation

In chapter 3 a reactor analysis based on the diffusion theory has been presented, which can be applied to a large variety of reactors (both fast and thermal).

In this chapter, we will approach the processes inside a reactor from a different point of view, which will lead to an equation for the calculation of the infinite and finite multiplication factor of a reactor. The method has been developed in the early years of nuclear energy and is only applicable to thermal reactors. Although this method provides considerably less detailed information and is less accurate, it does give a good insight in the parameters that are important reactor-physically and for that reason is still of value.

Whereas the spectrum of a fast reactor has the character of a degraded fission spectrum, the spectrum of the thermal reactor is composed of a fission spectrum, an epithermal spectrum of neutrons being slowed down and a thermal spectrum. The difference between both reactor types clearly finds expression in Figure 6.1, in which the fission density is shown per unit of lethargy

$$\Sigma_f \phi(u) = \Sigma_f E \phi(E) \quad .$$
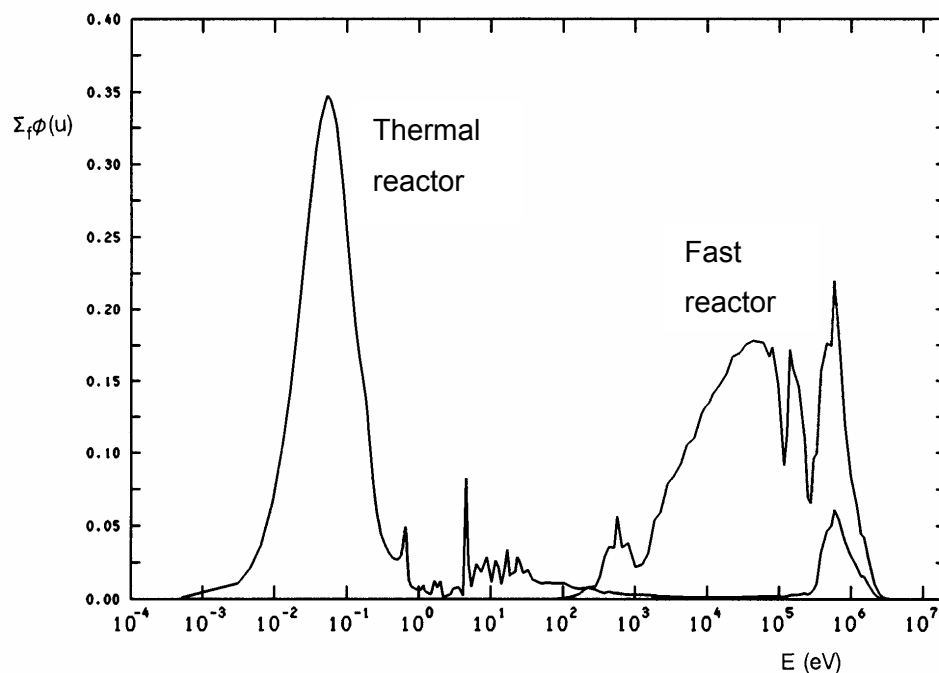
Figure 6.1. Fission density of neutrons in a thermal and a fast reactor

In fast reactors, fissions are caused by neutrons with a very broad energy distribution, so that for an accurate reactor analysis a division into many energy groups is necessary. In thermal reactors, the same accuracy can be achieved with less energy groups, because the most important neutron-physical processes occur in energy regions that can be clearly separated from each other.

Figure 6.2 shows the neutron cycle in a thermal reactor.
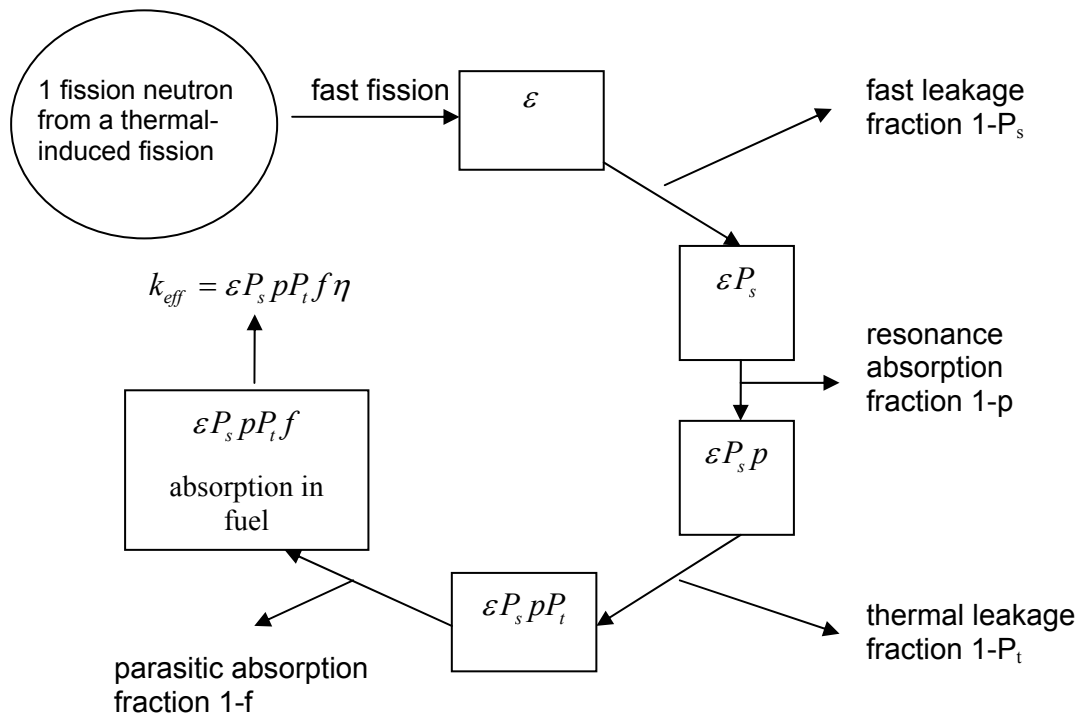
Figure 6.2. Neutron cycle in a thermal reactor

The fate of neutrons is chiefly determined by six processes:

1. The neutrons released upon fission can, as long as they have not yet been thermalised, cause so-called fast fission. As in thermal reactors natural or low-enriched (up to *circa* 4 %) uranium is used, mainly fast fission in ^{238}U occurs, for which the threshold energy is about 1 MeV, so that here the non-collided neutrons make the most important contribution.

2. During the largest part of the moderation process, leakage is the main neutron loss factor and absorption can be neglected. For this reason, the intermediate spectrum in good approximation can be described with $\phi(E) \propto 1/E$.

3. Resonance capture: during the last part of the moderation process, the neutrons 'pass through' the resonance region, where the probability of absorption in the nuclear fuel cannot

be neglected. An important part of this absorption consists of capture in ^{238}U. In addition to this loss, there is, however, also some fission of ^{235}U (see Figure 6.1).

4. Leakage of thermalised neutrons.

5. Parasitic capture of thermalised neutrons in the moderator and the construction materials (fuel cans, etc.).

6. Absorption in the nuclear fuel, partly consisting of parasitic capture and partly giving rise to fission.

One now defines six quantities:

1. The fast fission factor:

$$\varepsilon = \frac{number\ of\ fast\ neutrons}{number\ of\ fast\ neutrons\ produced\ by\ thermal\ fissions}$$

2. The fast non-leakage probability:

$$P_s = fraction\ of\ the\ fast\ neutrons\ that\ does\ not\ leak\ from\ the\ reactor$$

3. The resonance escape probability:

$$p = fraction\ of\ neutrons\ that\ passes\ through\ the\ resonance\ region\ without\ being\ absorbed$$

4. The thermal non-leakage probability:

$$P_t = fraction\ of\ the\ thermal\ neutrons\ that\ do\ not\ leak\ from\ the\ reactor$$

5. The thermal utilisation factor:

$$f = \frac{number\ of\ neutrons\ absorbed\ in\ the\ fuel}{total\ number\ of\ thermal\ neutrons\ absorbed}$$

6. The eta factor or neutron yield factor:

$$\eta = \frac{average\ number\ of\ fission\ neutrons\ released}{number\ of\ neutrons\ absorbed\ in\ the\ fuel}$$

On the basis of these definitions it can be easily seen that the infinite multiplication factor is given by the so-called four-factor equation

$$k_\infty = \varepsilon\, p f \eta \tag{6.1}$$

while the effective multiplication factor for a finite medium is given by

$$k_{eff} = k_\infty P_s P_t \tag{6.2}$$

The calculation of a thermal reactor now amounts to a calculation of the aforementioned six factors, which will be further analysed below. Before doing this, it is useful to notice that in the four-factor equation the resonance fission mentioned earlier is neglected. This is a consequence of the fact that this equation was developed when the first reactors, which used natural uranium as fuel and graphite as moderator, were realised. In these systems the mentioned omission is acceptable. For the current commercial reactors of the low-enriched light-water moderated type this simplification is not justified and the four-factor equation must be modified:

$$k_\infty = \varepsilon\, p f \eta + \varepsilon (1 - p) \eta_{res} \tag{6.3}$$

whereby η and η_{res} are the average eta factors for the thermal region and the resonance region, respectively. The effective multiplication factor then becomes

$$k_{eff} = \varepsilon\, p f \eta P_s P_t + \varepsilon (1 - p) \eta_{res} P_s \tag{6.4}$$

When calculating the factors in the four-factor equation, we must keep in mind that most reactors are composed of a large number of fuel rods provided with cladding, with moderator material around it, which often also serves as coolant (see Figure 6.3). In such a reactor lattice one can define a unit cell, which repeats itself many times. For the determination of k_∞ one can therefore limit oneself to a unit cell. One could calculate the flux behaviour in a cell by solving the diffusion equation, if one replaces the square cell by a cylindrical cell of equal geometric cross section.

The flux depends on the energy of the neutrons, because the source of neutrons is different for fast and (epi)thermal neutrons. Figure 6.4 shows characteristic examples.

For fast neutrons, the source is formed by the fission neutrons in the fuel rod. Therefore, here the flux is larger than in the moderator. For epithermal and thermal neutrons, the source is formed by neutrons that are moderated in the moderator, so that the flux in the rod is smaller

102

than in the moderator. In the case of resonance energies, the cross section in the rod is so large that the flux decreases very fast.

We will now further analyse the factors in the four-factor equation.
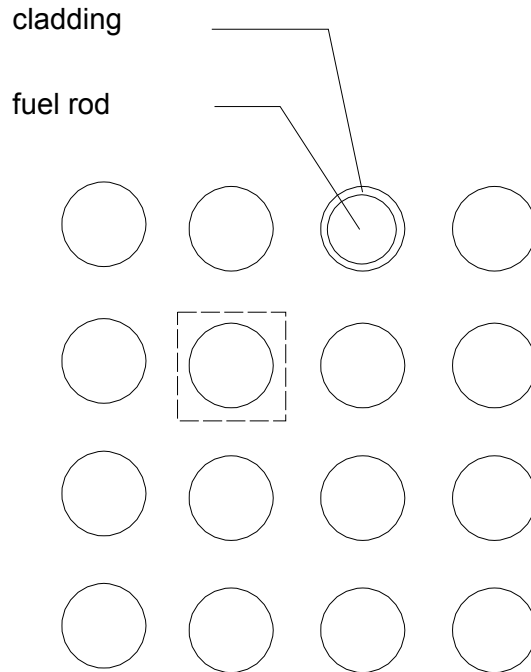

Figure 6.3. Definition of a unit cell
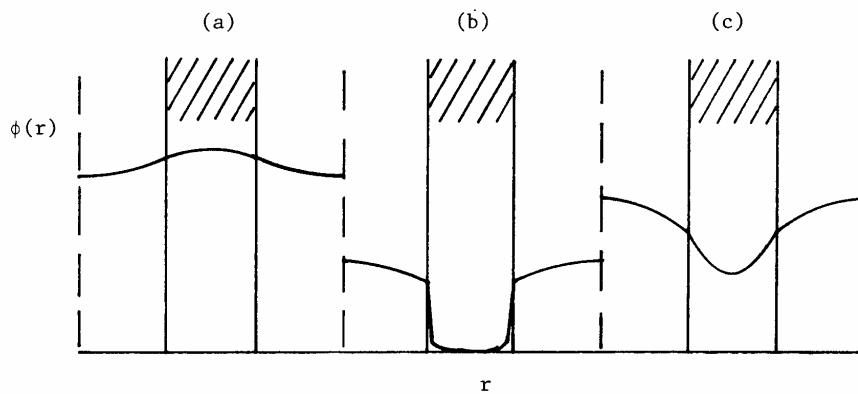
Figure 6.4. The neutron flux in a unit cell; (a) fast, (b) resonance, (c) thermal neutrons

6.2. The neutron yield factor

The eta factor is related to the nuclear fuel and hardly depends on the surrounding moderator. For fuel composed of ^{235}U and ^{238}U η is given by

$$\eta = \frac{\nu \Sigma_f}{\Sigma_f + \Sigma_c} = \nu \frac{N_5 \sigma_{f5}}{N_5 \sigma_{f5} + N_5 \sigma_{c5} + N_8 \sigma_{c8}} \qquad (6.5)$$

in which N_5 and N_8 are the atomic number densities of the isotopes ^{235}U and ^{238}U (when using other uranium isotopes or plutonium the equation is modified in a trivial way). Of course, the microscopic cross sections in this equation are averaged over the thermal region with the flux as weighting factor, analogous to (5.38). Equation (6.5) can also be written as

$$\eta = \nu \frac{e \sigma_{f5}}{e \sigma_{a5} + (1-e) \sigma_{c8}} \qquad (6.6)$$

where e is the atomic degree of enrichment

$$e = \frac{N_5}{N_5 + N_8} \qquad (6.7)$$

The microscopic cross sections for ^{235}U and ^{238}U for 2200 m/s neutrons are given in Table 6.1. For natural uranium η = 1.34. As a result of the ratios of the microscopic cross sections, η increases strongly for a low enrichment (see Figure 6.5); the limit value for pure ^{235}U is 2.08.
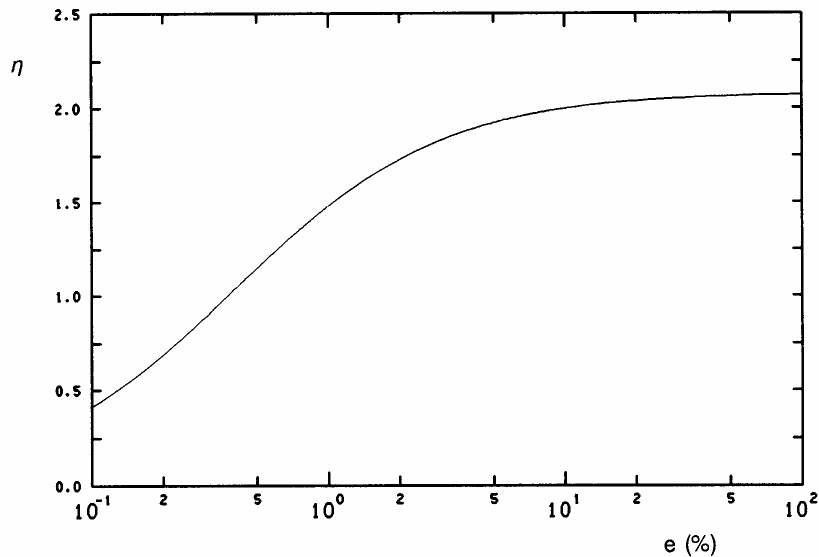

Figure 6.5. Neutron yield factor of uranium as a function of the degree of enrichment

104

Table 6.1. Microscopic cross sections at 2200 m/s

	ν	σ_f	σ_c
^{233}U	2.498	525.1	45.9
^{235}U	2.437	583.5	98.4
^{238}U	–	–	2.70
^{239}Pu	2.871	748.1	271.0

6.3. The thermal utilisation factor

The thermal utilisation factor is the fraction of the thermal neutrons that are absorbed in the nuclear fuel (all isotopes!) and is thus given by

$$f = \frac{\int_{V_F} \Sigma_{aF}\phi(\underline{r})dV}{\int_{V_F} \Sigma_{aF}\phi(\underline{r})dV + \int_{V_M} \Sigma_{aM}\phi(\underline{r})dV} = \frac{\Sigma_{aF}\phi_F V_F}{\Sigma_{aF}\phi_F V_F + \Sigma_{aM}\phi_M V_M}$$
$$= \frac{\Sigma_{aF}}{\Sigma_{aF} + \Sigma_{aM}\dfrac{\phi_M}{\phi_F}\dfrac{V_M}{V_F}}$$

(6.8)

with ϕ_F and ϕ_M the average flux in the fuel and the moderator. This equation can of course be extended for absorption in the fuel cladding. The ratio ϕ_M / ϕ_F is called the flux disadvantage factor and for thermal neutrons is larger than 1. This means that more neutrons are captured in the moderator than in the case of a flat flux in the unit cell. The thermal utilisation factor is dependent on the volume ratio of fuel and moderator and will increase with decreasing moderator-to-fuel ratio.

Notice that in our previous one-group analysis for a homogeneous reactor, the multiplication factor for an infinite system according to (3.14) is equal to

$$k_\infty = \frac{\nu\Sigma_f}{\Sigma_a} = \frac{\nu\Sigma_f}{\Sigma_a^F}\frac{\Sigma_a^F}{\Sigma_a^F + \Sigma_a^M} = \eta\,f$$

(6.9)

For this homogenised situation, the volume ratio of moderator and nuclear fuel indicates the mixing ratio of the materials.

6.4. The fast fission factor

The fission neutrons originating in the fuel rod have a probability that the first interaction takes place in the rod with the possibility of fast fission, predominantly by ^{238}U, as this usually is present in large quantities. Furthermore, a neutron can have a first interaction in another rod. If the first interaction occurs in the moderator, then the neutron will lose energy by collision and its energy will usually decrease to below 1 MeV, the fission threshold of ^{238}U, so that fast fission can no longer occur. These effects are illustrated in Figures 6.6 and 6.7. For most reactors, ε is between 1 and 1.10.
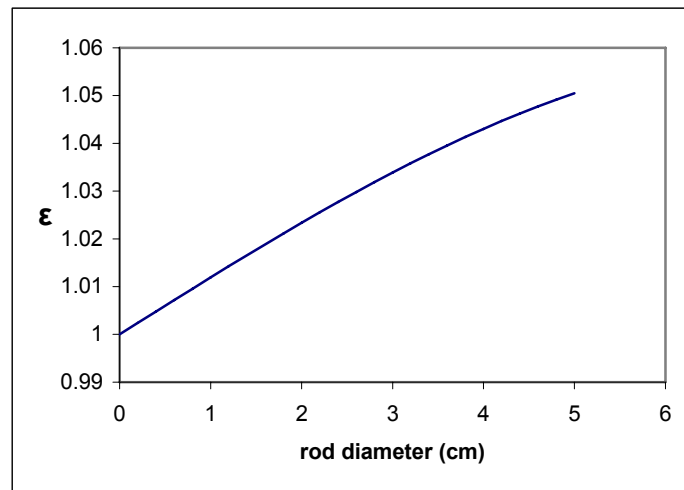

Figure 6.6. Fast fission factor for a 'solitary' cylindrical rod of natural uranium
*in water as a function of the rod diameter*
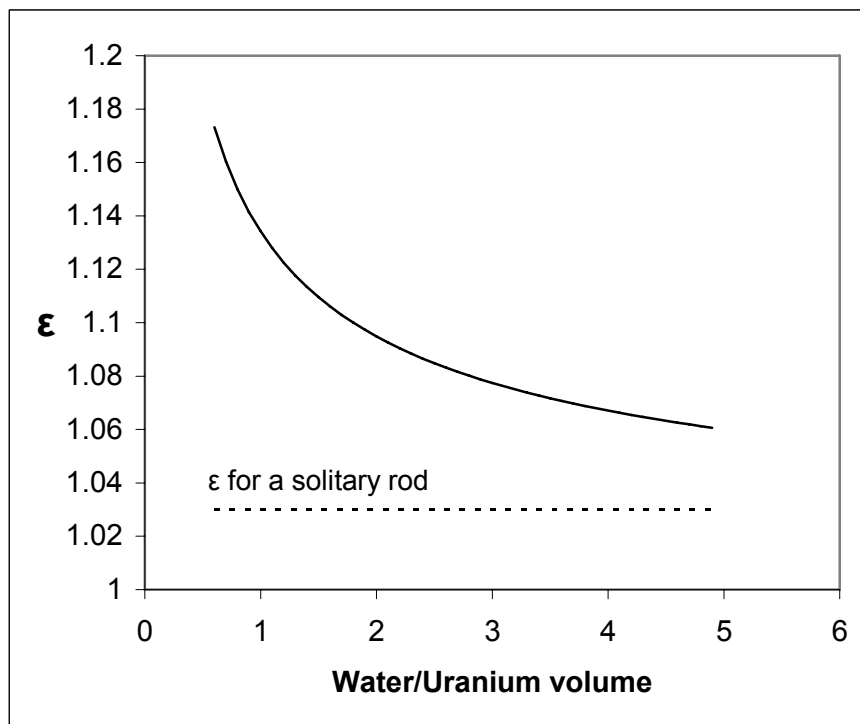
Figure 6.7. Fast fission factor for a lattice of natural-uranium rods
with a diameter of 2.5 cm in water

6.5. The resonance escape probability

In Section 5.6 it was indicated how the absorption in a resonance of the cross section can be calculated with the aid of the resonance integral according to (5.50). If we apply this to a single resonance and remember that for separate fuel and moderator the supply of the neutrons is given by the slowing-down density q_{br} in the moderator for an energy above the resonance, then the resonance escape probability p_i for resonance i is given by

$$p_i = 1 - \frac{1}{q_{br}V_M} N_F \phi_u V_F \int_i \frac{\sigma_a(E)}{1+\sigma_a(E)/\sigma_0} \frac{dE}{E} \tag{6.10}$$

The slowing-down density and the flux per unit of lethargy $\phi_u = E\phi(E)$ above the resonance are connected through (5.35), so that

$$p_i = 1 - \frac{N_F V_F}{\xi\Sigma_{sM}V_M} \int_i \frac{\sigma_a(E)}{1+\sigma_a(E)/\sigma_0} \frac{dE}{E} \tag{6.11}$$

For the resonance escape probability for all resonances we then find

$$p = \prod_i p_i \approx \exp\left(-\frac{N_F V_F}{\xi\Sigma_{sM}V_M} \sum_i \int_i \frac{\sigma_a(E)}{1+\sigma_a(E)/\sigma_0} \frac{dE}{E}\right)$$
$$= \exp\left(-\frac{N_F V_F}{\xi\Sigma_{sM}V_M} \int_{E_{th}}^{E_0} \frac{\sigma_a(E)}{1+\sigma_a(E)/\sigma_0} \frac{dE}{E}\right) = \exp\left(-\frac{N_F V_F}{\xi\Sigma_{sM}V_M} I_{eff}\right) \tag{6.12}$$

One calls the integral in this expression the effective resonance integral I_{eff}. In practical situations, this integral not only depends on the scattering cross section σ_0 per nuclear fuel atom, but also on the geometry of the unit cell (in the derivation given the spatial dependence of the flux was left out of consideration). Therefore, in the literature empirical relations have been developed for the effective resonance integral of the form

$$I_{eff} = A + B\sqrt{S/M} \tag{6.13}$$

with S the surface area of the fuel rod and M its mass. From this, one sees that with increasing rod diameter (so with decreasing S/M ratio) the effective resonance integral decreases and the resonance escape probability increases. This can be understood physically, as the absorption in a resonance will be concentrated at the surface of the rods, because of the very small free path

length of the neutrons at the resonance energy. The production of neutrons, however, takes place in the whole rod volume. Some empirical relations for I_{eff} at room temperature are

$$U: \quad I_{eff} = 2.95 + 25.8\sqrt{S/M} \quad 0.07 < \frac{S}{M} < 0.53\, cm^2/g \tag{6.14}$$

$$UO_2: \quad I_{eff} = 4.15 + 26.6\sqrt{S/M} \quad 0.08 < \frac{S}{M} < 0.7\, cm^2/g \tag{6.15}$$

with I_{eff} in barn if S in cm^2 and M in gram. As a result of the Doppler effect (Sections 1.4 and 4.4), the resonance integral also depends on the nuclear fuel temperature.

6.6. k_∞ as a function of the moderator-to-fuel ratio

In Figure 6.8 the quantities ε, p, f and η are shown as a function of the moderator-to-fuel ratio for a graphite-moderated, natural-uranium system.
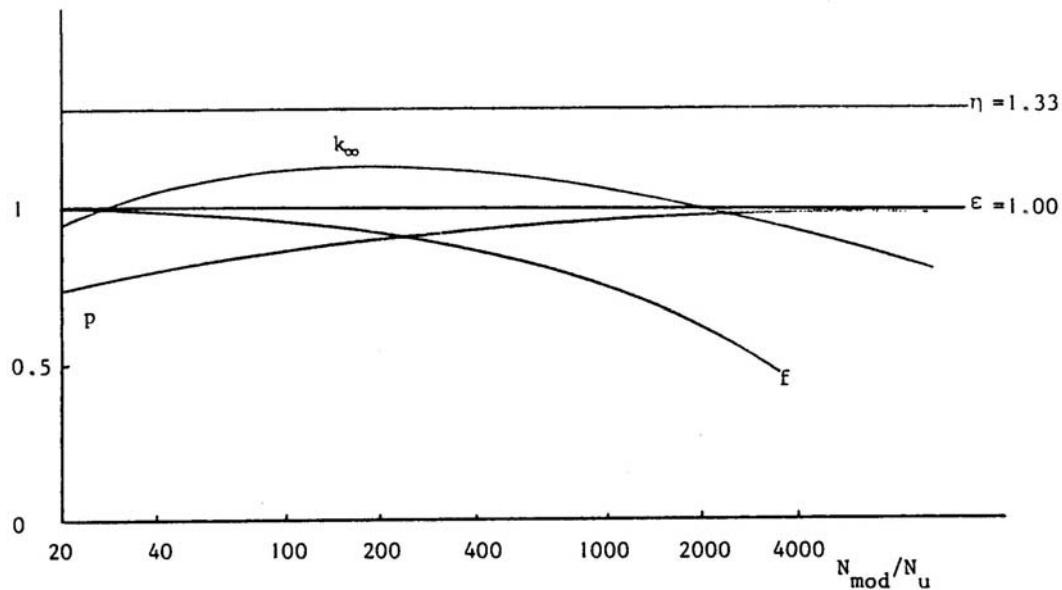
Figure 6.8. Dependence of k_∞ on the moderator-to-fuel ratio

As a result of the opposite behaviour of p and f, there is an optimum moderator-to-fuel ratio where the value of k_∞ is maximum. To the left of this optimum the reactor is undermoderated; the moderation then is insufficient and too many neutrons are lost by resonance absorption. To the right of the optimum the reactor is overmoderated; as too much moderator is present, there is too much parasitic absorption in this material.

From this figure one can also see that the moderator-to-fuel ratio is determining for the magnitude and the sign of the moderator temperature coefficient. If the temperature increases, the density of the moderator will decrease, in particular for water-moderated reactors. In an overmoderated reactor (to the right of the maximum), if the number of moderator nuclei decreases, the setpoint of the reactor will move to the left along the curve of k_∞ and k_∞ will increase, by which the reactivity increases. This yields a positive temperature coefficient. Therefore, one will choose the setpoint of the reactor to the left of the optimum, by which a negative temperature coefficient is obtained.

6.7. Leakage factors

From the one-group analysis (Section 3.1) we have already obtained an expression for the conservation factor of a reactor. Applied to the thermal neutrons this gives

$$P_t = \frac{1}{1 + B_g^2 \, L_t^2} \tag{6.16}$$

in which L_t is the diffusion length as given by (3.15) for thermal neutrons. For the fast neutrons one obtains an analogous expression by performing a two-group calculation:

$$P_s = \frac{1}{1 + B_g^2 L_f^2} \tag{6.17}$$

In the definition of the diffusion length for fast neutrons not only absorption of neutrons must be taken into account, but also neutrons that become thermal due to moderation, so that

$$L_f = \sqrt{D_s / \Sigma_{vs}} \tag{6.18}$$

with Σ_{vs} the macroscopic removal cross section for fast neutrons. In view of the analogy between the diffusion area and the moderation area, as shown in section 5.4 in the framework of Fermi age theory, L_f can be taken equal to $\tau^{1/2}$.
The effective multiplication factor then conformably (6.2) becomes

$$k_{eff} = \frac{k_\infty}{\left(1 + B_g^2 L_f^2\right)\left(1 + B_g^2 L_t^2\right)} \approx \frac{k_\infty}{1 + B_g^2\left(L_f^2 + L_t^2\right)} = \frac{k_\infty}{1 + B_g^2 M^2} \tag{6.19}$$

with which the migration surface area M^2 has been introduced:

$$M^2 = L_f^2 + L_t^2 \qquad (6.20)$$

This is a measure for the square of the crow-fly distance covered by a neutron in order to become moderated and subsequently absorbed as a thermal neutron (analogous to (2.32)). In light-water reactors the diffusion length for fast neutrons is much larger than for thermal neutrons, as a result of which fast leakage is also much more important than thermal leakage from the reactor (see Table 6.2).

Table 6.2. Transport quantities of some moderators

Material	L_t (cm)	L_f (cm)	M (cm)
H_2O	2.54	5.1	5.7
D_2O	160	11.4	160
Be	18.3	10.1	20.9
C	53.5	19.2	56.8

N.B. The value L_t depends on the purity of the material.

Chapter 7

Reactor types

7.1. Light-water reactors

In the preceding chapters we have limited ourselves completely to the analysis of the reactor core: how the composition can be chosen and how one calculates the dimensions of a critical reactor for a given composition. Although the reactor core forms the heart of the nuclear power station, in terms of dimensions the core is only a modest part of the nuclear power station. The principle of light-water reactors has already been outlined in Chapter 1.

The energy released during fission (mainly in the form of kinetic energy of the fission products; see Section 1.2, Table 1.4) is converted into heat in the nuclear fuel, as the fission products have a very small range (*circa* 5 μm). The heat developed in the fuel is removed by a coolant, which flows past the fuel elements. Whether or not through a steam generator, the heat is converted into mechanical energy in a steam turbine and finally into electrical energy in the generator (Figures 1.2 and 1.3).

The efficiency with which the heat from the reactor is converted into electricity is mainly determined by the temperature of the steam and of the cooling water in the condenser. As the temperature in the reactor is limited, the efficiency is low, *circa* 33 %. For comparison, the efficiency of a modern conventional power station (coal or oil fired) amounts to 40 – 50 %.

The boiling-water reactor

In the boiling-water reactor (BWR), steam is produced in the core, so that a mixture of water and steam leaves the core. Above the core a steam-water separator is present. The separated water is mixed with the feed water of the condenser and pumped into the core again. The water in the core is under a pressure of *circa* 70 bar. At this pressure the saturation temperature is 286 $^{\circ}$C. Because of the high pressure, the core with accessories must be placed in a pressure vessel.

The average volume fraction of steam in the core amounts to *circa* 35 %. At the outlet of the core this is considerably more (up to 70 %). The mass fraction of the steam (the steam quality) then is about 15 %.

The fuel elements of a BWR consist of UO_2 rods with lightly enriched uranium (4.5 %) in a zircaloy (zirconium alloy) cladding. In this way contact between uranium and cooling water is avoided, while the fission products (including the gaseous ones) remain confined in the nuclear fuel. A fuel element of a modern BWR consists of a rectangular lattice of e.g. 8x8 rods, which are assembled together in a can through which the cooling water flows. The diameter of the fuel

rods is *circa* 12.5 mm, the total length *circa* 4m. The distance between the rods (pitch) is *circa* 16 mm. The fuel elements are placed in the core in clusters of four with a cross-shaped control rod between these elements. The control rods consist of boron carbide (B_4C) and are moved into the core from below, as the steam-water separators and steam dryers are above the core.

As at the top of the core more steam is present and thus less moderation, the axial flux distribution is asymmetric and the maximum is in the lower half of the core. This is compensated for in some degree by the control rods inserted from below. Modern fuel designs incorporate partial length rods, that leave more open, steam-water filled, regions near the top of the core.

The control rods mainly serve for compensation of the burn-up of the nuclear fuel. The actual control of the reactor takes place via control of the recirculation flow of the feed water. If one increases this flow, the vapour bubble fraction in the core decreases, by which moderation is improved. This increases the reactivity (larger moderator-to-fuel ratio) and with that the power of the reactor. At a higher power the vapour bubble fraction increases again until the reactivity has decreases to zero, after which a new steady state has been obtained at higher power. The core of a BWR is approximately cylindrical. For a 1200 MWe reactor the height of the core is *circa* 4 m and the diameter *circa* 4.5 m. The average power density, connected to the thermal power, amounts to *circa* 50 kW/ℓ . Table 7.1 gives a number of characteristic data of a modern BWR nuclear power station.

The pressurized-water reactor

In another type of light-water reactor, the pressurized-water reactor (PWR), a much higher pressure of the cooling water (*circa* 150 bar) is applied, at which the boiling temperature is 343 ^{o}C. As the temperature of the water leaving the core amounts to about 315 ^{o}C, boiling does not occur in the core. The high pressure is obtained by a pressure generator (pressurizer). The steam required for the turbine is generated in a separate heat exchanger, the steam generator.

As a result of the better heat transfer in the core without boiling, the power density is larger than in a BWR: *circa* 100 kW/ℓ . The size of the core is thus smaller than that of a BWR of equal power. For a larger heat-transfer area the nuclear fuel rods are thinner (*circa* 10 mm) and are closer together (*circa* 12.5 mm). The moderator-to-fuel volume ratio is thus smaller than in a BWR. The density of the water, however, is higher because of the absence of steam.

A fuel element of a PWR consists of a lattice of e.g. 18x18 rods. In contrast with a BWR element, a PWR element is open; no can is applied. A number of fuel elements contain a finger-shaped control rod, which replaces the nuclear fuel at about 20 positions in the element. The control rods consist of an Ag-In-Cd alloy. For control of the reactivity change by burn-up and especially for compensation of the large overreactivity in a core with new fuel elements, boric acid is added to the cooling water and its concentration controlled. Table 7.2 gives a number of characteristic data of a modern PWR nuclear power station.

Table 7.1.Characteristic data of a modern BWR nuclear power station

Plant		
Core thermal power		3579 MWt
Electric output (gross/net)		1269/1233 MWe
Plant efficiency		33.5%
Core		
Active core height		3.76 m
Core diameter		4.65 m
Fuel inventory		138-t UO_2
Number of fuel assemblies		748
Assembly pitch		15.2 cm
Rod pitch		1.63 cm
Average power density		56 kW/liter
Fuel		
Fuel material		UO_2
Enrichment		Average 2.8% ^{235}U (initial core 1.77-2.1%)
Pellet dimensions (diam x height)		1.06 x 1.0 cm
Assembly array		8 x 8 with fuel channel around fuel rods
Total number of fuel rods		46.376
Cladding material		Zircaloy-2
Cladding outer diameter		1.25 cm
Cladding thickness		0.86 mm
Control		
Number of control rods		177
Material		Boron carbide (B_4C)
Control rod type		"Cruciform" blades inserted hydraulically from below between sets of four assemblies
Other control systems		Use of burnable poison
Vessel		
Material		SA533 (or 533B) manganese molybdenum nickel steel with an inner layer of cladding 3 mm of austenitic stainless steel
Wall thickness		16.4 cm
Vessel height		21.6 m
Vessel inner diameter		6 m
Vessel weight (including head)		885 t approximately

Coolant		
Material		Ordinary water (H_2O)-two phase
Pressure		7 MPa
Number of recirculation loops		2
Core coolant flow		13.2 Mg/hr
Core coolant outlet temperature		288°C
Core coolant inlet temperature		277°C
Feedwater flow rate		1.94 Mg/sec
Feedwater temperature		216°C
Average coolant exit quality		14.7% steam by weight
Fueling		
Type		Off-load, radial shuffling
Refueling sequence		1/3 of core every 18 months or 1/4 core every 12 months
Shutdown for refueling		60 days
Annual spent fuel discharge		32 t/yr
Design fuel burnup		28,400 MWd/t at equilibrium

Table 7.2.Characteristic data of a modern PWR nuclear power station

Plant		
Thermal power		3425 MWt
Electric output (gross/net)		1150/1100 MWe
Efficiency		33%
Core		
Active core (or fuel rod) height		3.7 m
Core diameter (equivalent)		3.4 m
Fuel inventory		101-t UO_2
Number of fuel assemblies		193
Assembly pitch		30.4 cm
Rod pitch		1.26 cm
Average core power density		104.5 kW/liter
Fuel		
Fuel material		UO_2
Enrichment		Three regions with 2.1, 2.6, 3.1%
Pellet dimensions (diam and length)		0.82 x 1.35 cm
Assembly array		17 x 17 (open type)
Total number of fuel rods		50,952
Cladding material		Zircaloy-4

Cladding outer diameter		0.95 cm
Cladding thickness		0.6 mm
Control		
Number of control clusters		53
Number of control rods per cluster		20
Absorber material		Ag – In – Cd
Absorber rod cladding		304 stainless steel
Control rod type		Cylindrical rods assembled into clusters inserted from above
Other control systems (first core)		Burnable poison rods, borosilicate glass
Vessel		
Material		SA533, Mg – Mo – Ni steel inner cladding
Wall thickness		21.9 cm
Vessel dimension (diam and height)		4.4 x 12.6 m
Coolant		
Material		Ordinary water (H_2O)-liquid phase
System pressure		15.5 MPa
Number of loops/steam generators		4
Mass flow		15.9 Mg/sec
Core inlet temperature		298°c
Core outlet temperature		326°C
Fueling		
Type		Off-load, radial shuffling
Refueling sequence		1/3 of core every 12 months
Shutdown period		30 days
Annual spent fuel discharge		30.4 t
Design fuel burnup		33,000 MWd/t

7.2. The fuel cycle of a light-water reactor

The fuel for a light-water reactor, uranium, is found as ore in the earth's crust. At the current uranium mining locations, the ore contains 0.1 to 0.5 % uranium. The uranium has the chemical formula U_3O_8 and has a yellow colour (yellow cake). For use in a light-water reactor, the natural uranium (0.7 % ^{235}U) must be enriched to 4-5 %. To this end, U_3O_8 is converted into UF_6, which becomes gaseous already at low temperature. The gas can be enriched by pumping it through membranes at high pressure, whereby the slightly lighter ^{235}U passes through the membrane somewhat easier (gaseous diffusion process; USA, France, former USSR). In the Netherlands (and in England and Germany), the ultracentrifuge process is applied. In this process, one brings the gas into very rapidly rotating centrifuges, by which the ^{238}U moves more

to the outside of the centrifuge due to its larger mass and so a certain separation is accomplished. Especially for the gaseous diffusion process the separation factor per step is very small, so that the process must be gone through many times (cascade process) in order to obtain the desired enrichment. For the future one has expectations of laser enrichment, which is currently still in the development stage.

From a feed stream F of natural uranium with percentage $x_F = 0.7$ % ^{235}U one obtains a product stream P with enrichment percentage x_P and waste stream W with percentage x_W. The total uranium flow and the flow of ^{235}U are given by

$$F = P + W \tag{7.1}$$

$$x_F F = x_P P + x_W W \tag{7.2}$$

From this it follows for the flow of enriched uranium that

$$P = \frac{x_F - x_W}{x_P - x_W} F \tag{7.3}$$

The percentage of ^{235}U in the waste 'tails' is about 0.2 %. If one wants to have an enrichment of 4 % as final product, it follows that one can produce 0.13 kg enriched uranium per kg natural uranium.

After enrichment the UF$_6$ is converted into UO$_2$, from which fuel pellets are sintered, which are finally assembled into a fuel element.

In the reactor the burn-up takes place. Thereby ^{235}U both undergoes fission and conversion into ^{236}U by neutron capture. From Table 6.1 it follows that the capture-to-fission ratio is about 0.16 in a thermal reactor. In addition, neutrons are captured in the ^{238}U, by which after β decay ultimately ^{239}Pu is formed, which is fissile by slow neutrons:

$$^{238}_{92}U + n \rightarrow {}^{239}_{92}U \xrightarrow{\beta^-} {}^{239}_{93}Np \xrightarrow{\beta^-} {}^{239}_{94}Pu$$
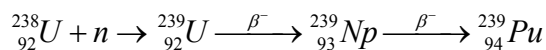
In Section 5.5 the conversion ratio C has already been defined as the ratio of the production rate of fissile nuclides to the consumption rate of fissile nuclides. This ratio appears to be 0.5 to 0.6 for light-water reactors, also due to the resonance capture in ^{238}U. Part of the formed Pu also undergoes fission in the reactor. Of the total energy produced from the nuclear fuel, about one third is coming from fission of Pu.

If a fuel element has been burned up sufficiently far, it will have to be replaced. In a pressurized-water reactor, one fourth to one third of the elements is replaced every year. The spent nuclear fuel then contains about 0.8 % ^{235}U.

With these data the uranium consumption of a reactor can be calculated. If a light-water reactor has produced 1000 MWyear of electricity (for such a yearly production a nuclear power station with a capacity of 1200 or 1300 Mwe is required with a load factor of 83 or 77 %, respectively), about 3000 MWyear of thermal energy has been produced. As 200 MeV or $3.2 \cdot 10^{-11}$ J is released upon fission, this means burn-up of about 1150 kg. About two thirds of this is ^{235}U, so that about 770 kg of ^{235}U is burned up. If the initial enrichment was 4 % and after consumption 0.8 % was left, about 24 tonnes of enriched uranium was required. This corresponds with about 185 tonnes of natural uranium before enrichment. Compare this with the required amount of coal with a heating value of 30 MJ/kg.

In addition to the burn-up of ^{235}U, Pu has been formed and partially burned up. Of the total amount of energy produced, about 1000 MWyear will have been obtained by burn-up of Pu, for which *circa* 385 kg Pu must have been burned up. With a conversion factor of 0.55, 0.55 x (770 + 385) = 635 kg ^{239}Pu has been formed. After usage, 250 kg is left, so that the spent nuclear fuel contains about 0.6 % Pu. The spent nuclear fuel further consists of *circa* 5 % fission products and 0.6 % ^{236}U. By repeated neutron capture other transuranium elements are also formed.

In a nuclear fuel reprocessing plant, the useful elements (U and Pu) can be extracted from the spent nuclear fuel and be used as fuel in the reactor again (possibly after re-enrichment). As the costs of this reprocessing are high and some countries are apprehensive of the spreading (proliferation) of the Pu for the production of nuclear weapons, reprocessing is no longer always applied. The amount of energy one can extract from spent nuclear fuel is limited by the amount of remaining nuclides that are necessary to be able to make the reactor critical. To this end, one could enhance the initial enrichment. However, one then encounters a technological limit: the radiation damage that occurs in the nuclear fuel during reactor operation and the formation of fission products, which swell the nuclear fuel. With the current nuclear fuels for light-water reactors one produces 3000 MWyear of thermal energy from 24 tonnes of enriched nuclear fuel, so that the degree of burn-up is about 45 MWd/kg. There is a tendency towards higher degrees of burn-up (70-100 MWd/kg), which makes it economical to start with a higher enrichment.

7.3. Other reactor types

Over the years a variety of reactor types have been developed in various countries with differences in construction, nuclear fuel, moderator and coolant. Currently, in addition to the light-water reactors, the following reactor types are of importance.

Gas-cooled reactors

These have especially been developed and applied in England. Graphite is used as the moderator, which makes it is possible to suffice with natural uranium. These reactors are called magnox reactors, after the cladding material of the fuel rods, which consists of a magnesium alloy. CO_2 is used as the coolant. In a later version (AGR = advanced gas-cooled reactor) enriched uranium is used in order to achieve a better nuclear fuel economy. A modern variant is the high-temperature reactor (HTR), in which graphite is used as the moderator also, but with helium as the coolant. Gas turbine In this reactor, the fuel cycle can be based on ^{233}U/^{232}Th, with which a high conversion ratio can be achieved. The fissile ^{233}U is obtained from the thorium by the conversion reaction

$$^{232}_{90}Th + n \rightarrow {}^{233}_{90}Th \xrightarrow{\beta^-} {}^{233}_{91}Pa \xrightarrow{\beta^-} {}^{233}_{92}U$$
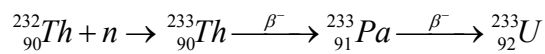
Heavy-water reactor

This type has especially been developed in Canada. Heavy water (D_2O) is applied as moderator. Due to the favourable neutron management, application of natural uranium is possible and one attains a relatively high conversion factor (*circa* 0.9). This type of reactor is called CANDU (Canadian deuterium-uranium) reactor.

Fast breeder reactors

The conversion ratio in a light-water reactor is 0.5 to 0.6, *i.e.* the production of new nuclear fuel is much less than its consumption. This is caused, among other things, by the relatively low value of the neutron yield factor η. For natural uranium this factor is 1.34 and for low-enriched uranium it is about 1.8. From Figure 7.1 one sees that for a thermal reactor ^{233}U is a much more favourable fuel with $\eta = 2.3$.

Of the neutrons released upon absorption in the nuclear fuel, one is required for continuation of the chain reaction, while neutrons are also lost as a result of parasitic absorption and leakage. Then *circa* one neutron remains, which can be used to convert a non-fissile nucleus into a fissile one. This should happen by addition of ^{232}Th. This fuel cycle is applied in a HTR, but in a HTR no breeding of additional nuclear fuel occurs.
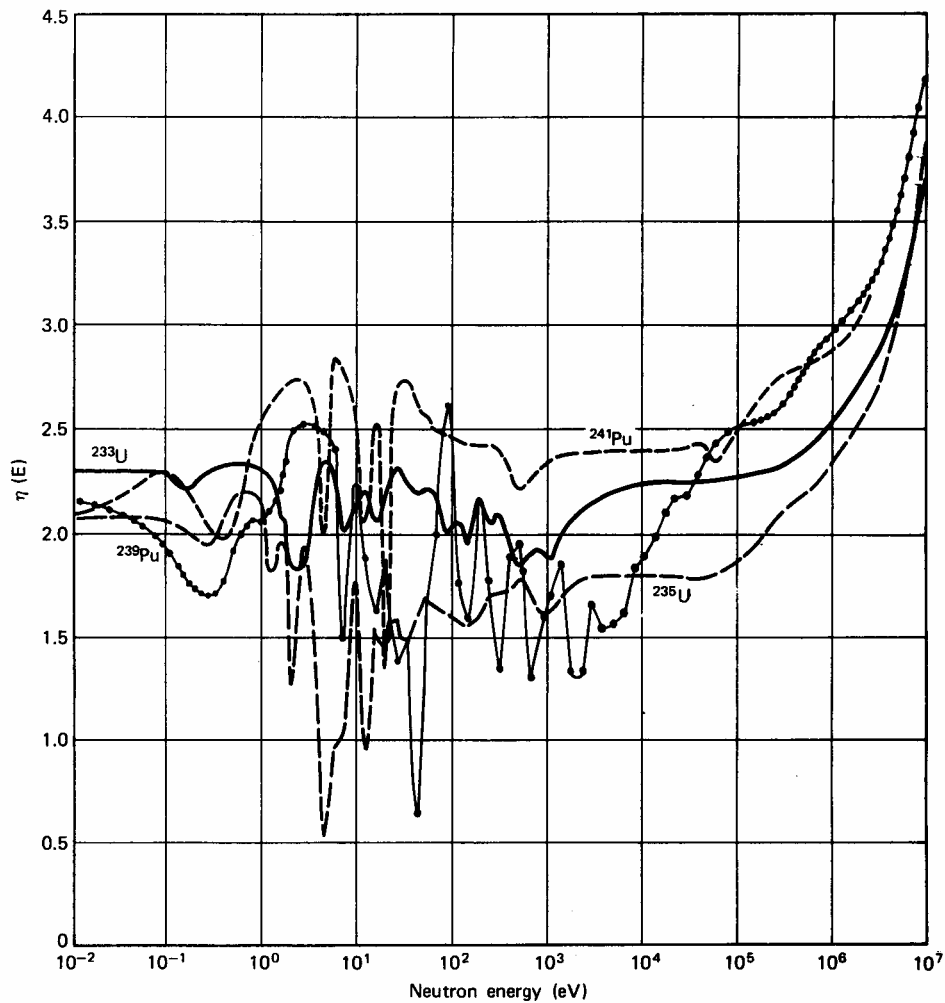
Figure 7.1. Neutron yield factor η as a function of the neutron energy for some fissile nuclides

If one wants to produce more nuclear fuel than one consumes, then an even higher value of η is necessary, which can only be realised with fast neutrons. In this case [239]Pu is a good nuclear fuel. The fast breeder reactor is based on this principle. In order to keep the neutron spectrum fast, one avoids the use of light materials such as a moderator. Liquid metal (sodium, lead or lead-bismuth) is applied as coolant, because it has favourable cooling properties and is not too light. The nuclear fuel consists of [239]PuO$_2$ mixed with UO$_2$. The uranium serves as breeding material for the fissile [239]Pu and thus does not have to be enriched. One can even use depleted uranium, which is left as waste in the enrichment of nuclear fuel for light-water reactors. If insufficient Pu is available for a first core, the reactor can also be started up with enriched uranium. After sufficient Pu has been produced, one can then feed other breeder reactors with it. The uranium requirement then becomes a factor 50 to 70 lower than for light-water reactors.

As the microscopic cross sections for fast neutrons are small, a large nuclear fuel density is required. Therefore, 15 to 20 % Pu is applied. In the core of the breeder reactor a net consumption of nuclear fuel takes place (breeding factor < 1). By choosing a small core with a relatively large neutron leakage, a blanket of fertile material (depleted uranium) can be placed

119

around the core, where breeding occurs almost exclusively. In this way, the breeding factor for the whole reactor can be 1.2 to 1.4.

For an economic application of the expensive nuclear fuel, a large power density is necessary: *circa* 500 kW/ℓ. Due to the good cooling properties of liquid sodium this heat can be removed in a safe manner. The temperature of the sodium is much higher than applicable for light-water reactors. Therefore, a higher thermal efficiency can be achieved, comparable to that of conventional power stations. The heat of the sodium must be transferred to water to generate steam. As direct contact between sodium and water can result in a violent reaction, an intermediate cooling circuit with sodium, which is no longer radioactive, is applied, which transfers its heat to a steam circuit.

Although the life of neutrons in a fast reactor is very short (10^{-7} to 10^{-6} s), here also reactor control is determined by the delayed neutrons, so that a fast reactor is no more difficult to control than a thermal reactor. As the fraction of delayed neutrons for Pu is much smaller than for ^{235}U (see Table 4.1), the margin for deviations in the reactivity is much smaller. Opposite to this stands that the change of the reactivity during the fuel cycle in a fast reactor is much smaller, because the net fuel consumption in the core is much smaller than in a light-water reactor.

Breeder reactors are not yet being applied commercially. Diverse prototypes have been built in various countries with capacities in the order of 300 MWe. Only in France a large breeder reactor (the Superphénix) with a capacity of 1200 MWe has been in operation. For the present, breeder reactors will not be able to compete with light-water reactors. Only if uranium becomes much more expensive, the breeder reactor with its small uranium consumption will acquire a more favourable position.

Research reactors

Reactors for research serve a completely different purpose from reactors for energy supply and for that reason differ strongly from the previously discussed reactors. A research reactor is used for the production of neutrons, which leave the reactor as, among other things, neutron beams and are used for e.g. research of matter, by studying the scattering of neutrons at a specimen. For a large intensity of neutrons a high leakage factor is required and thus a small core. By application of highly enriched uranium, core dimensions of e.g. 50x50x60 cm^3 can be obtained. Highly enriched nuclear fuel (93 % enrichment) used to be made available for research reactors by the American government. This highly enriched material is coming from a program for the production of nuclear weapons. In connection with controlling the proliferation of material for nuclear weapons, lightly enriched (< 20 %) uranium must now be used in research reactors. This does not matter much for the value of η (see Figure 6.5), but it has some influence on the resonance escape probability.

Unpressurised light water is applied as moderator and coolant. Because of this, the maximum allowable temperatures are low, which limits the maximum attainable neutron flux in the core. With special constructions so-called high-flux reactors can also be realised.

7.4. The international situation with regard to nuclear energy

Currently about 450 nuclear power stations are in operation worldwide. The majority is of the light-water type with a lead for the PWR. As a result of the economic recession of the 1970s and the increased social resistance against nuclear energy, the expansion of nuclear energy has proceeded much slower than one expected in about 1970. There are, however, substantial differences per country. The largest number of reactors is in the **United States** (104 in 2002). Since 1993 no new nuclear reactors - have been put into operation. The nuclear power installed has been increased by plant upgrading and by lifetime extension of several plants. The share of nuclear energy in electricity production amounts to *circa* 20 % and is almost completely provided by light-water reactors (both PWRs and BWRs). Important suppliers are Westinghouse (PWR) and General Electric (BWR).

In **Russia and neighbouring countries** nuclear energy is also applied at a large scale, although the share of nuclear energy in electricity production here also is modest. Two types are principally applied, *viz.* the Russian version of the pressurized-water reactor (VVER), which is exported to many other Eastern European countries, and a graphite-moderated, light-water cooled reactor (RBMK). The reactor in Tsjernobyl, where a serious accident happened in April 1986, was of the latter type. The positive temperature coefficient of this reactor type (positive reactivity with increasing temperature of the coolant), played an important part in this accident, reason why this type is no longer built.

Also **Japan**, which is almost destitute of natural resources, has a large number of reactors in operation (54 in 2002) and under construction (both PWR and BWR), built by own industry. It is operating the world's only two advanced reactors.

In Western Europe the situation strongly differs from country to country. **France** is the undisputed leader with respect to nuclear energy, with a share of *circa* 80 % in electricity production (59 nuclear reactors in 2002). This means that not all nuclear power stations can operate at base load (constantly supplying the maximum power, irrespective of the electricity demand), but continuously have to adapt the power to the demand. In France only PWRs are built by the supplier Framatome.

In **Sweden** (with own BWR supplier Asea-Atom, currently called ABB) and **Switzerland** *circa* 40 % of the electricity is generated with nuclear energy, in **Belgium** even 60 %. Germany, Finland and Spain rely for some 30% on nuclear energy.

121

In **England** the gas-cooled reactor is predominantly applied. As this type has no development possibilities any more, the most recently built nuclear power station is of the PWR type.

In **the Netherlands** only one nuclear energy station is in operation: Borssele since 1974, PWR type with a capacity of 477 MWe. After the accident with the Russian power station in Tsjernobyl, the government has postponed the decision for building at least two new power stations, each with a capacity of 900 to 1300 MWe.

As the safety of reactors plays an important part in the discussion about nuclear energy, development projects of newer types of reactors such as the SBWR (Simplified BWR) are taken part in and developments with respect to a new generation of reactors with characteristic features of inherent safety are watched. In these reactors the safety mechanisms are based as little as possible on systems that must be activated (opening or closing valves, starting pumps, etc.), but as much as possible on systems that automatically come into operation on the ground of physical principles.

Appendix

Definition of the solid angle

The magnitude of a solid angle Ω is defined by the area that is cut out of a sphere with radius R, divided by the square of the radius of the sphere (see Figure A.1):

$$\Omega = \frac{A}{R^2} \qquad\qquad (A.1)$$

with which the magnitude of the solid angle is independent of the chosen radius of the sphere. The solid angle is measured in steradians, abbreviated ster. In view of the definition (A.1) this is not an actual dimension in the sense of the S.I. For the maximum possible solid angle, which comprises all directions, the area would become equal to the total surface area of the sphere $4\pi R^2$, so that the maximum solid angle is 4π.
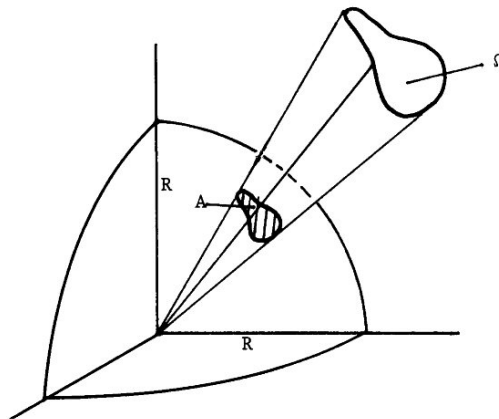

Figure A.1. Definition of a solid angle

Integrals over the direction $\underline{\Omega}$

The directional vector $\underline{\Omega}$ can be fixed with two scalar variables, a polar angle θ and an azimuthal angle ψ with $0 \leq \theta \leq \pi$ and $0 \leq \psi \leq 2\pi$ (see Figure A.2). When varying these angles, a solid angle $d\Omega$ that is equal to the surface area of a sphere of unit radius is described:

$$d\Omega = \sin\theta\, d\theta\, d\psi \qquad\qquad (A.2)$$

With this, any integration over $\underline{\Omega}$ can be written as a double integral over scalar variables. It is often easier to work with $\mu = \cos\theta$ instead of θ itself. Then

$$d\Omega = d\mu d\psi \tag{A.3}$$

with $-1 \leq \mu \leq 1$.
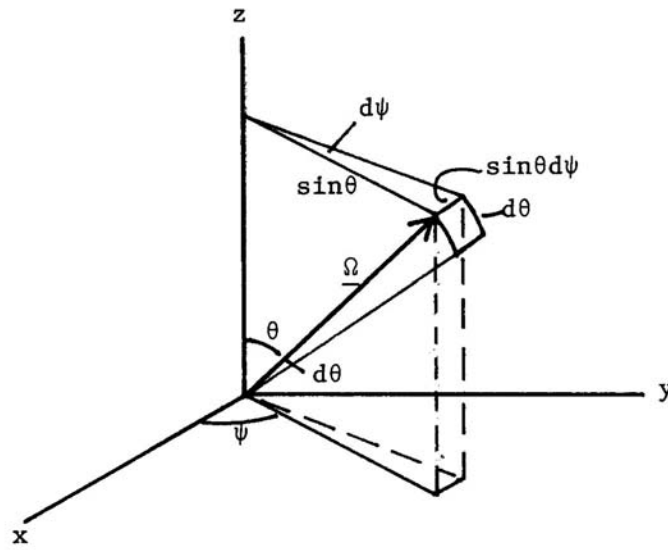
Figure A.2. Integration over the direction $\underline{\Omega}$

When working out integrals over $\underline{\Omega}$ over the whole solid angle 4π the following integrals are useful (verify these by writing them as elementary integrations):

$$\int_{4\pi} d\Omega = 4\pi \tag{A.4}$$

$$\int_{4\pi} \underline{\Omega} d\Omega = \underline{0} \tag{A.5}$$

$$\int_{4\pi} \underline{\Omega}(\underline{\Omega} \cdot \underline{a}) d\Omega = \frac{4\pi}{3} \underline{a} \tag{A.6}$$

with $\underline{a}$ a constant vector (independent of $\underline{\Omega}$). When choosing a co-ordinate system for defining θ and ψ, it is practical to choose the polar axis, from which θ is measured, along the vector $\underline{a}$. In the second and third integral the separated components of $\underline{\Omega}$ are required:

124

$$\underline{\Omega} = \begin{pmatrix} \sin\theta\cos\psi \\ \sin\theta\sin\psi \\ \cos\theta \end{pmatrix} \tag{A.7}$$

The nabla operator

The nabla operator $\underline{\nabla}$ can be interpreted as a vector with components

$$\underline{\nabla} = \left(\frac{\partial}{\partial x}, \frac{\partial}{\partial y}, \frac{\partial}{\partial z} \right) \tag{A.8}$$

Application on the scalar field $\phi(\underline{r}) = \phi(x,y,z)$ yields a vector

$$\underline{\nabla}\phi = grad\,\phi = \left(\frac{\partial\phi}{\partial x}, \frac{\partial\phi}{\partial y}, \frac{\partial\phi}{\partial z} \right) \tag{A.9}$$

In spherical co-ordinates with spherical symmetry:

$$\underline{\nabla}\phi = \frac{d\phi}{dr} \tag{A.10}$$

with direction equal to that of the co-ordinate vector $\underline{r}$.

Application of the nabla operator on a vector as internal product yields a scalar

$$\underline{\nabla}\cdot\underline{v} = div\,\underline{v} = \frac{\partial v_x}{\partial x} + \frac{\partial v_y}{\partial y} + \frac{\partial v_z}{\partial z} \tag{A.11}$$

Further, the operator of Laplace $\underline{\nabla}\cdot\underline{\nabla} = \nabla^2$, which operates on a scalar and has a scalar as result, can also be formed

$$\nabla^2 = \underline{\nabla}\cdot\underline{\nabla} = div\,grad\,\frac{\partial^2}{\partial x^2} + \frac{\partial^2}{\partial y^2} + \frac{\partial^2}{\partial z^2} \tag{A.12}$$

In spherical co-ordinates with spherical symmetry:

$$\nabla^2 = \frac{1}{r^2}\frac{d}{dr}\left(r^2\frac{d}{dr} \right) = \frac{d^2}{dr^2} + \frac{2}{r}\frac{d}{dr} \tag{A.13}$$

125

In cylindrical co-ordinates with rotational symmetry:

$$\nabla^2 = \frac{1}{r}\frac{d}{dr}\left(r\frac{d}{dr}\right) = \frac{d^2}{dr^2} + \frac{1}{r}\frac{d}{dr}$$

(A.14)

Divergence theory of Gauss

$$\int_V \underline{\nabla} \cdot \underline{v}\, dV = \int_S \underline{n} \cdot \underline{v}\, dS$$

(A.15)

Expansion in Legendre polynomials

Legendre polynomials $P_n(\mu)$ are defined by

$$P_n(\mu) = \frac{1}{2^n n!}\frac{d^n}{d\mu^n}\left(\mu^2 - 1\right)^n$$

(A.16)

with $\quad P_0(\mu) = 1$

$\quad\quad\quad P_1(\mu) = \mu$

$\quad\quad\quad P_2(\mu) = \frac{1}{2}(3\,\mu^2 - 1)$

$\quad\quad\quad P_3(\mu) = \frac{1}{2}(5\,\mu^3 - 3\,\mu)$

A recurrent relation exists between the Legendre polynomials:

$$(n+1)P_{n+1}(\mu) - (2n+1)\mu P_n(\mu) + nP_{n-1}(\mu) = 0$$

(A.17)

At the interval $-1 \leq \mu \leq 1$ the Legendre polynomials are orthogonal:

$$\int_{-1}^{1} P_m(\mu)P_n(\mu)d\mu = \quad 0 \quad\quad m \neq n$$

$$\frac{2}{2n+1} \quad\quad m = n$$

(A.18)

This orthogonality enables the expansion of a real function $f(\mu)$, quadratic integration of which is possible at the interval $-1 \leq \mu \leq 1$, but which further is arbitrary, in a series of Legendre polynomials:

$$f(\mu) = \sum_{n=0}^{\infty} \frac{2n+1}{2} f_n P_n(\mu) \tag{A.19}$$

in which the coefficients f_n are given by

$$f_n = \int_{-1}^{1} f(\mu) P_n(\mu) d\mu \tag{A.20}$$

An extension of such a series expansion is the expansion of a function that depends on the unit vector $\underline{\Omega}$ in so-called spherical harmonics, which has been applied in the expansion of the angle-dependent flux $\phi(\underline{\Omega})$ according to (2.15).

Literature

a. General books about reactor physics ([*] = very useful as supplement to this text):

1. [*] Bennet, D.J.:   The Elements of Nuclear Power.

          Longman, London, England, 1972.

2. [*] Caspers, L.M. and D.J. v.d. Hoek:

          Kernreactorkunde, een beknopte inleiding (in Dutch).

          VSSD, Delft, 1976.

3. [*] Fassbender, J.:   Einführung in die Reaktorphysik (in German).

          Thiemig-Taschenbücher, part 12.

          Thiemig, München, Germany, 1967.

4. [*] Glasstone, S. and M.C. Edlund:

          The Elements of Nuclear Reactor Theory.

          D. van Nostrand, New York, USA, 1952.

5. Isbin, H.S.:   Introductory Nuclear Reactor Theory.

          Reinhold Publishing corporation, New York, USA, 1963.

6. [*] Knief, R.A.:   Nuclear Engineering.

          Taylor and Francis, London, UK, 1992.

6. Meghreblian, R.V. and D.K. Holmes:

          Reactor Analysis.

          McGraw-Hill, New York, USA, 1960.

7. [*] Onega, R.J.:   An Introduction to Fission Reactor Theory.

          University Publications, Blacksburg, 1975.

8. Ott, K.O. and W.A. Bezella:

          Introductory Nuclear Reactor Statics.

          American Nuclear Society, La Grange Park, Illinois USA, 1989.

9. Weinburg, A.M. and E.P. Wigner:

    The Physical Theory of Neutron Chain Reactors.

    University of Chicago Press, Chicago, USA, 1958.

10. Zweifel, P.F.:   Reactor Physics.

    McGraw-Hill, New York, USA, 1973.

b. Specialized books:

1. Beckurts, K.H. and K. Wirtz:

    Neutron Physics.

    Springer Verlag, Berlin, Germany, 1964.

    (Discussion of neutron transport theory and measuring techniques)

2. Bell, G.I. and S. Glasstone:

    Nuclear Reactor Theory.

    Van Nostrand, New York, USA, 1970.

    (Profound discussion of neutron transport theory)

3. Duderstadt, J.J. and L.J. Hamilton:

    Nuclear Reactor Analysis.

    John Wiley and Sons, New York, USA, 1976.

    (Profound discussion of a broad spectrum of topics in reactor physics)

4. Hetrick, D.L.:   Dynamics of Nuclear Reactors.

    University of Chicago Press, Chicago, USA, 1971.

    (Profound discussion of reactor dynamics)

5. Ott, K.O. and R.J. Neuhold:

    Introductory Nuclear Reactor Dynamics.

    American Nuclear Society, La Grange Park, Illinois USA, 1985.

6. Rahn, F.J., A.G. Adamantides, J.E. Kenton and C.Braun:

    A Guide to Nuclear Power Technology.

    John Wiley and Sons, New York, USA, 1984.

    (Comprehensive description of all components of nuclear power stations of various reactor types)

7. Silvenoinen, P.:   Reactor Core Fuel Management.

                         Pergamon Press, Oxford, England, 1976.

                         (Discussion of nuclear fuel management in a reactor)

8. Stacey, W.M.:   Nuclear Reactor Physics.

                         John Wiley & Sons Inc., New York, USA, 2001.

                         (Profound discussion of a broad spectrum of topics in reactor physics)

c. More general reading-matter concerning nuclear reactors and nuclear energy:

1. Andriesse, C.D. and A. Heertje (editors):

                         Kernenergie in Beweging (in Dutch).

                         Keesing Boeken, Amsterdam, 1982.

                         (Contains a large number of contributions on reactors and the fuel
                         cycle, environment and radiation and social aspects of nuclear
                         energy)

2. Hoogenboom, J.E.:

                         Kernreactoren voor Electriciteitsproduktie (in Dutch).

                         Nederlands Tijdschrift voor Natuurkunde $\underline{A53}$ (2/3), (1987), pp. 49-
                         56.

                         And other articles in this 'Nuclear Energy issue' of the Nederlands
                         Tijdschrift voor Natuurkunde.

d. Specific data:

1. Hughes, D.J. and R.B. Schwartz:

                         Neutron Cross Sections. report BNL-325, second edition.

                         Brookhaven National Laboratory, Upton, USA, 1958.

                         (Classical report with numerical and graphical representation of cross
                         sections of many materials and nuclides; a more modern publication
                         is:)

2. Metane, V., C.L. Dunford and P.F. Rose:

Neutron Cross Sections, Vol. 2. (graphical representation). Academic Press, Boston, USA, 1988.

3. Mughabghab, S.F., M. Divadeenam and V.E. Holden:

Neutron Cross Sections. Vol. 1. (thermal cross sections and resonance parameters). Academic Press, Boston, USA, 1981.

4. Rose, P.F. and C.L. Dunford:

Data Formats and Procedures for the Evaluated Nuclear Data File ENDF-6, report ENDF-102/BNL-NCS 44945, Rev. 10/91. Brookhaven National Laboratory, Upton, USA, 1991.

(Description of the format of the computer files ENDF/B-VI and JEF-2 with numerical values of cross sections; the computer files are present at the IRI).

Websites with relevant information:

www.kernenergie.nl: Dutch portal to relevant websites

www.kerncentrale.nl: website of the Borssele 2004+ foundation. with background information on nuclear energy

www.worldnuclear.org: website of the world's nuclear news agency

www.world-nuclear.org: website of the World Nuclear Association with a tremendous amount of detailed information on nuclear energy

www.iaea.org: website of the International Atomic Energy Agency containing factsheets on nuclear energy topics

www.kerntechniek.nl: website of the Netherlands Nuclear Society and the Nuclear Technology Section of the Royal Institute of Engineers (KIvI)